A core mitophagic machinery promotes selective degradation of paternal mitochondria in mouse embryos and MEF cells

Thesis by

Rebecca Bloom Rojansky

In Partial Fulfillment of the Requirements for

the degree of

Doctor of Philosophy

CALIFORNIA INSTITUTE OF TECHNOLOGY

Pasadena, California

2016

(Defended April 18, 2016)

Rebecca Bloom Rojansky

ORCID: 0000-0002-3735-8159

ACKNOWLEDGEMENTS

First, I would like to thank my advisor, Dr. David Chan, through whose model, guidance, and support I learned how to think critically about science. I would also like to thank Dr. Hsiuchen Chen both for her invaluable help with animal work, as well as for her efforts in keeping us all running smoothly. I thank my committee, Dr. Dianne Newman, Dr. Angela Stathopoulos, and Dr. Shu-ou Shan, for granting me their time and insight, and for their support in pursuing this degree.

I am most grateful to Dr. Shirley Pease, and Jennifer Costanza. Without their expertise I could not even have begun this project. Dr. Pease generously opened her lab to me and provided insight on countless occasions, and her knowledge and experience is only matched by her kindness.

I would like to acknowledge the past and present members of the Chan lab, including Dr. Prashant Mishra, Dr. Nickie Chan, Dr. Anh Pham, Dr. Anna Salazar, Dr. Elisabeth Yun Wang, Dr. Anand Vaidya, Dr. Anne Chomyn, Dr. Huu Ngo, Dr. Oliver Loson, Dr. Chunshik Shin, Raymond Liu, Greg Varuzhanyan, Ruohan Wang, Katherine Kim, and Dr. Kurt Reichermeier for their insights, mentorship, and friendship.

I am lucky to have had a wonderful friend and colleague in Meera Rao. I can’t thank her enough for her support.

I want to thank my family for encouraging my inquisitive mind, providing me with opportunities to grow, and for supporting me through every challenge. Their boundless love is an anchor in everything I do.

Finally, I thank James Parle for his love, wisdom, humor, and above all honesty, for supporting me through good times and bad, and for believing in me more than I believed in myself.

ABSTRACT

The maternal mode of mitochondrial inheritance is conserved across mammalian species; however, little is known about how mitochondria from the sperm are eliminated from early mammalian embryos. Mitophagy, the regulated degradation of mitochondria in the lysosome, has been proposed as a possible mechanism. Mitophagy is an important means by which the cell responds to changes in mitochondrial fitness, and has been observed under a number of physiological and non-physiological circumstances, including, but not limited to, hypoxia, mitochondrial depolarization, mitochondrial fission, and erythrocyte differentiation.

Here we examine the core component of mitophagy proteins involved in three physiological states: respiration-induced mitophagy in cultured mouse fibroblasts, mitophagy of dysfunctional mitochondria in the absence of mitochondrial fusion, and degradation of paternal mitochondria in pre-implantation mouse embryos. We find that a common pathway is used for elimination of mitochondria, involving mitochondrial depolarization, and the E3 ubiquitin ligases PARKIN and MUL1. We find that PARKIN and MUL1 play partially redundant roles in elimination of paternal mitochondria that is also dependent on PINK1 kinase, the fission factor, FIS1, and the autophagy receptor, p62. We find that p62 is specifically recruited to defective mitochondria in fusion deficient cells by a mechanism independent of ubiquitin binding. Our results elucidate the molecular mechanism of strict maternal transmission of mitochondria and uncover a collaboration between MUL1 and PARKIN in mitophagy.

TABLE OF CONTENTS

LIST OF FIGURES AND TABLES

Chapter 1

INTRODUCTION

Mitochondrial Homeostasis

Mitochondria are vital organelles that are essential for aerobic respiration. Originally independent prokaryotic cells, they were engulfed and co-opted by eukaryotic hosts for their ability to perform oxidative phosphorylation to produce ATP. This primordial history also points to another of the mitochondrion's unique traits: its genome. Mitochondria are the only organelles that carry and maintain their own DNA, termed mtDNA. In mammals, mtDNA follows a maternal inheritance pattern that is distinct from that of the nuclear DNA. Furthermore, mitochondria are highly dynamic structures that exist as part of a network, which is constantly remodeling itself to maintain the function of the population as a whole. As highly active organelles, mitochondria can accumulate damage to proteins, lipids, and DNA.

A variety of quality control mechanisms have been discovered to mitigate this damage. Mitochondria have their own proteolytic system which degrades misfolded proteins (Haynes and Ron, 2010), and they utilize the proteasome to degrade damaged outer mitochondrial membrane proteins (Taylor and Rutter, 2011). Moreover mitochondria can degrade oxidized proteins via the recently discovered mitochondria-derived vesicles, which bud off damaged mitochondria and are degraded in the lysosome along with their contents (Sugiura et al., 2014).

In addition, damaged mitochondria can be segregated from healthy mitochondria by mitochondrial fission, and healthy mitochondria can combine their components by mitochondrial fusion (Chen et al., 2005; Twig et al., 2008). Finally, dysfunctional mitochondria that are sequestered by coordinated fission and fusion can be degraded by a specialized form of selective macroautophagy, called mitophagy. Mitophagy leads to degradation of mitochondria in the lysosome (Ashrafi and Schwarz, 2013), and has been suggested to be an important mechanism for protection against alcohol-induced liver injury (Williams et al., 2015), neurodegenerative disease (Palikaras and Tavernarakis, 2012) cancer (Chourasia et al., 2015), and even aging (Richard et al., 2013).

Here we present work investigating the players in three specialized forms of mitophagy: first, mitophagy induced by elevated respiration, which we refer to as OXPHOS-induced mitophagy; second, mitophagy of paternal mitochondria in the pre-implantation mouse embryo; and third, mitophagy of dysfunctional mitochondria at steady-state in cells lacking mitochondrial fusion. In particular, we explore the requirement for the mitophagy receptor protein, p62, in all of these processes, and show a novel cooperation between the newly identified mitochondrial resident E3 ligase, Mulan (MUL1), and the established PINK1/PARKIN mitophagy pathway. In the following sections we will briefly discuss elements of normal mitochondrial physiology, including mtDNA, respiration, and mitochondrial dynamics, and then focus on our current understanding of mitophagy, and one way in which the cell responds to their dysfunction.

Respiration

Energy production goes through three stages: glycolysis in the cytosol, the Krebs cycle in the mitochondrial matrix, and oxidative phosphorylation across the mitochondrial inner membrane. Glycolysis, which breaks down glucose into pyruvate, can proceed in the presence or absence of oxygen, and although it generates much less ATP than oxidative phosphorylation, it is the main energy generation method used by highly proliferative cells including tumor cells, as well as many immortalized cell lines in standard in vitro culture systems. This "aerobic glycolysis" is known as the Warburg effect (Diaz-Ruiz et al., 2011). The advantages of this metabolic switch are unknown; however, it is hypothesized that it may be advantageous in the hypoxic environment found within solid tumors (Gatenby and Gillies, 2004). Another feature of many tumor cells is glucose-induced suppression of respiration, called the Crabtree effect (Crabtree, 1929). Both the Warburg and Crabtree effects are facilitated by the high glucose concentration often provided in cell culture media. Both are also reversible. Immortalized cells can be induced to increase respiration within 30 minutes of a shift in culture medium from glucose-containing to glucose-free medium that instead contains galactose or ketone bodies as a carbon source (Mishra et al.). This elevated respiration has a rapid effect on mitochondrial morphology. While cells grown in standard glucose-containing media have predominantly fragmented or short tubular mitochondria, within 24 hours of a shift to media lacking glucose, but containing galactose or ketone bodies, mitochondria form long tubules

(Mishra et al.). Metabolic state, therefore, profoundly affects mitochondrial physiology, beyond a simple increase or decrease in flow across the electron transport chain. Recent studies by our lab and others discussed below, and in Chapter 2, have begun to shed light on the fact that another physiological process, mitochondrial turnover by mitophagy, is also influenced by respiratory state (Melser et al., 2013).

The Krebs cycle in the mitochondrial matrix generates the high-energy molecules NADH, and $FADH_2$. Oxidative phosphorylation (OXPHOS) utilizes these high-energy molecules to generate an electrical potential across the inner mitochondrial membrane (IMM). This is accomplished by a series of coupled redox reactions that transport electrons through the respiratory complexes of the IMM. NADH enters the electron transport chain at complex I, and $FADH_2$ enters at complex II. Electrons from these molecules are passed in a stepwise manner to eventually reduce O_2 to H_2O at complex IV. During this process protons move from the mitochondrial matrix to the intermembrane space, which creates an electrochemical gradient composed of a pH gradient, and an electrical potential. This potential drives the synthesis of ATP from ADP as protons flow through ATP synthase (complex V) and re-enter the matrix. Complex I is the primary point at which electrons enter the respiratory chain, and hence damage to complex I is detrimental to mitochondrial function (Brandt, 2006; Papa et al., 2008). Seven hydrophobic subunits, composing the central core of the complex I, are encoded by mtDNA, so mtDNA mutations often disrupt complex I function. Loss of complex I function has also been observed in mitochondrial fusion mutants, and

drugs that inhibit complex I function produce Parkinson's-like disease phenotypes in animal models, and in humans (Chen and Chan, 2009; Chen et al., 2005). Mitochondria are the main source of reactive oxygen species (ROS) in the cell. Mitochondrial dysfunction due to mtDNA mutations or high respiratory activity can lead to oxidative stress, which results in oxidation of proteins, lipids, and DNA. Oxidative stress can induce mitochondrial degradation by mitophagy (Frank et al., 2012b), and may play a role in neurodegenerative diseases such as Parkinson's (Henchcliffe and Beal, 2008; Uttara et al., 2009). Our understanding of the link between respiration and mitophagy, however, is incomplete, and further studies of the mechanisms by which OXPHOS leads to mitophagy are necessary.

Mitochondrial DNA

In the 1970s, Dr. Lynn Margulis proposed that mitochondria originated as endosymbionts - prokaryotic cells engulfed by a host cell, and maintained for their ability to undergo aerobic respiration. Consistent with this theory, mitochondria are the only animal organelles that carry their own DNA. The mitochondrial genome (mtDNA) consists of a roughly 16.6 kb double-stranded circular genome, which encodes 13 proteins, all of which are subunits of the respiratory chain complexes. These include seven subunits of complex I, one of complex III, three of complex IV, and two of complex V. mtDNA replicates independently from nuclear DNA, and requires its own mitochondrially-targeted machinery for this process. mtDNA also codes for 22 tRNAs and two rRNAs that

are required for mitochondrial protein synthesis (Reeve et al., 2008). The majority of mitochondrial proteins are encoded by the nuclear DNA, and transported to mitochondria by specialized import machinery described in more detail in the section on PINK1/PARKIN. Each mitochondrion contains one to ten thousand copies of its mtDNA, and these are arranged in nucleoids, a cluster of mtDNAs and proteins involved in replication and transcription. Mitochondria also contain their own DNA repair mechanisms; however, these are poorly understood, and mtDNA is subject to more mutations than nuclear DNA (Wei, 1998). The ROS generated in the mitochondria may contribute to this mtDNA damage. mtDNA is inherited exclusively through the maternal lineage (discussed in more detail in the section on paternal mitochondria), and mtDNA mutations are either inherited or acquired. mtDNA exists at high copy numbers, and this may help reduce the impact of mutations, which may exist in conjunction with wild-type mtDNA in a single mitochondrion. This mixture of mitochondrial haplotypes is known as heteroplasmy (Dimauro and Davidzon, 2005; Trifunovic and Larsson, 2008). Mitochondria reproduce by clonal expansion, and mtDNA is provided to daughter mitochondria by replication. Mitochondrial dysfunction can result when a certain threshold of mutant mtDNA is reached and usually manifests as defective OXPHOS (Rossignol et al., 2003). OXPHOS deficiency is particularly damaging for highly active cells that are dependent on ATP production, such as neurons, and skeletal and cardiac muscle cells. Thus mtDNA mutations are associated with encephalomyopathies, and neuromuscular disorders (Schapira, 2006). Additionally, the frequency of mtDNA mutations increases with age (Khrapko

and Vijg, 2009; Trifunovic and Larsson, 2008). Consistent with the deleterious effects of mtDNA mutations, recent evidence suggests that under conditions of heteroplasmy, mitophagy may be particularly important to remove dysfunctional organelles and reduce mutational burden (Dai et al., 2014).

Mitochondrial Dynamics

Mitochondria can take a vast array of shapes and sizes. In mouse embryonic fibroblast cells (MEFs) mitochondria usually exist as tubules of varying lengths. A variety of stressors, including temperature shock, and protonophore treatment, induce these mitochondria to fragment, forming the compact spherical organelles that are the classic textbook representation of mitochondria. Under conditions that favor aerobic respiration, these same mitochondria fuse and elongate to form a long tubular network. These morphology changes can occur as a part of normal physiology. In mouse oocytes and early embryos, mitochondria begin as compact, spherical organelles, and ultimately they elongate to form short tubules. Similarly, mitochondria in apoptotic cells are fragmented, while mitochondria from cells in the G1-S phase of the cell cycle exhibit elongated mitochondria (Barsoum et al., 2006; Jagasia et al., 2005; Mitra et al., 2009).

These striking changes in morphology are due to the coordination of two opposing processes: fusion and fission of mitochondria (Detmer and Chan, 2007; Hoppins et al., 2007). These two processes are believed to strike a delicate balance in order to maintain healthy mitochondrial morphology and segregate

dysfunctional mitochondria from the rest of the network (Chen and Chan, 2009; Jezek and Plecita-Hlavata, 2009). In fact, our lab has recently shown that lethality due to defective mitochondrial fusion in mice can be rescued by an additional loss of mitochondrial fission (Chen et al., 2015).

Mitochondrial Fusion

Fusion is the process by which mitochondria join together forming filamentous networks. Mitochondria are composed of an outer and an inner membrane with an inter-membrane space between the two, and a matrix compartment within the inner membrane. Fusion of two mitochondria requires the junction of both the outer and the inner membranes, respectively. Therefore, the fusion process actually occurs as two separate fusion events, outer membrane fusion and inner membrane fusion, and each relies on dynamin-related large GTPase proteins. Mitofusin 1 and 2 (MFN1 and MFN2, Fzo1 in yeast) are together required for outer membrane fusion (Koshiba et al., 2004; Meeusen et al., 2004). The MFNs are anchored to the outer mitochondrial membrane by two transmembrane domains such that both their N and C termini are exposed to the cytoplasm. MFN1 and MFN2 contain two 4,3 hydrophobic heptad repeat motifs, and the anti-parallel coiled coil interaction of the second of these domains on opposing mitofusins tethers the outer membranes of opposing mitochondria together during fusion (Koshiba et al., 2004). Homo- and heterotypic interactions between MFN1 and MFN2 have been observed (Chen et al., 2003; Rojo et al., 2002), but in vitro, at least, the latter are more efficient (Hoppins et al., 2011).

While normally coupled to outer membrane fusion, inner membrane fusion is mediated by a distinct GTPase, Optic atrophy protein 1 (OPA1 or Mgm1 in yeast) (Chen et al., 2005; Cipolat et al., 2004; Griparic et al., 2004; Meeusen et al., 2006; Olichon et al., 2003; Song et al., 2007; Song et al., 2009), and can be decoupled from outer membrane fusion. OPA1 is anchored to the inner membrane by a single transmembrane domain, and its C-terminus is exposed to the inter-membrane space. In the absence of OPA1, fusion intermediates are observed that have distinct matrix units surrounded by a fused outer membrane, suggesting that inner and outer membrane fusion are truly distinct processes (Hoppins et al., 2007; Song et al., 2009). OPA1 exists as a mixture of isoforms resulting from differential RNA splicing and proteolytic processing. Long isoforms contain the transmembrane domain whereas short isoforms do not (Chan, 2012; Delettre et al., 2001). Debate still exists as to which isoforms of OPA1 are minimally sufficient to undergo fusion. It was discovered that re-expression of either short isoforms or non-cleavable long isoforms of OPA1 in OPA1-null cells failed to rescue inner membrane fusion, whereas expression of a single cleavable long isoform was sufficient to reconstitute this process, suggesting that both long and short isoforms or the act of cleavage itself is required for inner membrane fusion (Song et al., 2007). However, other studies have shown that un-cleavable long-form OPA1 is sufficient for fusion (Tondera et al., 2009), or that short-form OPA1 is actually involved in fission (Anand et al., 2014). A recent study in our laboratory suggests that long forms of OPA1 interact between opposing inner

membranes, while cleavage to short form dissolves this complex, thus facilitating fusion (Mishra et al., 2014). This matter remains open to further study.

Mitochondrial fusion is the key process underlying mitochondrial morphology (Chen et al., 2003); however, it also plays a role in maintaining mitochondrial function and mtDNA stability, and is thought to protect the functional status of the mitochondrial population by facilitating content mixing amongst mitochondria (Chen et al., 2007; Chen et al., 2010; Detmer and Chan, 2007). Inner membrane fusion is exquisitely sensitive to mitochondrial energetic status. Loss of mitochondrial membrane potential ($\Delta\Psi_m$) by protonophore treatment reduces mitochondrial fusion and induces proteolytic cleavage of OPA1 (Chen et al., 2007; Duvezin-Caubet et al., 2006; Griparic et al., 2007; Ishihara et al., 2006; Song et al., 2007). It is speculated that this reduced fusion helps segregate dysfunctional mitochondria for degradation by mitophagy. Additionally, under endogenous conditions, mitochondrial fusion shows a selective preference for fusion between mitochondria with intact $\Delta\Psi_m$, suggesting that fusion may be a mechanism for separating active and inactive mitochondria for the same purpose. Conversely, high levels of mitochondrial fusion proteins reduce mitophagy (Twig et al., 2008). Work from our lab has shown that cells lacking mitochondrial fusion due to loss of MFN1 and MFN2 (MFN-null) have fragmented mitochondria as well as severe defects in respiratory capacity, cell growth rate, and $\Delta\Psi_m$ (Chen et al., 2005). In these cells, the fragmented mitochondria become functionally heterogeneous, with widely divergent $\Delta\Psi_m$, protein levels, and mtDNA levels and mutation load. In mice, this dysfunction has

severe consequences. Loss of fusion proteins in all tissues is lethal, and loss of fusion exclusively in muscle cells results in a lethal mitochondrial myopathy (Chen et al., 2010). The fate of the dysfunctional mitochondria in MFN-null cells is unknown; however, recent evidence from our lab and others suggests that mitophagy may be upregulated in the absence of fusion (Narendra et al., 2008). Hence mitochondrial fusion may be viewed as a key mechanism for maintaining a healthy mitochondrial network and preventing mitochondrial degradation (Twig et al., 2008).

Mitochondrial Fission

Mitochondrial fission is an equally important mechanism for maintaining the integrity of the mitochondrial network. Fission itself is mediated by dynamin-related protein (DRP1) (Smirnova et al., 2001). DRP1 is a cytosolic protein that must be recruited to mitochondria in order to facilitate division. A number of resident mitochondrial proteins can act as DRP1 recruitment factors and the varying roles of each is still under investigation. These include mitochondrial fission 1 (FIS1), mitochondrial fission factor (MFF), and mitochondrial dynamics protein 49 and 51 (MID49, MID51). Overexpression of these proteins increases DRP1 localization to the mitochondria (Gandre-Babbe and van der Bliek, 2008; James et al., 2003; Otera et al., 2010a; Palmer et al., 2011; Yoon et al., 2003; Zhao et al., 2011). While FIS1 and MFF promote fission of mitochondria by DRP1, MID49 and MID51 reduce this activity by sequestering DRP1 (Dikov and Reichert, 2011; Palmer et al., 2011; Zhao et al., 2011). Interestingly, recent work

by our lab suggests that the suppression of fission by MID51 is dependent on nucleotide availability. When mitochondria are uncoupled with protonophore, carbonyl cyanide m-chlorophenylhydrazone (CCCP) or respiration is inhibited with complex III inhibitor, Antimycin A, and ADP is provided and MID51 stimulates DRP1 oligomerization and fission (Loson et al., 2014).

Like mitochondrial fusion, fission also plays a role in quality control of mitochondria. Fission generates two daughter mitochondria, and in so doing segregates functional contents into one daughter, and dysfunctional contents into the other, generating one hyperpolarized, healthy daughter, and one depolarized, dysfunctional daughter (Twig et al., 2008). In the latter, OPA1 and MFN levels are reduced, preventing the dysfunctional mitochondrion from fusing with healthy mitochondria within the cell. Instead, the damaged mitochondrion can now be selectively degraded by mitophagy. Indeed it is hypothesized that mitochondrial fission may be essential for mitophagy progression, as small fragmented mitochondria may be required in order for the phagophore to engulf the organelle.

Mitophagy

As illustrated above, mitochondrial physiology is complex and dynamic. Changes in respiratory state and morphology as well as mutations to mtDNA can drastically change the fitness of the mitochondrial population. Mitophagy is one of the primary means of responding to these changes in fitness. It enables dysfunctional mitochondria to be selectively degraded, preventing them from fusing with functional mitochondria in the cell, and reducing the impact of

damaging ROS they might produce. Mitophagy has been observed in a variety of different cellular contexts, including, but not limited to nutrient starvation, mitochondrial depolarization (due to physiologic or pharmacologic causes), increased OXPHOS, reduced fusion, erythrocyte differentiation, heteroplasmy, hypoxia, and fertilization. As more research is dedicated to this topic, this list continues to grow. Our understanding of the molecular mechanisms of mitophagy is in its infancy; however, new players in this process continue to be uncovered, and further studies will likely clarify what features are shared amongst these different forms of mitophagy, and which are unique. In the next section, we will begin by discussing the general process of macroautophagy, as the core components are utilized in the final stages of mitophagy. Then we will discuss the current understanding of the mechanisms by which mitophagy can be induced, and how these may interface with the core autophagy machinery.

Macroautophagy

Autophagy means "self-eating" and is a general mechanism for the degradation of cellular components by the lysosome. Autophagy can be divided into three classes: microautophagy, chaperone-mediated autophagy, and macroautophagy. The main distinction between the three lies in the mechanism by which contents arrive in the lysosome. Microautophagy involves the direct invagination of the lysosomal membrane and random incorporation of cytoplasmic material (Mijaljica et al., 2011). Chaperone-mediated autophagy is the pathway through which individual proteins containing a KFERQ-like

pentapeptide motif are transported across the lysosomal membrane by the cytosolic chaperone heat shock cognate 70 kDa protein (HSC70) and the lysosomal-associated membrane protein 2A (LAMP2A) (Kaushik and Cuervo, 2008). Macroautophagy is the most morphologically distinct and best-studied pathway, in which specialized autophagosomal vesicles first engulf cargo and subsequently fuse with lysosomes. Hereafter macroautophagy will be referred to as autophagy.

Autophagy Discovery

Autophagy was first identified by electron microscopy. In characterizing developing kidney cells, Clark noted mitochondria within the degradative vesicles of brush border cells (Clark, 1957). Subsequently, Ashford and Porter found that perfusion of rat livers with glucagon induced an accumulation of lysosomes, almost all of which contained mitochondrial remnants (Ashford and Porter, 1962). Mechanistic studies revealed that during macroautophagy, double-membrane-compartments formed around and sequestered cytoplasmic material. They were subsequently observed to acidify and display characteristics of lysosomes (Deter et al., 1967). These compartments are now called autophagosomes. Further immunoelectron microscopy studies identified the endoplasmic reticulum as the site of origin of autophagosomal membranes (Dunn, 1990); however, this model is still contested, and many alternative hypotheses exist, including the recent suggestion that under starvation conditions the mitochondria may be the source of autophagosomal lipids (Hailey et al., 2010).

Detailed genetic dissection of autophagy became possible with the discovery of the autophagy pathway in yeast in the early 1990s. When yeast cells were transferred to starvation media, autophagic bodies were observed to accumulate in the central vacuole. These vesicles contained cytoplasmic ribosomes, endoplasmic reticulum, and mitochondria, making them analogous to the autophagosomes observed in mammalian cells (Takeshige et al., 1992). The autophagy mutants identified in yeast are now referred to as the APG mutants (ATG in mammalian cells) (Thumm et al., 1994).

The first mutant identified was *apg1*, in which nitrogen starvation in the presence of the protease inhibitor PMSF was lethal (Tsukada and Ohsumi, 1993). This enabled rapid screening, and the isolation of 16 complementation groups of apg mutants. Using an immunofluorescence assay for uptake of fatty acid synthetase into the vacuole, an independent group identified the same mutants, which they named *aut* mutants (Thumm et al., 1994). It is now appreciated that there are more than 30 autophagy genes. Of these, ATG1-10, 12-14, 16-18, 29, and 31 are essential for autophagosome formation (Nakatogawa et al., 2009). The proteins encoded by these genes can be functionally subdivided into six classes: the serine/threonine kinase, ATG1 (ULK1/2 in mammals), and its regulatory proteins, the PI3 Kinase complex, the transmembrane protein ATG9, the ATG2-ATG18 complex, and two ubiquitin-like conjugation systems.

Autophagy Mechanism

Autophagy begins with a degradation cue, such as ubiquitination of a substrate. Typically, when four or more ubiquitin molecules are linked by their K48 residues, they are recognized by the 19S proteasomal subunits and degraded by the proteasome (Elsasser and Finley, 2005). Ubiquitin chains with K63 or K27 linkeages serve as signals for degradation by autophagy (Kraft et al., 2010). Evidence for the involvement of ubiquitin in autophagy is still emerging. A direct demonstration of this is that artificial substrates with ubiquitin chains can be recognized by the autophagy machinery and degraded in lysosomes (Kim et al., 2008) A more indirect proof is that the degradation of excess ribosomes during nutrient starvation depends on the deubiquitinating enzyme UBP3/BRE5 (Kraft et al., 2008). Additionally, there may be other signals not yet appreciated, as ubiquitin independent mechanisms have been proposed. The ubiquitin-chains, and possibly other signals, are recognized by autophagy receptor proteins that can be broad or selective in scope. These receptors are generally believed to bind directly to core autophagy machinery at the isolation membrane. An autophagosome is formed around the substrate, and in mammals subsequently fuses with an endosome to generate an amphisome (in yeast, this step is skipped). The amphisome then fuses with the lysosome to form an autolysosome. Once the amphisome and lysosome fuse, the contents as well as the inner membrane of the autophagosome are subject to degradation (Armstrong and Hart, 1971; Baba et al., 1995; Tooze, 2013).

Here we will briefly discuss the signaling mechanism in starvation-induced autophagy and the biogenesis of the autophagosome, reserving a detailed discussion of signaling mechanisms to mitophagy specifically.

AMPK and mTOR signaling in Starvation-induced Autophagy

The first and best-understood pathway for autophagy induction is nutrient starvation. Starvation upregulates bulk autophagy in all organisms studied to date. The details of its signaling mechanism are still a topic of much investigation, but several key players are well established. UNC51-like kinase 1 (ULK1) must be phosphorylated in order to begin the "initiation" step of autophagy described below. Two kinases are known to regulate ULK1 phosphorylation, 5' AMP-activated protein kinase (AMPK), and mammalian target of Rapamycin (mTOR). AMPK is a sensor of cellular ATP levels, and its role in autophagy is dependent on glucose availability. The first illustration that AMPK directly impacts the autophagy pathway showed that under glucose starvation conditions AMPK has an activating effect on ULK1. A dominant-negative kinase-dead mutant of AMPK suppresses ULK1 autophosphorylation and wild type AMPK binds to ULK1, phosphorylates it at serine 317 and 777, and is sufficient to induce its autophosphorylation in vitro (Kim et al., 2011). ULK1 has been shown to be required for mitophagy caused by hypoxia or mitochondrial uncouplers; however, its role in other mitophagy systems has not been addressed (Wu et al., 2014).

The role of mTOR, on the other hand, seems to be primarily in sensing amino acid levels. Under normal conditions, mTOR inhibits autophagy (Galluzzi

et al., 2014; Jung et al., 2010; Sengupta et al., 2010) and is itself strongly inhibited during amino acid starvation. Rapamycin, the mTOR inhibitor for which it is named, robustly induces autophagy even when nutrients are available (Noda and Ohsumi, 1998). mTOR forms two complexes, TOR complex 1 (TORC1) and TOR complex 2 (TORC2). TORC1 inhibits autophagy across model systems (Blommaart et al., 1995; Diaz-Troya et al., 2008; Noda and Ohsumi, 1998; Ravikumar et al., 2004; Scott et al., 2004). TORC1 was found to directly phosphorylate ULK1 on serine 757, a site distinct from ULK1 autophosphorylation. This phosphorylation disrupts the interaction between ULK1 and AMPK (Kim et al., 2011). Furthermore, in yeast, TORC1 was shown to directly hyperphosphorylate ATG13, preventing its interaction with ULK1-homologue, ATG1, and thereby inhibiting autophagy induction (Kamada et al., 2010). The integration of AMPK and mTOR signals is complex and beyond the scope of this work, but both serve as a gateway to the next step in the pathway: autophagosome biogenesis.

Autophagosome Biogenesis

Autophagosome biogenesis roughly follows the stages outlined in Figure 1.1, initiation, nucleation, and expansion. Upon activation of autophagy, a majority of ATG proteins accumulate at the pre-autophagosomal structure (PAS), which in yeast is a single punctate structure closely apposed to the vacuole. In mammalian cells, a similar structure may be found on the endoplasmic reticulum, called the omegasome (Itakura and Mizushima, 2010), but this remains to be

conclusively proven. At the PAS, proteins of the UNC51-like kinase (ULK) complex (ULK1, ULK2, ATG13, FAK family kinase interacting protein of 200 kDa (FIP200) and ATG101) begin to form the isolation membrane (Lamb et al., 2013). Now, a local pool of phosphatidylinositol 3-phosphate (PI3P) is formed when the activated ULK complex in turn activates a class III PI3K complex containing beclin 1 (ATG6 in yeast), vacuolar protein sorting 15 (VPS15), VPS34, and ATG14 (which, in mammals, may also be involved in fusion of the autophagosome to the late endosome) (Diao et al., 2015). Additionally, ATG9 transmembrane protein helps traffic source membrane for phagophore elongation. Finally, a complex consisting of ATG5, ATG12, and ATG16 is recruited and it modifies microtubule-associated protein 1 light chain 3 (MAP1LC3, or just LC3, and ATG8 in yeast) by lipidation with phosphatidylethanolamine (PE). This allows LC3 to associate with the autophagosomal membrane, which is essential for autophagy progression.

LC3, its processing, and function

It is worth discussing LC3 in more detail, as it and its modifying proteins are essential for autophagy and it is used as a marker of autophagosomes in this work, as well as many others. The first mammalian ATG8 protein to be identified was LC3B, and was initially found associated with microtubule-associated proteins (MAPs) 1A and 1B (Kuznetsov and Gelfand, 1987). It was much later that its role in autophagy was identified (Kabeya et al., 2000). In humans there are actually two subfamilies of ATG8-like proteins: the LC3 family and the

GABARAP family. The former consists of two splice variants of LC3A, LC3B, LC3B2 and LC3C, and the latter of GABARAP, GABARAPL1/GEC1, GABARAPL2/GATE-16, and GABARAPL3. All are ubiquitously expressed, but LC3B is the most commonly used for the study of autophagy. ATG8-like proteins share a common processing mechanism, which we will discuss in the context of the LC3 family (Shpilka et al., 2011).

LC3 proteins are synthesized as precursor proteins and are proteolytically cleaved by ATG4 to reveal a conserved terminal glycine residue. This truncated form of the protein is called LC3-I, and is unable to associate with autophagosomes until it is lipidated in an ubiquitin-like conjugation pathway. Ubiqutitin-like modifier-activating enzyme ATG7 is an E1-like protein that activates ATG12 for its conjugation with ATG5 and ATG8 for its conjugation with PE. Ubiquitin-like conjugating enzyme ATG3 is an E2-like protein that in conjunction with the E3-like ATG12-ATG5-ATG16 complex covalently links PE to ATG8 (Ichimura et al., 2000; Tanida et al., 2003). This phospholipid conjugated ATG8, which runs as a faster migrating band on a denaturing polyacrylamide gel, is called LC3-II, and can be cleaved again by ATG4 to reverse the lipidation (Kabeya et al., 2004; Kirisako et al., 2000).

Yeast ATG8 has no paralogues, and hence its essential role in autophagy was easily identified (Lang et al., 1998). By contrast, the redundancy within the mammalian system made this less obvious. More recent studies of ATG3 knockout mice and cultured cells overexpressing a dominant-negative mutant of ATG4 have clarified that LC3 lipidation is essential for autophagy. ATG3

knockout mice exhibit a complete loss of LC3 conjugate formation, and electron microscopy shows aberrant isolation membranes that fail to close (Sou et al., 2008). Furthermore, loss of ATG3 in mice is lethal at 1 day after birth, consistent with other studies showing a necessary burst of autophagy during the neonatal starvation period (Kuma et al., 2004). Dominant-negative ATG4 sequesters free LC3 and shows similar open isolation membranes as in ATG3-knockout mice as well as accumulation of LC3 due to lack of degradation in autophagosomes (Fujita et al., 2008).

Historically, assessment of autophagy *in vivo* required electron microscopy, but more recently a variety of tools for probing autophagy have been developed. Although its precise function in autophagy is still unknown, LC3 was proposed as a good marker for monitoring autophagy. It is present exclusively on isolation membranes, autophagosomes, and to a lesser extent, autolysosomes, and unlike proteins upstream in the biogenesis pathway it does not dissociate from the isolation membrane when autophagosome biogenesis is complete, but instead remains on the membrane even after fusion with lysosomes (at which point the it becomes more dilute, and hence less easily detected) (Kabeya et al., 2000). For these reasons GFP-LC3 transgenic mice were generated which demonstrated that imaging of LC3 in tissues did not interfere with endogenous autophagic processes and could be used to indicate the distribution of autophagosomes in the cell (Mizushima et al., 2004).

Autophagy Adaptors

Selective autophagy, such as mitophagy, often utilizes receptors that physically link labeled substrates with the canonical autophagy activation machinery. However, the mechanism of this interaction is still unclear, as direct binding to LC3 has been shown to be insufficient to recruit the phagophore in some cases (Itakura and Mizushima, 2011b). A class of adaptor proteins has been proposed which interact directly with ULK1. These include ATG11 in yeast, and Huntingtin (HTT) in *Drosophila* and mammals (Kamber et al., 2015; Rui et al., 2015), forming a bridge between substrate receptors and the isolation membrane components. These adaptors may have regulatory roles as well, activating the autophagy machinery to localize isolation membrane formation to the areas of substrate availability. However, non-canonical autophagy pathways also exist which do not involve ULK1 or other core autophagy genes, and are indicative of how much more we have yet to understand about this topic.

Mitophagy Machinery

PINK/PARKIN Pathway

The PINK1/PARKIN pathway of mitochondrial degradation is the best characterized form of mitophagy, and mounting evidence suggests that it is probably active in a number of different mitophagy contexts. The proteins involved in this pathway were first identified as genes mutated in familial forms of Parkinson's disease (PD). PD is a neurodegenerative disorder characterized by stereotypic motor symptoms, including bradykinesia, hypokinesia, cogwheel rigidity, resting tremor, and postural instability, and is the most common

movement disorder, and the second most common neurodegenerative disorder (Winklhofer and Haass, 2010). In PD, Loss of dopaminergic neurons in the substantia nigra pars compacta (SNPC) leads to a dopamine deficiency in the striatum, and the consequent dysregulation of basal ganglia circuitries underlies the motor symptoms. The disease can be sporadic or genetic in cause, and both forms exhibit loss of dopaminergic neurons in the SNPC; however, sporadic PD exhibits proteinaceous deposits within neuronal cell bodies (Lewy bodies) and processes (Lewy neurites), a characteristic observed much less frequently in genetic disease (Spillantini et al., 1997). Therefore, there may be both common and distinct mechanisms of cell damage in the two forms of PD.

Sporadic PD is the most common form, and can be due to environmental (including pesticide exposure) or genetic factors. Little is known about the specific etiology of the disease and the pathogenesis is likely complex; however, identification of genes responsible for more rare familial forms of PD opened the field for more in depth research. Among these are autosomal dominant mutations in the gene encoding α-synuclein and leucine-rich repeat kinase 2 (LRRK2), and recessive mutations in the genes encoding parkin RBR E3 ubiquitin protein ligase (PARKIN), PTEN-induced putative kinase 1 (PINK1), protein deglycase DJ-1 (DJ-1), and ATPase 13A2 (ATP13A2) (Di Fonzo et al., 2007; Ramirez et al., 2006; Winklhofer and Haass, 2010).

Mounting evidence suggests that mitochondrial dysfunction may be at the center of PD pathogenesis. In the late 1970s and early 1980s two separate reports were made of young drug addicts having developed Parkinsonism after

intravenous injection of a toxic byproduct of opioid synthesis. In both cases the neurotoxic compound was 1-methyl-4-phenyl-1,2,3,6-tetrahydropyridine (MPTP). Treatment with dopaminergic agents alleviated symptoms, and necropsy indicated damage to the SNPC without evidence of Lewy bodies (Davis et al., 1979; Langston et al., 1983). This finding is consistent with the degenerative pattern observed in non-human primates treated with MPTP (Forno et al., 1993; Hantraye et al., 1993; Moratalla et al., 1992; Varastet et al., 1994). The effects of dopamine agonist therapy in MPTP model systems and sporadic PD are similar, making it a common model for PD in laboratory studies, including in mice, where it has a similar, albeit milder effect (Betarbet et al., 2002).

Studies of the molecular mechanism of MPTP-toxicity showed that a metabolite of MPTP, MPP^+ concentrates in the mitochondria of neurons and inhibits Complex I causing ROS accumulation (Chan et al., 1991; Dreschel and Granger, 2009; Fabre et al., 1999; Hantraye et al., 1996; Hasegawa et al., 1990; Nicklas et al., 1985; Pennathur et al., 1999; Przedborski et al., 1996; Ramsay et al., 1986). Complex I dysfunction is also observed in post-mortem SNPD of sporadic PD patients (Janetzky et al., 1994) and subunits of complex I from frontal cortex mitochondria were found to be oxidatively damaged in autopsied patients with PD (Keeney et al., 2006) consistent with complex I dysfunction. Furthermore, rotenone, another inhibitor of complex I, induces α-synuclein-rich inclusion bodies like those observed in sporadic PD (Betarbet et al., 2000). Thus, evidence suggests that aberrant Complex I activity, and ROS may play a role in PD pathogenesis.

The etiology of mitochondrial dysfunction in sporadic PD is unclear, but some evidence points to elevated mtDNA mutation burden. Analysis of mtDNA in neurons from patients with PD showed higher levels of mtDNA deletions specifically in substantia nigra neurons than in age-matched controls (Bender et al., 2006). Additionally patients with rare mutations in mtDNA replication machinery, such as in the mtDNA polymerase POLG, or helicase Twinkle, exhibit parkinsonism (Baloh et al., 2007; Luoma et al., 2004), and variants in the POLG CAG-repeat region may predispose for sporadic PD (Luoma et al., 2007). There is no clear evidence that mtDNA mutations are actually causative of PD, they may instead occur as a result of increased cellular stress. Nonetheless, evidence is clear that mitochondrial dysfunction is sufficient to cause Parkinsonism across species and is associated with sporadic PD in patients.

Familial variants of PD are essentially clinically indistinguishable from sporadic PD other than early onset and slower progression (Bonifati, 2007), and interestingly, current knowledge of the biology of PD related genes is consistent with the mitochondrial dysfunction, oxidative stress, and protein aggregopathy observed in sporadic PD. Mutations in PARKIN and PINK1 are the most common cause of autosomal recessive Parkinsonism (Valente et al., 2004). The first evidence that PARKIN and PINK1 operate as part of the same pathway came from drosophila. Deletion dParkin or dPink1 led to the same phenotypes: muscle degeneration, disrupted spermatogenesis, and loss of dopaminergic neurons. Conversely, overexpression of dParkin in the dPink1 null flies could partially rescue the defects, whereas overexpression of dPink1 in a dParkin null

background could not, suggesting that dPink1 functions upstream of dParkin. Swollen and fragmented mitochondria could be observed in the flight muscles of the mutant flies early in the disease progression, consistent with a role for mitochondria in onset of the pathology (Clark et al., 2006; Greene et al., 2003; Park et al., 2006; Whitworth et al., 2005; Yang et al., 2006). Oxidative stress was proposed as a root cause of the defects, as overexpression of glutathione *S*-transferase could rescue dopaminergic neuron loss (Whitworth et al., 2005). In mice, loss of PARKIN or PINK1 also results in a common phenotype with mitochondrial and nigrostriatal dysfunction (Gautier et al., 2008; Kitada et al., 2009; Palacino et al., 2004).

PARKIN is a cytosolic E3 ubiquitin ligase, which is recruited to defective mitochondria and activated specifically upon mitochondrial depolarization (Narendra et al., 2008). How mitochondrial dysfunction signals to PARKIN was recently uncovered, and involves an elegant cascade of proteolytic processing of the mitochondrial resident protein, PINK1. PINK1 is a serine/threonine kinase with an N terminal mitochondrial targeting signal (MTS). The majority of PINK1 mutations found in PD impair the kinase activity, suggesting that this function might be important in maintenance of mitochondrial function (Silvestri et al., 2005; Valente et al., 2004; Zhou et al., 2008). A series of papers by Narendra et al. and others characterized the mechanism by which PINK1 recruits PARKIN selectively to depolarized mitochondria (Figure 1.2). By monitoring PINK1-YFP accumulation on mitochondria after treatment with CCCP, Narendra et al. found that full-length PINK1 accumulates on mitochondria within five minutes of

depolarization. When MFN-null MEFs, which have heterogeneous $\Delta\Psi_m$, were transfected with PINK1-YFP, the investigators found that PINK1 selectively labeled depolarized mitochondria. They further observed that PARKIN recruitment to depolarized mitochondria was dependent on PINK1 localization to mitochondria. No PARKIN localization was observed in PINK-null MEFs and this localization could be rescued by expression of exogenous PINK1 but not PINK1 lacking its N-terminal MTS (Narendra et al., 2010b). Ectopic PARKIN had been previously shown to induce mitophagy of depolarized mitochondria (Narendra et al., 2008), and with 24 hour treatment with CCCP loss of mitochondria could be quantified in WT MEFs. This loss was only achieved in PINK1-null MEFs with exogenous expression of PINK1 (Narendra et al., 2010b). Taken together, these results suggest that PINK1 is responsible for PARKIN recruitment to mitochondria. The selective recruitment of PARKIN to depolarized mitochondria was explained by biochemical analysis of PINK1 post-translational processing. Full-length PINK1, which is a 63 kDa protein anchored in the outer mitochondrial membrane, is cleaved to a 52 kDa cytosolic fragment that can be degraded by the proteome (Lin and Kang, 2008). Narendra et al. showed that in the presence of CCCP, levels of full-length PINK1 rise, whereas after CCCP is washed-out, levels of full-length PINK1 fall. In the presence of an ubiquitin proteasome system (UPS) inhibitor, MG132, levels of the 52 kDa short form of PINK1 rise, suggesting that this cleaved form is unstable under normal conditions (Lin and Kang, 2008; Narendra et al., 2010b). This data supports the model that PINK1 is cleaved and subsequently degraded under basal conditions. In the

setting of mitochondrial damage, however, full-length PINK1 is stabilized and able to recruit PARKIN, leading to degradation (Figure 1.2).

Work by several other groups further detailed the proteolytic mechanism by which PINK1 serves as a signal of mitochondrial dysfunction. Under basal conditions, PINK1 is imported through the outer mitochondrial membrane (OMM) by the translocase of the outer membrane (TOM) complex and fed through the inner mitochondrial membrane (IMM) in the translocase of the inner membrane (TIM) complex, where it is first cleaved, as are most imported proteins, by the mitochondrial processing peptidase (MPP) (Greene et al., 2012). PINK1 is cleaved a second time by the rhomboid protease, presenilin-associated rhomboid-like protein (PARL) between amino acids A103 and F104 in its hydrophobic domain, which spans the IMM (Deas et al., 2011; Jin et al., 2010; Meissner et al., 2011). This cleavage product is the 52 kDa form of PINK1 that escapes to the cytosol where its N-terminal phenylananine is recognized by the N-degron type 2 E3 ubiquitin ligases and degraded by the UPS (Yamano and Youle, 2013). Thus, under basal conditions, very little PINK1 is detectable on mitochondria. However, stressors including mitochondrial depolarizing agents, OXPHOS inhibitors, genetic or environmental stress, or unfolded proteins prevent import of proteins through the TIM complex, and hence processing of PINK1 is blocked, since it never reaches the IMM where PARL and MPP reside. Full-length PINK1 accumulates, bound to the Tomm7 subunit of the TOM complex, which has been suggested to be involved in releasing OMM proteins laterally into the OMM (Hasson et al., 2013; Lazarou et al., 2012; Okatsu et al., 2013). Indeed,

PINK1 contains a second, weaker targeting signal that directs it to the OMM (Zhou et al., 2008) and it may be by this domain that PINK1 is stabilized there. Alternatively, the association of PINK1 with the TOM complex might facilitate re-import and degradation should mitochondrial $\Delta\Psi_m$ be restored. Making PINK1 a switch turning mitochondrial degradation on or off (Lazarou et al., 2012).

Many mitochondrial stressors result in loss of $\Delta\Psi_m$, and this may be a unifying mechanism for translation mitochondrial damage into targeted degradation. Mechanisms may exist, however, for degradation of mitochondria that do not involve depolarization. One such mechanism involves unfolded proteins in the mitochondrial matrix. In two recent papers, an unfolded protein expressed in the matrix stabilized PINK1 at the OMM and activated PARKIN without membrane depolarization (Jin and Youle, 2013). Accumulation of further unfolded protein by reduction in Lon protease, a matrix protease known to degrade unfolded proteins, further increased PINK1 accumulation (Jin and Youle, 2013). Similar experiments were performed in Drosophila where knockdown of LON protease also resulted in an increase in PINK1 on mitochondria (Thomas et al., 2014). However, differential sedimentation generating mitochondrial and postmitochondrial fractions from lysates of LON knockdown flies showed an accumulation of all processed forms of PINK1 in primarily the mitochondrial but also the postmitochondrial fractions. In contrast to the results in MEFs, this data suggests that LON might promote PINK1 degradation in the matrix, a confounding finding in light of previous work, suggesting that PINK1 processed by PARL is primarily degraded in the cytoplasm (Yamano and Youle, 2013). The precise mechanism for PINK1 accumulation on

mitochondria due to unfolded mitochondrial proteins is still unknown, but in broad strokes it is clear that in both Drosophila and mammals mitochondrial damage results in PINK1 stabilization on the OMM and PARKIN activation (Pickrell and Youle, 2015). Until recently, it remained unknown how PINK1 recruits PARKIN to mitochondria and how PARKIN is activated. Co-immunoprecipitation experiments suggest that PINK1 and PARKIN directly bind one another (Sha et al., 2010; Xiong et al., 2009), however PINK1 and PARKIN appear predominantly in complexes of different sizes by size exclusion chromatography and native PAGE (Lazarou et al., 2012; Thomas et al., 2011). Interestingly, ectopic expression of PINK1 on peroxisomes can recruit PARKIN to that organelle and induce pexophagy (Lazarou et al., 2012) suggesting that the substrate of Pink1 kinase activity is not specific to mitochondria. PINK1 has also been shown to directly phosphorylate PARKIN at a residue within its ubiquitin-like (UBL) domain (S65). This phosphorylation stimulates both PARKIN recruitment to mitochondria and E3 ligase activity (Kondapalli et al., 2012; Shiba-Fukushima et al., 2012). However, this phosphorylation event cannot be the sole mechanism for PINK1 mediated PARKIN recruitment to mitochondria, because mutant forms of PARKIN lacking the UBL domain, or mutated at S65 still translocate to mitochondria in PINK1 dependent manner (Kane et al., 2014). This data was somewhat confounding because it suggested that some other cytosolic substrate must be phosphorylated by PINK1, yet in vitro reconstitution of PARKIN activation could apparently be achieved with PINK1 and PARKIN alone (Lazarou et al., 2013). This conundrum was only resolved by a recent discovery that PINK1 phosphorylates ubiquitin at S65, and this

phospho-ubiquitin activates PARKIN (Kane et al., 2014; Kazlauskaite et al., 2014a; Koyano et al., 2014). This is perhaps not surprising given that the PARKIN UBL domain by its very nature is homologous to ubiquitin (Kondapalli et al., 2012). Several lines of evidence demonstrate that phospho-S65 ubiquitin mediates the activation of PARKIN by PINK1. First, mass spectrometry of PINK1-null cells compared to wild-type cells treated with CCCP showed that phospho-S65 ubiquitin was produced only in wild-type cells (Kane et al., 2014). Similar results were obtained in CCCP-treated cells with overexpression of PINK1 (Kazlauskaite et al., 2014b). In a purified, cell-free system, PINK1 was shown to phosphorylate ubiquitin at S65 (Kazlauskaite et al., 2014b) and PARKIN was shown to bind to phospho-mimetic S65D ubiquitin (Kane et al., 2014). Phospho-ubiquitin could also activate PARKIN's E3 ligase activity in vitro (Kane et al., 2014; Kazlauskaite et al., 2014b) and a phospho-S65 mimetic PARKIN with an S65D mutation displayed greater ubiquitin ligase activity than wild-type PARKIN if it was incubated with phospho-ubiquitin, suggesting that phosphorylation not just of ubiquitin, but also of the PARKIN UBL could activate PARKIN (Kazlauskaite et al., 2014b; Koyano et al., 2014). However, while phospho-mimetic S65D ubiquitin alone was sufficient to activate PARKIN, phospho-mimetic S65D PARKIN was not active (Kane et al., 2014; Kazlauskaite et al., 2014b). In live cells, replacing ubiquitin with an S65A phospho-incompetent mutant prevented PARKIN translocation to mitochondria (Kane et al., 2014), suggesting that phospho-ubiquitin is required for targeting PARKIN to mitochondria. One theory is that phosphorylation of existing ubiquitin chains on OMM proteins might be the first step in recruiting PARKIN. Consistent

with this, phospho-ubiquitin peptides could be isolated from peptides of OMM proteins by mass spectrometry (Kane et al., 2014). Ordureau et al. suggest a model with an additional role for direct phosphorylation of PARKIN. In this model, phosphorylation of PARKIN by PINK1 may occur first, localizing it to mitochondria and allowing it to begin ubiquitinating substrates, which then serve as the substrates for further phosphorylation by PINK1, and after being phosphorylated, these phospho-ubiquitin chains further accelerate PARKIN activity. In their immunoprecipitation experiments, PARKIN could bind phosphorylated ubiquitin with 21 times higher affinity if was also phosphorylated. Furthermore, it was found that the active site of PARKIN becomes exposed when PARKIN is activated by S65 phosphorylation but not when it is activated by phospho-S65 ubiquitin (Ordureau et al., 2014). This may indicate that PARKIN may first be directly phosphorylated by PINK1 before activation by phospho-S65 ubiquitin. However, in vivo studies in Drosophila indicate that this may not be strictly necessary, since PINK1-null or PARKIN-null flies can be partially rescued even with a phospho-incompetent form of PARKIN (Shiba-Fukushima et al., 2012). It remains unclear whether ubiquitin must be present on mitochondrial proteins to begin with and be phosphorylated by PINK1 in order to recruit PARKIN, or whether phosphorylation of PARKIN itself is enough to begin the process. The source of this ubiquitination, if not PARKIN, is yet unknown.

PINK1 has been shown to phosphorylate other mitochondrial proteins; however, most are unrelated to mitophagy (Plun-Favreau et al., 2007; Pridgeon et al., 2007) and those involved in related processes (transport and dynamics) are not

essential for mitophagy. MIRO1, a protein involved in mitochondrial trafficking on microtubules is phosphorylated by PINK1. This phosphorylation event was suggested to activate PARKIN-mediated proteasomal degradation of MIRO1, and hence arrest mitochondrial motility (Wang et al., 2011), but this result could not be replicated (Kazlauskaite et al., 2014a; Liu et al., 2012b). MFN2 was found to be phosphorylated by PINK1 leading to ubiquitination by PARKIN and degradation (Chen and Dorn, 2013); however, PARKIN translocation cannot be dependent on MFN2 because it proceeds normally in MFN-null cells (Narendra et al., 2008). Interestingly, Mitofusins are ubiquitinated in yeast lacking PINK1 and PARKIN (Neutzner et al., 2008), which is evidence that ubiquitinated proteins may be available on the OMM for PINK1 to phosphorylate prior to PARKIN translocation.

Once on the mitochondria, PARKIN primarily forms K48- and K63-linked ubiquitin chains (Chan et al., 2011). K63-linked ubiquitin chains may be involved autophagy receptor recruitment, including p62 (Geisler et al., 2010; Narendra et al., 2010a; Okatsu et al., 2010; Sims et al., 2012; van Wijk et al., 2012) and NBR1 (van Wijk et al., 2012), discussed below. K48-linked ubiquitin chains probably lead to extraction of proteins from the OMM (called outer mitochondrial membrane -associated degradation or OMMAD) and subsequent proteasomal degradation (Chan et al., 2011; Kim et al., 2013; Yoshii et al., 2011). However, it is not clear what role this may play in mitophagy, as proteasomal activity is necessary for PARKIN-mediated mitophagy (Chan et al., 2011; Tanaka et al., 2010). Given the protective nature of mitochondrial fusion, alteration of the levels of MFN1 and MFN2 by PARKIN ubiquitination and proteasomal degradation

could play a role in accelerating mitophagy (Gegg et al., 2010; Poole et al., 2010; Tanaka et al., 2010; Ziviani et al., 2010). However, 36 OMM proteins have been shown to be ubiquitinated by PARKIN (Sarraf et al., 2013), which may indicate that the chain-linkage type and density of ubiquitin on mitochondria may be more important than the specific substrate.

Other E3 Ligases

There are three recently identified mitochondrial resident E3 ubiquitin ligases that could also facilitate mitophagy. Among these, one paper has proposed the OMM E3 ligase, RNF185, as a regulator of mitophagy (Tang et al., 2011). RNF185 was shown to ubiquitinate BCL family protein, BNIP1, with K63 linkage, allowing it to bind to receptor p62 and recruit autophagosomes. This result has yet to be confirmed. Another OMM E3 ubiquitin ligase, Mulan (MUL1) can compensate for PARKIN activity and can ubiquitinate MFNs independently of PARKIN (Yun et al., 2014b); however, its role in mitophagy is not clear. The third mitochondrial resident E3 ligase is MARCH5, which has been shown to bind FIS1, DRP1, and MFN2, and has been proposed to regulate mitochondrial fission (Karbowski et al., 2007). A possible function in mitophagy remains to be addressed. Another non-mitochondrial E3 ligase has been proposed as a mitophagy player. When overexpressed, the ER resident Glycoprotein 78 (GP78) E3 ligase can induce degradation of mitochondria by autophagy that is PARKIN independent (Fu et al., 2013); however, this experiment was done in the setting of

CCCP treatment, which is non-physiological, so its true role in mitophagy is still tenuous.

Receptors

One common feature of many selective autophagy receptors is a short linear peptide sequence that binds directly to LC3, called the LIR motif (for LC3 interacting region) (Alemu et al., 2012; Birgisdottir et al., 2013; Kalvari et al., 2014). Canonical LIR domains are characterized by a [W/F/Y]XX[L/I/V] sequence (square brackets indicate alternative amino acids, X is any residue), and often follow acidic residues or phosphorylation sites, which exert a regulatory effect on LC3 binding. Selective autophagy receptors can be divided into two broad classes based on their ability to bind ubiquitin (Khaminets et al., 2016). Ubiquitin-dependent autophagy receptors contain ubiquitin-binding domains (UBD) by which they can recognize ubiquitylated substrates and physically link them to the LC3-II coated autophagosome via an LIR motif. However, whether this binding is required for their function is unknown. While the core autophagy machinery has been well conserved over evolution, selective autophagy machinery has expanded to allow for high specificity (Liu et al., 2014). Here we will discuss some of the machinery of the mammalian mitophagy system that is currently appreciated.

Ubiquitin-dependent autophagy/mitophagy Receptors P62 and NBR1

Sequestosome 1 (SQSTM1) or p62 is a selective autophagy receptor with UBD and LIR domains as well as several specific protein interaction domains (Figure 1.3). Originally, p62 was identified as a cargo receptor for the selective removal of misfolded protein aggregates by autophagy (Bjorkoy et al., 2005; Komatsu et al., 2007; Pankiv et al., 2007), but more recently an additional role as a receptor for mitophagy has been elucidated (Geisler et al., 2010). The neighbor of BRCA1 (NBR1) shares sequence similarity with p62 and has a similar function as a receptor in removal of protein aggregates (Kirkin et al., 2009). Although NBR1 has been shown to be involved in pexophagy (Deosaran et al., 2013), and it was found by mass spectrometry on mitochondria undergoing mitophagy (Chan et al., 2011), its role in mitophagy is disputed (Shi et al., 2015). Both receptors are cytosolic under basal conditions, and contain a UBD at their C-terminus, which can bind polyubiquitin (Isogai et al., 2011). The NBR1 ubiquitin-associated (UBA) domain has equal affinity for K63- and K48-linked polyubiquitin chains, whereas, in the context of mitophagy, the p62 UBA domain shows strong preference for K63- and K27-linked polyubiquitin chains (Geisler et al., 2010) and its affinity is increased by phosphorylation at serine 403 (S403), within the UBA (Matsumoto et al., 2011), which is a novel type of autophagy regulation.

In HeLa cells overexpressing wild type PARKIN and treated with CCCP, mitochondria exhibit K63-linked polyubiquitiation (Narendra et al., 2010a) and K27-linked ubiquitination (Geisler et al., 2010). This ubiquitination is dependent on PARKIN function, and can be abolished by overexpression of a ligase-dead PARKIN mutant R275W (Narendra et al., 2010a). Two separate groups of

investigators found that p62 is recruited to mitochondria when mitophagy is induced by mitochondrial depolarization with PARKIN overexpression (Geisler et al., 2010; Narendra et al., 2010a); however, these investigators differ in their interpretation of the role of p62 in mitophagy. By measuring the compaction index of mitochondria (proximity of mitochondria to the nucleus) in wild-type and p62 knockout MEFs, Narendra et al. conclude that P62 mediates the aggregation of mitochondria. However when this group counted the number of cells lacking mitochondria after CCCP treatment, in cells lacking p62 by either genetic knockout or siRNA, they found no difference relative to wild-type cells, indicating that p62 was not required for mitophagy (Narendra et al., 2010a). By contrast, when Geisler et al. performed the same experiment in p62 siRNA treated cells, they found significantly less clearance of mitochondria relative to wild-type cells, indicating that p62 was required for mitophagy (Geisler et al., 2010). Whether p62 is required for mitophagy or only for mitochondrial clustering has yet to be clarified, but in either case, it seems to be targeted to damaged mitochondria that are labeled with specific polyubiquitin chains.

P62 contains an N-terminal PB1 domain which facilitates self-oligomerization as well as binding to many other proteins. This domain is likely the means by which p62 aggregates form (Komatsu et al., 2007; Lamark et al., 2003). It is believed that oligomerization increases the avidity of p62 for LC3B clusters, and it may also facilitate membrane curvature (Wurzer et al., 2015). NBR1 also oligomerizes, but it does so via its coiled-coil domain (CC1) (Kirkin et al., 2009). Hetero-oligomers of p62 and NBR1 as well as oligomers with other

proteins can also form (Lamark et al., 2003). Both receptors also contain LIR domains, which enable degradation of cargo as well as the receptors themselves via autophagy (Ichimura et al., 2008b; Rozenknop et al., 2011). NBR1 contains two LIR domains. The first, located N-terminal to its UBA domain (LIR1) interacts with LC3 and GABARAP subfamily proteins, whereas the more cryptic LIR between the two coiled-coil domains (LIR2) can provide redundant affinity for ATG8-homologues in the absence of LIR1 (Kirkin et al., 2009).

Nix

Nascent reticulocytes contain membrane-bound organelles including golgi, rough endoplasmic reticulum, endocytic vesicles, and mitochondria (Gronowicz et al., 1984; Koury et al., 2005). As they mature, reticulocytes lose all membrane-bound organelles, including mitochondria. NIX/BNIP3L is an outer mitochondrial membrane protein that mediates mitophagy during this maturation process (Sandoval et al., 2008; Schweers et al., 2007). NIX is constitutively targeted to mitochondria by its C-terminal mitochondrial targeting sequence, and its cytosolic N-terminus contains an LIR motif like many autophagy receptors (Novak et al., 2010). Unlike most receptors, however, NIX may actually play a role in triggering mitophagy. A study of reticulocytes in NIX knockout mice showed that mitochondria persisted despite normal clearance of ribosomes, and in the absence of NIX mitochondria failed to colocalize with LC3 by immunostaining, consistent with a role as an LC3-binding receptor. However, flow cytometric analysis of reticulocytes stained with tetramethylrhodamine, ethyl

ester (TMRE), a cell permeant, positively-charged dye that accumulates in mitochondria with intact $\Delta\Psi_m$, showed that whereas wild-type reticulocytes exhibited depolarized mitochondria, mitochondria in NIX knockout reticulocytes maintained $\Delta\Psi_m$, indicating a role for NIX upstream of targeting to the autophagosome. Additionally, with treatment of NIX knockout reticulocytes with carbonyl cyanide *p*-trifluoromethoxyphenylhydrazone (FCCP), a protonophore that abolishes $\Delta\Psi_m$, mitochondria were cleared and could be seen in autophagic vacuoles, suggesting that some other mechanism exists to link defective mitochondria to the autophagosome downstream of NIX (Sandoval et al., 2008). This function places NIX in cooperation with the PINK1/PARKIN pathway of mitophagy, which targets depolarized mitochondria (Ding et al., 2010). In contrast to the role of NIX in erythrocyte maturation, wherein healthy mitochondria are targeted for degradation, the PINK1/PARKIN pathway targets only damaged mitochondria (Narendra et al., 2008).

A new role for NIX was recently discovered in OXPHOS-induced mitophagy. High OXPHOS activity due to replacement of glucose with glutamine in cell culture media, was found to induce mitophagy revealed by a high rate of mitochondrial protein degradation and LC3 accumulation. Levels of the small GTPase, Ras homolog enriched in brain protein (RHEB) were found to increase under these conditions, and overexpression of RHEB could induce mitophagy even under normal growth conditions, consistent with a role for RHEB in triggering mitophagy. This mitophagy was found to be NIX dependent as well. Knockdown of NIX could prevent RHEB induced mitophagy, and a complex was

isolated that contained RHEB, NIX, and LC3. Under these conditions it was proposed that mitophagy enhances the efficiency of OXPHOS by removing damaged mitochondria (Melser et al., 2013). How increased OXPHOS translates to RHEB expression is unknown, and whether this condition also involves the PINK1/PARKIN pathway was not addressed.

Stress induced mitophagy

High OXPHOS activity may qualify as a form of energetic stress, since it demands high respiratory substrate concentrations, and creates elevated levels of ROS. This broader category includes starvation and mitochondrial dysfunction. In starvation, low nutrient availability leads to less ATP generation, whereas with inherent mitochondrial dysfunction, the low ATP generation is due to impaired synthesis. All these energetic stresses regulate mitophagy slightly differently, and although it is likely that they impinge upon the same core processes, a universal mitophagy pathway is yet to be identified. In the case of starvation, while autophagy is increased, as described previously, for the purpose of recycling nutrients, mitophagy is inhibited, probably to retain mitochondria to process the newly generated catabolites. Mitochondria avoid degradation in this case by elongation, sterically hindering engulfment by the autophagosome (Rambold et al., 2011). This is accomplished by inhibitory phosphorylation of DRP1 by Protein kinase A (PKA) due to rising cAMP levels, resulting in inhibition of fission. Mitochondrial dysfunction leading to PINK1/PARKIN activation does the reverse. PINK1 phosphorylation of MFN2 leads to its ubiquitination and

degradation, resulting in mitochondrial fragmentation and mitophagy (Chen and Dorn, 2013). These mechanisms illustrate a common link between energetic stress, mitophagy, and mitochondrial dynamics. Future work may identify a common pathway by which these factors are linked.

Another type of cellular stress that impinges upon mitochondrial respiration is hypoxia. Recently, the OMM protein, FUNDC1, was shown to have mitophagy adaptor function under hypoxia (Liu et al., 2012a). Under normal conditions, FUNDC1 is phosphorylated in its LIR domain, inhibiting interaction with LC3. Hypoxia induces its dephosphorylation and promotes mitophagy, perhaps maintaining the proper stoichiometry of mitochondria given available oxygen. Additionally, expression of the NIX homologue, BNIP3, which also binds LC3, is induced under hypoxia, yet another means for reducing mitochondrial mass in the absence of oxygen (Hanna et al., 2012).

Mitochondrial Fission and Mitophagy

While mitochondrial fusion seems to be protective, there are several links between mitochondrial fission and mitophagy. In yeast, the DRP1 homologue, DNM1 is required for some types of mitophagy (Abeliovich et al., 2013; Frank et al., 2012a; Mao et al., 2013). Consistent with this, phenotypes due to deletion of dPink1 or dParkin in *Drosophila* can be reversed by enhancing mitochondrial fission (Deng et al., 2008; Yang et al., 2008). PINK1 and PARKIN have also been implicated in pinching off a newly identified class of vesicles, the so-called mitochondria-derived vesicles (MDVs), from mitochondria (Sugiura et al., 2014;

Yang and Yang, 2013). MDVs ultimately fuse with the lysosome for degradation. While it is not know whether other fusion machinery is involved in this process, this micro-fission event suggests yet another way that fission and mitophagy machinery may intersect.

Fis1/TBC1D15

Yet another interesting link between mitophagy and mitochondrial fission was recently identified in the protein FIS1. In yeast, the MDV1/FIS1 complex is the only adaptor for DRP1 on the mitochondria (Mozdy et al., 2000); however, in mammalian cells the situation is more complicated. FIS1 is conserved humans and mice, but as of now no one has been able to show a requirement for FIS1 in recruiting DRP1 to mitochondria. Instead, DRP1 recruitment is mediated by MFF, MID49 and MID51 (Koirala et al., 2013). There is still debate as to whether loss of FIS1 has any effect on mitochondrial morphology (Otera et al., 2010b). However, recently a FIS1 binding protein was identified that opened up new channels of investigation. RAB GTPase regulator domain-containing protein, TBC1D15, is a cytosolic protein that was shown to bind to FIS1 constitutively and regulate mitochondrial morphology independently of Drp1. Whereas knockdown of FIS1 has little obvious effect on mitochondrial morphology, knockdown of TBC1D15 causes more obvious elongation with or without FIS1 knockdown, possibly pointing to an additional recruitment mechanism independent of FIS1 (Onoue et al., 2013). Subsequent work questioned the role for TBC1D15 in mitochondrial morphology and instead placed FIS1 and

TBC1D15 downstream of PINK1/PARKIN in restricting autophagosome biogenesis around mitochondria. Knockout of either FIS1 or TBC1D15 as well as a related protein, TBC1D17, impaired mitochondrial clearance by mitophagy, and led to accumulation of aberrantly structured LC3-labeled autophagosomal membranes during PINK1/PARKIN mediated mitophagy (Yamano et al., 2014). Similar results were seen in vivo in *C. elegans* where mutations in FIS1 also caused accumulation of LC3 aggregates and impaired mitochondrial clearance after treatment with Antimycin A (Shen et al., 2014). While it is intriguing to think that FIS1 may be a master mitophagy regulator on the mitochondria, it is unknown if the role of FIS1 and TBC1D15/TBC1D17 is restricted to mitophagy due to mitochondrial depolarization, or whether other types of mitophagy might also utilize this machinery.

Mitophagy of paternal mitochondria during fertilization

In humans and many mammals, mtDNA is maternally inherited, and hence mutations in mitochondrially-encoded genes follow the female line (Giles et al., 1980). Such mutations may cause encephalomyopathies or other neuromuscular disorders (DiMauro and Schon, 2003), and have also been used as a molecular clock to date evolutionary events. Although heteroplasmy is not strictly avoided in mammals, as it can occur through random mutation, uniparental inheritance seems to be enforced nonetheless. Only one case of truly biparental inheritance in humans has ever been identified, and this finding has neither been reproduced in another laboratory, nor revealed by meta-analysis of previously identified heteroplasmic

sequences (Bandelt et al., 2005).

The evolutionary rationale for this pattern of inheritance remains disputed. It has been suggested that maternal and paternal mtDNAs may be incompatible, that the disappearance of paternal mtDNA signal is actually due to dilution rather than degradation (Luo et al., 2013), or that mtDNA may be greatly damaged during transport in the sperm and hence must be degraded (Birky, 1995). PCR assays designed to detect paternal mtDNA reveal that whereas embryos from intraspecific crosses in mice never retain paternal mtDNA, it does persist in offspring of interspecific crosses, suggesting that neither incompatibility nor dilution are the only factors limiting paternal mitochondrial inheritance (Song et al., 2014). Additionally, one study of polyploid human embryos produced by IVF showed that occasionally paternal mtDNA can persist at least to the blastocyst stage in these faulty ova (St John et al., 2000), suggesting that under certain conditions an ovum may fail to restrict mitochondrial content, despite the fact that the ratio of maternal to paternal mitochondria remains imbalanced (Sawada et al., 2002).

The mechanism behind this degradation in mammals is unknown; however, evidence exists supporting a role for selective proteolysis by the proteasome as well as for mitophagy. These may actually be related processes, as work from our lab and others suggest that activation of the proteasome may be a necessary step preceding mitophagy (Chan et al., 2011).

Several mechanisms have been identified in different model systems that might also be active in mammals, some directed at the DNA itself and beginning during spermatogenesis. In *Drosophila*, mtDNA is removed from the spermatozoa

during its development in a process dependent on the mitochondrial endonuclease, EndoG (DeLuca and O'Farrell, 2012). Similarly, in Japanese Medaka fish the amount of mtDNA is reduced during spermatogenesis, and remaining mtDNA disappears during fertilization before the destruction of mitochondrial structures (Nishimura et al., 2006). Similarly, downregulation of mtDNA copy number has been found in rat, mouse, and human spermatogenesis (Rantanen et al., 2001; Rantanen and Larsson, 2000). This reduction seems to be important for sperm quality, as in human sperm, the ratio of mtDNA copies per cell in progressive verses nonprogressive sperm is estimated at 700:1200 (Diez-Sanchez et al., 2003).

In mammalian fertilization, at least, mtDNA depletion is not the only mechanism. Ubiquitin signaling also clearly plays a role in mitochondrial degradation. In bovine, mouse, and primate eggs, sperm mitochondria are transiently tagged with ubiquitin during their development, and again after fertilization whereas oocyte mitochondria are not (Sutovsky et al., 1999). When anti-ubiquitin antibody is added to oocytes prior to fertilization, sperm mitochondria no longer become ubiquitinated and persist for at least 40 hours post fertilization by which point they would otherwise have been degraded (Sutovsky et al., 2000). The specific type of ubiquitin linkage on sperm mitochondria is unknown, and it may be a signal for the UPS, or mitophagy machinery.

Activity of the ubiquitin-proteasome pathway in mitochondrial inheritance has been tested using proteasome inhibitors. Inhibition of the 26S proteasome with MG132 causes paternal mitochondria to remain intact for at least 120-hours. Importantly, however, MG132 also causes arrest of the cell cycle, and when the

treatment is removed and the cell cycle resumes, mitochondria proceed to degradation (Sutovsky et al., 2000). Since even in untreated embryos paternal mitochondria are not degraded until the four cell stage, these results remain inconclusive as to whether the effect of the proteasome on mitochondria is direct or somehow linked to cell cycle progression.

Mitophagy represents an alternative pathway for paternal mitochondrial removal. Ammonium chloride (NH_4Cl), a so-called "lysosomotropic agent", is a weak base that increases intralysosomal pH, inhibiting protein degradation in the lysosome (Rote and Rechsteiner, 1983). When applied to bovine embryos 20 hours post-fertilization, NH_4Cl prevents the destruction of the sperm mitochondria until at least the eight-cell stage, without inhibiting cell division, suggesting that lysosomal activity may also be required for loss of paternal mitochondria.

Further support for mitophagy in fertilization comes from two recent studies in *C. elegans* that show accumulation of markers of the autophagosome around paternal mitochondria in early stage embryos and persistence of these mitochondria in mutant cells defective in autophagosome formation (Al Rawi et al., 2011; Sato and Sato, 2011). Similarly, fertilized mouse oocytes show accumulation of autophagosome markers around the sperm midpiece after but not before fertilization and lysosomes labeled with LysoTracker can be seen associated with sperm mitochondria inside the embryo (Sutovsky et al., 2000). Experiments with autophagy indicator mice, which contain a GFP-labeled autophagy protein, LC3, show that autophagy is involved in embryogenesis. No LC3 expression is seen in the egg prior to insemination, but dots of LC3 appear from the one to four-cell stage

after fertilization (Tsukamoto et al., 2008). Levels of GFP-LC3 rapidly decrease after the four-cell stage, which coincides with the final stage of paternal mitochondrial degradation. Accordingly, in matings where both egg and sperm are autophagy mutants, development does not proceed past the four to eight cell stage, precisely the point by which paternal mitochondria should be essentially cleared from the embryo (Tsukamoto et al., 2008). These data strongly suggest that mitophagy plays an important role in mitochondrial inheritance; however, studies are needed to conclusively show whether mitophagy is required for parental mitochondrial degradation in mammals.

It is yet unknown what signals paternal mitochondria bear that distinguish them from maternal mitochondria, and what other requirements there may be that facilitate the degradation, such as mitochondrial morphology, given the previously discussed association between mitophagy and mitochondrial fission. The process of degradation must be highly specific, as paternal mitochondria persist in interspecies crosses. It is possible that the signal on paternal mitochondria involves one or more ubiquitinated proteins. So far the only mitochondrial protein that has been shown to be ubiquitinated in spermatozoa is Prohibitin, and it has both K48 and K63 types of ubiquitin chains so it could signal either the UPS or mitophagy machinery (Thompson et al., 2003). However, since this is an inner membrane protein, it is not the most probable candidate for a degradation signal. It is possible that bulk ubiquitination of mitochondria by an E3 ligase such as PARKIN may be required rather than ubiquitination of any specific proteins, and that upstream mechanisms dictate specificity, rather than the ubiquitination itself. Identification of further

ubiquitinated outer mitochondrial membrane proteins on sperm mitochondria will be informative.

Measuring Mitophagy

In the following chapters, we utilize fluorescence microscopy to measure mitophagy in MEF cells and mouse embryos. It is worth discussing here the various experimental methods for assessing mitophagy (as distinct from autophagy more broadly), as each has advantages and drawbacks. The gold standard is electron microscopy. Indeed, this was the method by which the process was first discovered. And although it enables visualization of mitochondria within double membrane vesicles, which is pathognomonic for mitophagy, it is nearly impossible to quantify, and a very difficult method to pursue. Loss of mtDNA nucleoids is one way to monitor mitophagy if combined with pharmacological or genetic perturbations of the autophagy pathway as a negative control. This method is specific for loss of mtDNA, but it does not always reflect mitophagy, and may be very noisy, as there are other methods for modulating mtDNA independent of mitophagy. One commonly used technique is to detect loss of mitochondrial outer membrane proteins such as TOM20 by western or immunostaining. This, however, cannot distinguish the loss of these proteins due to proteasomal degradation rather than mitophagy. Measurement of matrix proteins, by immunological methods or mitochondrial loading with $\Delta\Psi_m$-independent dyes such as mitotracker green, is a more accurate assessment of mitophagy. Matrix proteins, however, are recycled at different rates, and may not

be very precise proxies for mitophagy. An alternative method is the expression of exogenous fluorophores targeted to the mitochondrial matrix. In Chapter 2 below, we utilize matrix-targeted Dendra2, a monomeric photoconvertable protein which fluoresces green under normal conditions, and can be photoconverted to red emission by exposure to UV light (Pham et al., 2012a). Loss of fluorescence of this matrix-targeted protein can be used as a reporter of mitochondrial degradation. Recently, a matrix-targeted fluorescent reporter using the coral-derived protein Keima (mt-Keima), which exhibits pH-dependent excitation and resistance to lysosomal proteases, was used to measure mitophagy (Katayama et al., 2011). This is a more direct measure, since it changes its excitation wavelength from 440 to 586 in the acidic lysosome during autophagy, so a distinct population of mitochondria can be detected. Similar experiments have been done to monitor general autophagy, using LC3 tagged with both EGFP and mCherry based on the same principle, since mCherry is more acid-stable than EGFP (Gump et al., 2014). In our lab we have adapted this experiment to mitochondria, by targeting this fusion protein to the mitochondrial matrix, and we use this protein to assess mitophagy in Chapters two and three.

Thesis Overview

The importance of mitophagy in maintaining mitochondrial function is well appreciated. Studies in the last decade have clearly established a key role for PINK1 and PARKIN in mitochondrial quality control; however, it is not clear whether all or even most mitophagy pathways converge on PINK1/PARKIN. It is

increasingly becoming clear that there is a high degree of selectivity within the mitophagy system due to the array of receptors so far implicated in different mitophagy contexts. Selective mitophagy receptors can function by ubiquitin dependent or ubiquitin independent mechanisms, and since many have similar domain structures, it remains unknown how exactly the specificity is encoded in either case. Similarly, we do not know how much overlap there is mechanistically between mitophagy induced by different means. Further studies are needed to determine whether these are truly disparate pathways for mitophagy, or whether there are more universal rules governing mitophagy in mammalian cells. Toward this end, we developed three systems in which to study mitophagy: OXPHOS-induced mitophagy in MEFs, degradation of paternal mitochondria in mouse embryos, and selective clearance of dysfunctional mitochondria within MFN-null cells. We utilized fluorescent reporters to directly analyze mitochondrial degradation in these systems, and we demonstrated a core set of proteins that function across systems in an effort to integrate our understanding of mitophagy in mammals.

Chapter 2

The maternal mode of mitochondrial inheritance in mammals is well accepted; however, the mechanism that governs loss of paternal mitochondria remains disputed. Although clear evidence in *C. Elegans* implicates mitophagy, it has not been conclusively shown that this is also the case in mammals. In an effort to directly test the role of mitophagy in mammalian fertilization, we took a two-

staged approach. First, we developed a cell culture based system in which to identify candidate proteins involved in a physiological type of mitophagy induced by increased OXPHOS. Then, we tested the role of these proteins in mouse embryos by shRNA knockdown. We show that in both systems, the E3 ubiquitin ligases PARKIN and MUL1 play partially redundant roles in mitophagy, and that the process also requires FIS1, as well as the autophagy adaptor, p62 and PINK1. These results suggest that a core mitophagy mechanism, which may occur in response to a variety of stressors, is involved in the maternal transmission of mitochondria.

Chapter 3

Functional heterogeneity of mitochondria in cells lacking mitochondrial fusion has been previously described by our lab and others. MFN-null cells have a mixed population of healthy mitochondria and dysfunctional mitochondria that are depolarized, contain mtDNA mutations, altered protein content, and have reduced respiratory capacity. Some studies have suggested that the PINK1/PARKIN machinery is recruited to these dysfunctional mitochondria, but the means by which functional and dysfunctional mitochondria are distinguished has not been well addressed. Using our fluorescence based mitophagy assay, we show that MFN-null cells exhibit an increase in mitophagy, and that the mitophagy receptor, p62 is recruited specifically to defective mitochondria that lack mtDNA and $\Delta\Psi_m$. We further show that p62 is required for mitophagy in

these cells. Contrary to previous theories, we show that its ubiquitin-binding domain is dispensable for p62 recruitment to mitochondria. Rather, we find that a protein-protein interaction domain is sufficient to localize p62 to mitochondria, suggesting another layer of specificity in this mitophagy context.

Chapter 4

Here we discuss open topics in mitophagy based on the findings of the preceding chapters. We will address experiments that explore the role of MUL1 in mitophagy and specifically how it interacts with the PINK1/PARKIN mitophagy pathway. Next we will consider tools that are now available to study mitophagy including high-throughput methods, and the mitophagy mouse. Finally, we will discuss experiments focused on the long-term effects of paternal mitochondrial persistence in adult animals, addressing the puzzling reason why maternal inheritance of mitochondria came into being.

FIGURE LEGENDS

Figure 1.1 Schematic of mammalian macroautophagy. Initiation at the phagophore assembly site (PAS) mediated by an ULK1-associated complex. Nucleation of the phagophore is mediated by the vacuolar protein sorting 34 (VPS34) PI3K. Expansion of the phagophore membrane requires the conjugation of phosphatidyl ethanolamine (PE) to LC3 by way of two ubiquitin-like conjugation systems. The closed autophagosome fuses with the lysosome, forming the autolysosome.

Figure 1.2 PINK1/PARKIN mitophagy pathway. Mitochondrial damage leads to impaired protein translocation through the mitochondrial outer membrane. PINK1 accumulates on the mitochondrial outer membrane, resulting in phosphorylation of ubiquitin and PARKIN. Phospho-ubiquitin activates PARKIN, which further ubiquitinates mitochondria. Ubiquitination triggers subsequent recruitment of the phagophore. FIS1 and TBC1D15 facilitate phagophore elongation and curvature around mitochondrial cargo.

Figure 1.3 Domain structure of NBR1 and p62. The N-terminal Phox and Bem1 (PB1) domain facilitates homo- and hetero-oligomerization of p62 and NBR1 as well as further protein-protein interactions. The zinc finger (ZZ) domain can bind DNA, and may modulate protein binding. The first NBR1 coiled coil domain (CC1) facilitates NBR1 homo-dimerization. Coiled-coil domain 2 (CC2) is of unknown

function. The LC3 interacting regions (LIR) of both proteins bind LC3 family proteins, with LIR1 of NBR1 having higher affinity than LIR2. The ubiquitin association domain (UBA) may facilitate binding to ubiquitinated autophagy substrates. The UBA of p62 has higher affinity for K63-linked ubiquitin chains, whereas the UBA of NBR1 shows equal affinity for K63 and K48-linked chains.

Figure 1.1

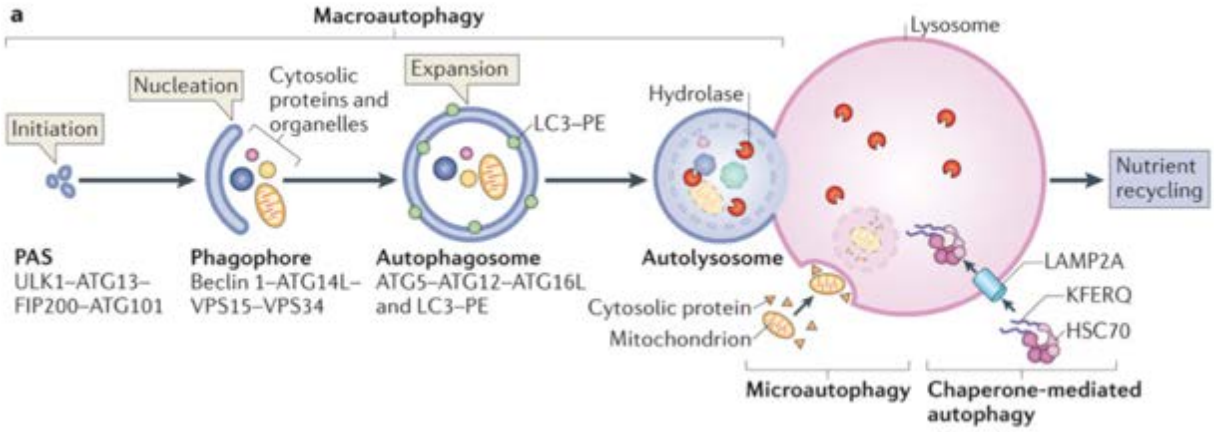

From (Kaur and Debnath, 2015)

Figure 1.2

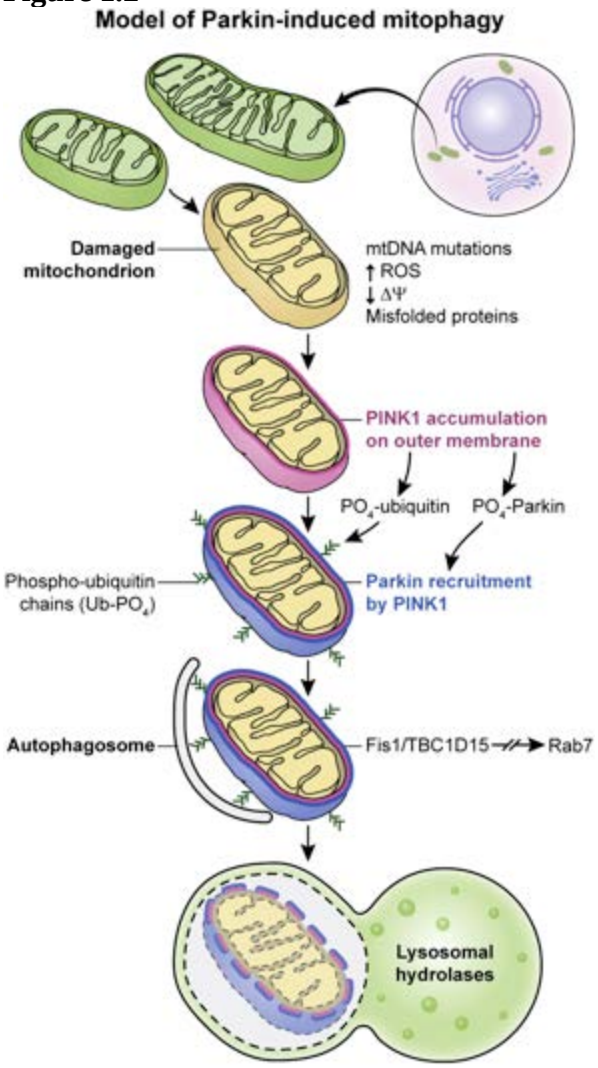

From (Pickrell and Youle, 2015)

Figure 1.3

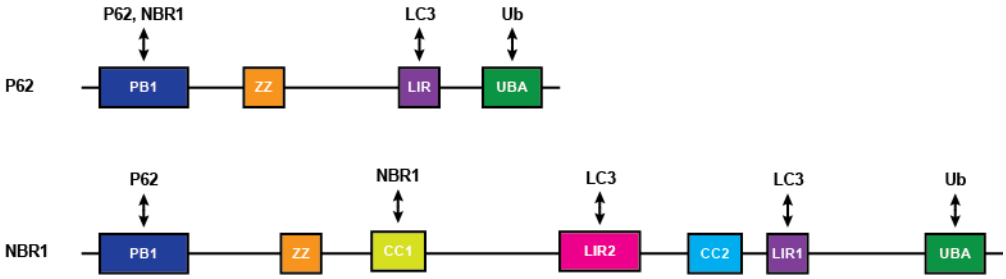
P62, NBR1
LC3
Ub
P62
PB1
ZZ
LIR
UBA
P62
NBR1
LC3
LC3
Ub
NBR1
PB1
ZZ
CC1
LIR2
CC2
LIR1
UBA

REFERENCES

Abeliovich, H., Zarei, M., Rigbolt, K.T., Youle, R.J., and Dengjel, J. (2013). Involvement of mitochondrial dynamics in the segregation of mitochondrial matrix proteins during stationary phase mitophagy. Nature communications *4*, 2789.

Al Rawi, S., Louvet-Vallee, S., Djeddi, A., Sachse, M., Culetto, E., Hajjar, C., Boyd, L., Legouis, R., and Galy, V. (2011). Postfertilization autophagy of sperm organelles prevents paternal mitochondrial DNA transmission. Science *334*, 1144-1147.

Alemu, E.A., Lamark, T., Torgersen, K.M., Birgisdottir, A.B., Larsen, K.B., Jain, A., Olsvik, H., Overvatn, A., Kirkin, V., and Johansen, T. (2012). ATG8 family proteins act as scaffolds for assembly of the ULK complex: sequence requirements for LC3-interacting region (LIR) motifs. J Biol Chem *287*, 39275-39290.

Anand, R., Wai, T., Baker, M.J., Kladt, N., Schauss, A.C., Rugarli, E., and Langer, T. (2014). The i-AAA protease YME1L and OMA1 cleave OPA1 to balance mitochondrial fusion and fission. J Cell Biol *204*, 919-929.

Armstrong, J.A., and Hart, P.D. (1971). Response of cultured macrophages to Mycobacterium tuberculosis, with observations on fusion of lysosomes with phagosomes. J Exp Med *134*, 713-740.

Ashford, T.P., and Porter, K.R. (1962). Cytoplasmic components in hepatic cell lysosomes. J Cell Biol *12*, 198-202.

Ashrafi, G., and Schwarz, T.L. (2013). The pathways of mitophagy for quality control and clearance of mitochondria. Cell death and differentiation *20*, 31-42.

Baba, M., Osumi, M., and Ohsumi, Y. (1995). Analysis of the membrane structures involved in autophagy in yeast by freeze-replica method. Cell Struct Funct *20*, 465-471.

Baloh, R.H., Salavaggione, E., Milbrandt, J., and Pestronk, A. (2007). Familial parkinsonism and ophthalmoplegia from a mutation in the mitochondrial DNA helicase twinkle. Arch Neurol *64*, 998-1000.

Bandelt, H.J., Kong, Q.P., Parson, W., and Salas, A. (2005). More evidence for non-maternal inheritance of mitochondrial DNA? J Med Genet *42*, 957-960.

Barsoum, M.J., Yuan, H., Gerencser, A.A., Liot, G., Kushnareva, Y., Graber, S., Kovacs, I., Lee, W.D., Waggoner, J., Cui, J., *et al.* (2006). Nitric oxide-induced mitochondrial fission is regulated by dynamin-related GTPases in neurons. The EMBO journal *25*, 3900-3911.

Bender, A., Krishnan, K.J., Morris, C.M., Taylor, G.A., Reeve, A.K., Perry, R.H., Jaros, E., Hersheson, J.S., Betts, J., Klopstock, T., *et al.* (2006). High levels of mitochondrial DNA deletions in substantia nigra neurons in aging and Parkinson disease. Nat Genet *38*, 515-517.

Betarbet, R., Sherer, T.B., and Greenamyre, J.T. (2002). Animal models of Parkinson's disease. Bioessays *24*, 308-318.

Betarbet, R., Sherer, T.B., MacKenzie, G., Garcia-Osuna, M., Panov, A.V., and Greenamyre, J.T. (2000). Chronic systemic pesticide exposure reproduces features of Parkinson's disease. Nat Neurosci *3*, 1301-1306.

Birgisdottir, A.B., Lamark, T., and Johansen, T. (2013). The LIR motif - crucial for selective autophagy. J Cell Sci *126*, 3237-3247.

Birky, C.W., Jr. (1995). Uniparental inheritance of mitochondrial and chloroplast genes: mechanisms and evolution. Proc Natl Acad Sci U S A *92*, 11331-11338.

Bjorkoy, G., Lamark, T., Brech, A., Outzen, H., Perander, M., Overvatn, A., Stenmark, H., and Johansen, T. (2005). p62/SQSTM1 forms protein aggregates degraded by autophagy and has a protective effect on huntingtin-induced cell death. J Cell Biol *171*, 603-614.

Blommaart, E.F., Luiken, J.J., Blommaart, P.J., van Woerkom, G.M., and Meijer, A.J. (1995). Phosphorylation of ribosomal protein S6 is inhibitory for autophagy in isolated rat hepatocytes. J Biol Chem *270*, 2320-2326.

Bonifati, V. (2007). Genetics of parkinsonism. Parkinsonism Relat Disord *13 Suppl 3*, S233-241.

Brandt, U. (2006). Energy converting NADH:quinone oxidoreductase (complex I). Annu Rev Biochem *75*, 69-92.

Chan, D.C. (2012). Fusion and fission: interlinked processes critical for mitochondrial health. Annu Rev Genet *46*, 265-287.

Chan, N.C., Salazar, A.M., Pham, A.H., Sweredoski, M.J., Kolawa, N.J., Graham, R.L., Hess, S., and Chan, D.C. (2011). Broad activation of the ubiquitin-proteasome system by Parkin is critical for mitophagy. Hum Mol Genet *20*, 1726-1737.

Chan, P., DeLanney, L.E., Irwin, I., Langston, J.W., and Di Monte, D. (1991). Rapid ATP loss caused by 1-methyl-4-phenyl-1,2,3,6-tetrahydropyridine in mouse brain. J Neurochem *57*, 348-351.

Chen, H., and Chan, D.C. (2009). Mitochondrial dynamics--fusion, fission, movement, and mitophagy--in neurodegenerative diseases. Hum Mol Genet *18*, R169-176.

Chen, H., Chomyn, A., and Chan, D.C. (2005). Disruption of fusion results in mitochondrial heterogeneity and dysfunction. J Biol Chem *280*, 26185-26192.

Chen, H., Detmer, S.A., Ewald, A.J., Griffin, E.E., Fraser, S.E., and Chan, D.C. (2003). Mitofusins MFN1 and MFN2 coordinately regulate mitochondrial fusion and are essential for embryonic development. J Cell Biol *160*, 189-200.

Chen, H., McCaffery, J.M., and Chan, D.C. (2007). Mitochondrial fusion protects against neurodegeneration in the cerebellum. Cell *130*, 548-562.

Chen, H., Ren, S., Clish, C., Jain, M., Mootha, V., McCaffery, J.M., and Chan, D.C. (2015). Titration of mitochondrial fusion rescues Mff-deficient cardiomyopathy. The Journal of Cell Biology *211*, 795-805.

Chen, H., Vermulst, M., Wang, Y.E., Chomyn, A., Prolla, T.A., McCaffery, J.M., and Chan, D.C. (2010). Mitochondrial fusion is required for mtDNA stability in skeletal muscle and tolerance of mtDNA mutations. Cell *141*, 280-289.

Chen, Y., and Dorn, G.W., 2nd (2013). PINK1-phosphorylated mitofusin 2 is a Parkin receptor for culling damaged mitochondria. Science *340*, 471-475.

Chourasia, A.H., Boland, M.L., and Macleod, K.F. (2015). Mitophagy and cancer. Cancer & metabolism *3*, 4.

Cipolat, S., Martins de Brito, O., Dal Zilio, B., and Scorrano, L. (2004). OPA1 requires mitofusin 1 to promote mitochondrial fusion. Proc Natl Acad Sci U S A *101*, 15927-15932.

Clark, I.E., Dodson, M.W., Jiang, C., Cao, J.H., Huh, J.R., Seol, J.H., Yoo, S.J., Hay, B.A., and Guo, M. (2006). Drosophila pink1 is required for mitochondrial function and interacts genetically with parkin. Nature *441*, 1162-1166.

Clark, S.L., Jr. (1957). Cellular differentiation in the kidneys of newborn mice studies with the electron microscope. J Biophys Biochem Cytol *3*, 349-362.

Crabtree, H.G. (1929). Observations on the carbohydrate metabolism of tumours. Biochem J *23*, 536-545.

Dai, Y., Zheng, K., Clark, J., Swerdlow, R.H., Pulst, S.M., Sutton, J.P., Shinobu, L.A., and Simon, D.K. (2014). Rapamycin drives selection against a pathogenic heteroplasmic mitochondrial DNA mutation. Human Molecular Genetics *23*, 637-647.

Davis, G.C., Williams, A.C., Markey, S.P., Ebert, M.H., Caine, E.D., Reichert, C.M., and Kopin, I.J. (1979). Chronic Parkinsonism secondary to intravenous injection of meperidine analogues. Psychiatry Res *1*, 249-254.

Deas, E., Plun-Favreau, H., Gandhi, S., Desmond, H., Kjaer, S., Loh, S.H., Renton, A.E., Harvey, R.J., Whitworth, A.J., Martins, L.M., *et al.* (2011). PINK1 cleavage at position A103 by the mitochondrial protease PARL. Hum Mol Genet *20*, 867-879.

Delettre, C., Griffoin, J.M., Kaplan, J., Dollfus, H., Lorenz, B., Faivre, L., Lenaers, G., Belenguer, P., and Hamel, C.P. (2001). Mutation spectrum and splicing variants in the OPA1 gene. Hum Genet *109*, 584-591.

DeLuca, S.Z., and O'Farrell, P.H. (2012). Barriers to male transmission of mitochondrial DNA in sperm development. Dev Cell *22*, 660-668.

Deng, H., Dodson, M.W., Huang, H., and Guo, M. (2008). The Parkinson's disease genes pink1 and parkin promote mitochondrial fission and/or inhibit fusion in Drosophila. Proc Natl Acad Sci U S A *105*, 14503-14508.

Deosaran, E., Larsen, K.B., Hua, R., Sargent, G., Wang, Y., Kim, S., Lamark, T., Jauregui, M., Law, K., Lippincott-Schwartz, J., *et al.* (2013). NBR1 acts as an autophagy receptor for peroxisomes. J Cell Sci *126*, 939-952.

Deter, R.L., Baudhuin, P., and De Duve, C. (1967). Participation of lysosomes in cellular autophagy induced in rat liver by glucagon. J Cell Biol *35*, C11-16.

Detmer, S.A., and Chan, D.C. (2007). Functions and dysfunctions of mitochondrial dynamics. Nat Rev Mol Cell Biol *8*, 870-879.

Di Fonzo, A., Chien, H.F., Socal, M., Giraudo, S., Tassorelli, C., Iliceto, G., Fabbrini, G., Marconi, R., Fincati, E., Abbruzzese, G., *et al.* (2007). ATP13A2 missense mutations in juvenile parkinsonism and young onset Parkinson disease. Neurology *68*, 1557-1562.

Diao, J., Liu, R., Rong, Y., Zhao, M., Zhang, J., Lai, Y., Zhou, Q., Wilz, L.M., Li, J., Vivona, S., *et al.* (2015). ATG14 promotes membrane tethering and fusion of autophagosomes to endolysosomes. Nature *520*, 563-566.

Diaz-Ruiz, R., Rigoulet, M., and Devin, A. (2011). The Warburg and Crabtree effects: On the origin of cancer cell energy metabolism and of yeast glucose repression. Biochimica et Biophysica Acta (BBA) - Bioenergetics *1807*, 568-576.

Diaz-Troya, S., Perez-Perez, M.E., Florencio, F.J., and Crespo, J.L. (2008). The role of TOR in autophagy regulation from yeast to plants and mammals. Autophagy *4*, 851-865.

Diez-Sanchez, C., Ruiz-Pesini, E., Lapena, A.C., Montoya, J., Perez-Martos, A., Enriquez, J.A., and Lopez-Perez, M.J. (2003). Mitochondrial DNA content of human spermatozoa. Biol Reprod *68*, 180-185.

Dikov, D., and Reichert, A.S. (2011). How to split up: lessons from mitochondria. The EMBO journal *30*, 2751-2753.

Dimauro, S., and Davidzon, G. (2005). Mitochondrial DNA and disease. Ann Med *37*, 222-232.

DiMauro, S., and Schon, E.A. (2003). Mitochondrial respiratory-chain diseases. N Engl J Med *348*, 2656-2668.

Ding, W.X., Ni, H.M., Li, M., Liao, Y., Chen, X., Stolz, D.B., Dorn, G.W., 2nd, and Yin, X.M. (2010). Nix is critical to two distinct phases of mitophagy, reactive oxygen species-mediated autophagy induction and Parkin-ubiquitin-p62-mediated mitochondrial priming. J Biol Chem *285*, 27879-27890.

Dreschel, N.A., and Granger, D.A. (2009). Methods of collection for salivary cortisol measurement in dogs. Horm Behav *55*, 163-168.

Dunn, W.A., Jr. (1990). Studies on the mechanisms of autophagy: formation of the autophagic vacuole. J Cell Biol *110*, 1923-1933.

Duvezin-Caubet, S., Jagasia, R., Wagener, J., Hofmann, S., Trifunovic, A., Hansson, A., Chomyn, A., Bauer, M.F., Attardi, G., Larsson, N.G., *et al.* (2006). Proteolytic processing of OPA1 links mitochondrial dysfunction to alterations in mitochondrial morphology. J Biol Chem *281*, 37972-37979.

Elsasser, S., and Finley, D. (2005). Delivery of ubiquitinated substrates to protein-unfolding machines. Nat Cell Biol *7*, 742-749.

Fabre, E., Monserrat, J., Herrero, A., Barja, G., and Leret, M.L. (1999). Effect of MPTP on brain mitochondrial H2O2 and ATP production and on dopamine and DOPAC in the striatum. J Physiol Biochem *55*, 325-331.

Forno, L.S., DeLanney, L.E., Irwin, I., and Langston, J.W. (1993). Similarities and differences between MPTP-induced parkinsonsim and Parkinson's disease. Neuropathologic considerations. Adv Neurol *60*, 600-608.

Frank, M., Duvezin-Caubet, S., Koob, S., Occhipinti, A., Jagasia, R., Petcherski, A., Ruonala, M.O., Priault, M., Salin, B., and Reichert, A.S. (2012a). Mitophagy is triggered by mild oxidative stress in a mitochondrial fission dependent manner. Biochim Biophys Acta *1823*, 2297-2310.

Frank, M., Duvezin-Caubet, S., Koob, S., Occhipinti, A., Jagasia, R., Petcherski, A., Ruonala, M.O., Priault, M., Salin, B., and Reichert, A.S. (2012b). Mitophagy is triggered by mild oxidative stress in a mitochondrial fission dependent manner. Biochimica et Biophysica Acta (BBA) - Molecular Cell Research *1823*, 2297-2310.

Fu, M., St-Pierre, P., Shankar, J., Wang, P.T., Joshi, B., and Nabi, I.R. (2013). Regulation of mitophagy by the Gp78 E3 ubiquitin ligase. Mol Biol Cell *24*, 1153-1162.

Fujita, N., Hayashi-Nishino, M., Fukumoto, H., Omori, H., Yamamoto, A., Noda, T., and Yoshimori, T. (2008). An Atg4B mutant hampers the lipidation of LC3 paralogues and causes defects in autophagosome closure. Mol Biol Cell *19*, 4651-4659.

Galluzzi, L., Pietrocola, F., Levine, B., and Kroemer, G. (2014). Metabolic control of autophagy. Cell *159*, 1263-1276.

Gandre-Babbe, S., and van der Bliek, A.M. (2008). The novel tail-anchored membrane protein Mff controls mitochondrial and peroxisomal fission in mammalian cells. Mol Biol Cell *19*, 2402-2412.

Gatenby, R.A., and Gillies, R.J. (2004). Why do cancers have high aerobic glycolysis? Nat Rev Cancer *4*, 891-899.

Gautier, C.A., Kitada, T., and Shen, J. (2008). Loss of PINK1 causes mitochondrial functional defects and increased sensitivity to oxidative stress. Proc Natl Acad Sci U S A *105*, 11364-11369.

Gegg, M.E., Cooper, J.M., Chau, K.Y., Rojo, M., Schapira, A.H., and Taanman, J.W. (2010). Mitofusin 1 and mitofusin 2 are ubiquitinated in a PINK1/parkin-dependent manner upon induction of mitophagy. Hum Mol Genet *19*, 4861-4870.

Geisler, S., Holmstrom, K.M., Skujat, D., Fiesel, F.C., Rothfuss, O.C., Kahle, P.J., and Springer, W. (2010). PINK1/Parkin-mediated mitophagy is dependent on VDAC1 and p62/SQSTM1. Nat Cell Biol *12*, 119-131.

Giles, R.E., Blanc, H., Cann, H.M., and Wallace, D.C. (1980). Maternal inheritance of human mitochondrial DNA. Proc Natl Acad Sci U S A *77*, 6715-6719.

Greene, A.W., Grenier, K., Aguileta, M.A., Muise, S., Farazifard, R., Haque, M.E., McBride, H.M., Park, D.S., and Fon, E.A. (2012). Mitochondrial processing peptidase regulates PINK1 processing, import and Parkin recruitment. EMBO Rep *13*, 378-385.

Greene, J.C., Whitworth, A.J., Kuo, I., Andrews, L.A., Feany, M.B., and Pallanck, L.J. (2003). Mitochondrial pathology and apoptotic muscle degeneration in Drosophila parkin mutants. Proc Natl Acad Sci U S A *100*, 4078-4083.

Griparic, L., Kanazawa, T., and van der Bliek, A.M. (2007). Regulation of the mitochondrial dynamin-like protein OPA1 by proteolytic cleavage. J Cell Biol *178*, 757-764.

Griparic, L., van der Wel, N.N., Orozco, I.J., Peters, P.J., and van der Bliek, A.M. (2004). Loss of the intermembrane space protein Mgm1/OPA1 induces swelling and localized constrictions along the lengths of mitochondria. J Biol Chem *279*, 18792-18798.

Gronowicz, G., Swift, H., and Steck, T.L. (1984). Maturation of the reticulocyte in vitro. J Cell Sci *71*, 177-197.

Gump, J.M., Staskiewicz, L., Morgan, M.J., Bamberg, A., Riches, D.W.H., and Thorburn, A. (2014). Autophagy variation within a cell population determines cell fate through selective degradation of Fap-1. Nat Cell Biol *16*, 47-54.

Hailey, D.W., Rambold, A.S., Satpute-Krishnan, P., Mitra, K., Sougrat, R., Kim, P.K., and Lippincott-Schwartz, J. (2010). Mitochondria supply membranes for autophagosome biogenesis during starvation. Cell *141*, 656-667.

Hanna, R.A., Quinsay, M.N., Orogo, A.M., Giang, K., Rikka, S., and Gustafsson, A.B. (2012). Microtubule-associated protein 1 light chain 3 (LC3) interacts with Bnip3 protein to selectively remove endoplasmic reticulum and mitochondria via autophagy. J Biol Chem *287*, 19094-19104.

Hantraye, P., Brouillet, E., Ferrante, R., Palfi, S., Dolan, R., Matthews, R.T., and Beal, M.F. (1996). Inhibition of neuronal nitric oxide synthase prevents MPTP-induced parkinsonism in baboons. Nat Med *2*, 1017-1021.

Hantraye, P., Varastet, M., Peschanski, M., Riche, D., Cesaro, P., Willer, J.C., and Maziere, M. (1993). Stable parkinsonian syndrome and uneven loss of striatal dopamine fibres following chronic MPTP administration in baboons. Neuroscience *53*, 169-178.

Hasegawa, E., Takeshige, K., Oishi, T., Murai, Y., and Minakami, S. (1990). 1-Methyl-4-phenylpyridinium (MPP+) induces NADH-dependent superoxide formation and enhances NADH-dependent lipid peroxidation in bovine heart submitochondrial particles. Biochemical and biophysical research communications *170*, 1049-1055.

Hasson, S.A., Kane, L.A., Yamano, K., Huang, C.H., Sliter, D.A., Buehler, E., Wang, C., Heman-Ackah, S.M., Hessa, T., Guha, R., *et al.* (2013). High-content genome-wide RNAi screens identify regulators of parkin upstream of mitophagy. Nature *504*, 291-295.

Haynes, C.M., and Ron, D. (2010). The mitochondrial UPR – protecting organelle protein homeostasis. Journal of Cell Science *123*, 3849-3855.

Henchcliffe, C., and Beal, M.F. (2008). Mitochondrial biology and oxidative stress in Parkinson disease pathogenesis. Nat Clin Pract Neuro *4*, 600-609.

Hoppins, S., Edlich, F., Cleland, M.M., Banerjee, S., McCaffery, J.M., Youle, R.J., and Nunnari, J. (2011). The soluble form of Bax regulates mitochondrial fusion via MFN2 homotypic complexes. Mol Cell *41*, 150-160.

Hoppins, S., Lackner, L., and Nunnari, J. (2007). The machines that divide and fuse mitochondria. Annu Rev Biochem *76*, 751-780.

Ichimura, Y., Kirisako, T., Takao, T., Satomi, Y., Shimonishi, Y., Ishihara, N., Mizushima, N., Tanida, I., Kominami, E., Ohsumi, M., *et al.* (2000). A ubiquitin-like system mediates protein lipidation. Nature *408*, 488-492.

Ichimura, Y., Kumanomidou, T., Sou, Y.S., Mizushima, T., Ezaki, J., Ueno, T., Kominami, E., Yamane, T., Tanaka, K., and Komatsu, M. (2008). Structural basis for sorting mechanism of p62 in selective autophagy. J Biol Chem *283*, 22847-22857.

Ishihara, N., Fujita, Y., Oka, T., and Mihara, K. (2006). Regulation of mitochondrial morphology through proteolytic cleavage of OPA1. The EMBO journal *25*, 2966-2977.

Isogai, S., Morimoto, D., Arita, K., Unzai, S., Tenno, T., Hasegawa, J., Sou, Y.S., Komatsu, M., Tanaka, K., Shirakawa, M., *et al.* (2011). Crystal structure of the ubiquitin-associated (UBA) domain of p62 and its interaction with ubiquitin. J Biol Chem *286*, 31864-31874.

Itakura, E., and Mizushima, N. (2010). Characterization of autophagosome formation site by a hierarchical analysis of mammalian Atg proteins. Autophagy *6*, 764-776.

Itakura, E., and Mizushima, N. (2011). p62 Targeting to the autophagosome formation site requires self-oligomerization but not LC3 binding. J Cell Biol *192*, 17-27.

Jagasia, R., Grote, P., Westermann, B., and Conradt, B. (2005). DRP-1-mediated mitochondrial fragmentation during EGL-1-induced cell death in C. elegans. Nature *433*, 754-760.

James, D.I., Parone, P.A., Mattenberger, Y., and Martinou, J.C. (2003). hFis1, a novel component of the mammalian mitochondrial fission machinery. J Biol Chem *278*, 36373-36379.

Janetzky, B., Hauck, S., Youdim, M.B., Riederer, P., Jellinger, K., Pantucek, F., Zochling, R., Boissl, K.W., and Reichmann, H. (1994). Unaltered aconitase activity, but decreased complex I activity in substantia nigra pars compacta of patients with Parkinson's disease. Neurosci Lett *169*, 126-128.

Jezek, P., and Plecita-Hlavata, L. (2009). Mitochondrial reticulum network dynamics in relation to oxidative stress, redox regulation, and hypoxia. Int J Biochem Cell Biol *41*, 1790-1804.

Jin, S.M., Lazarou, M., Wang, C., Kane, L.A., Narendra, D.P., and Youle, R.J. (2010). Mitochondrial membrane potential regulates PINK1 import and proteolytic destabilization by PARL. J Cell Biol *191*, 933-942.

Jin, S.M., and Youle, R.J. (2013). The accumulation of misfolded proteins in the mitochondrial matrix is sensed by PINK1 to induce PARK2/Parkin-mediated mitophagy of polarized mitochondria. Autophagy *9*, 1750-1757.

Jung, C.H., Ro, S.H., Cao, J., Otto, N.M., and Kim, D.H. (2010). mTOR regulation of autophagy. FEBS Lett *584*, 1287-1295.

Kabeya, Y., Mizushima, N., Ueno, T., Yamamoto, A., Kirisako, T., Noda, T., Kominami, E., Ohsumi, Y., and Yoshimori, T. (2000). LC3, a mammalian homologue of yeast Apg8p, is localized in autophagosome membranes after processing. The EMBO journal *19*, 5720-5728.

Kabeya, Y., Mizushima, N., Yamamoto, A., Oshitani-Okamoto, S., Ohsumi, Y., and Yoshimori, T. (2004). LC3, GABARAP and GATE16 localize to autophagosomal membrane depending on form-II formation. J Cell Sci *117*, 2805-2812.

Kalvari, I., Tsompanis, S., Mulakkal, N.C., Osgood, R., Johansen, T., Nezis, I.P., and Promponas, V.J. (2014). iLIR: A web resource for prediction of Atg8-family interacting proteins. Autophagy *10*, 913-925.

Kamada, Y., Yoshino, K., Kondo, C., Kawamata, T., Oshiro, N., Yonezawa, K., and Ohsumi, Y. (2010). Tor directly controls the Atg1 kinase complex to regulate autophagy. Molecular and cellular biology *30*, 1049-1058.

Kamber, R.A., Shoemaker, C.J., and Denic, V. (2015). Receptor-Bound Targets of Selective Autophagy Use a Scaffold Protein to Activate the Atg1 Kinase. Mol Cell *59*, 372-381.

Kane, L.A., Lazarou, M., Fogel, A.I., Li, Y., Yamano, K., Sarraf, S.A., Banerjee, S., and Youle, R.J. (2014). PINK1 phosphorylates ubiquitin to activate Parkin E3 ubiquitin ligase activity. J Cell Biol *205*, 143-153.

Karbowski, M., Neutzner, A., and Youle, R.J. (2007). The mitochondrial E3 ubiquitin ligase MARCH5 is required for Drp1 dependent mitochondrial division. The Journal of Cell Biology *178*, 71-84.

Katayama, H., Kogure, T., Mizushima, N., Yoshimori, T., and Miyawaki, A. (2011). A sensitive and quantitative technique for detecting autophagic events based on lysosomal delivery. Chemistry & biology *18*, 1042-1052.

Kaur, J., and Debnath, J. (2015). Autophagy at the crossroads of catabolism and anabolism. Nat Rev Mol Cell Biol *16*, 461-472.

Kaushik, S., and Cuervo, A.M. (2008). Chaperone-mediated autophagy. Methods Mol Biol *445*, 227-244.

Kazlauskaite, A., Kelly, V., Johnson, C., Baillie, C., Hastie, C.J., Peggie, M., Macartney, T., Woodroof, H.I., Alessi, D.R., Pedrioli, P.G., *et al.* (2014a). Phosphorylation of Parkin at Serine65 is essential for activation: elaboration of a Miro1 substrate-based assay of Parkin E3 ligase activity. Open Biol *4*, 130213.

Kazlauskaite, A., Kondapalli, C., Gourlay, R., Campbell, D.G., Ritorto, M.S., Hofmann, K., Alessi, D.R., Knebel, A., Trost, M., and Muqit, M.M. (2014b). Parkin is activated by PINK1-dependent phosphorylation of ubiquitin at Ser65. Biochem J *460*, 127-139.

Keeney, P.M., Xie, J., Capaldi, R.A., and Bennett, J.P., Jr. (2006). Parkinson's disease brain mitochondrial complex I has oxidatively damaged subunits and is functionally impaired and misassembled. J Neurosci *26*, 5256-5264.

Khaminets, A., Behl, C., and Dikic, I. (2016). Ubiquitin-Dependent And Independent Signals In Selective Autophagy. Trends Cell Biol *26*, 6-16.

Khrapko, K., and Vijg, J. (2009). Mitochondrial DNA mutations and aging: devils in the details? Trends Genet *25*, 91-98.

Kim, J., Kundu, M., Viollet, B., and Guan, K.L. (2011). AMPK and mTOR regulate autophagy through direct phosphorylation of Ulk1. Nat Cell Biol *13*, 132-141.

Kim, N.C., Tresse, E., Kolaitis, R.M., Molliex, A., Thomas, R.E., Alami, N.H., Wang, B., Joshi, A., Smith, R.B., Ritson, G.P., *et al.* (2013). VCP is essential for mitochondrial quality control by PINK1/Parkin and this function is impaired by VCP mutations. Neuron *78*, 65-80.

Kim, P.K., Hailey, D.W., Mullen, R.T., and Lippincott-Schwartz, J. (2008). Ubiquitin signals autophagic degradation of cytosolic proteins and peroxisomes. Proc Natl Acad Sci U S A *105*, 20567-20574.

Kirisako, T., Ichimura, Y., Okada, H., Kabeya, Y., Mizushima, N., Yoshimori, T., Ohsumi, M., Takao, T., Noda, T., and Ohsumi, Y. (2000). The reversible modification regulates the membrane-binding state of Apg8/Aut7 essential for autophagy and the cytoplasm to vacuole targeting pathway. J Cell Biol *151*, 263-276.

Kirkin, V., Lamark, T., Sou, Y.S., Bjorkoy, G., Nunn, J.L., Bruun, J.A., Shvets, E., McEwan, D.G., Clausen, T.H., Wild, P., *et al.* (2009). A role for NBR1 in autophagosomal degradation of ubiquitinated substrates. Mol Cell *33*, 505-516.

Kitada, T., Pisani, A., Karouani, M., Haburcak, M., Martella, G., Tscherter, A., Platania, P., Wu, B., Pothos, E.N., and Shen, J. (2009). Impaired dopamine release and synaptic plasticity in the striatum of parkin-/- mice. J Neurochem *110*, 613-621.

Koirala, S., Guo, Q., Kalia, R., Bui, H.T., Eckert, D.M., Frost, A., and Shaw, J.M. (2013). Interchangeable adaptors regulate mitochondrial dynamin assembly for membrane scission. Proceedings of the National Academy of Sciences of the United States of America *110*, E1342-E1351.

Komatsu, M., Waguri, S., Koike, M., Sou, Y.S., Ueno, T., Hara, T., Mizushima, N., Iwata, J., Ezaki, J., Murata, S., *et al.* (2007). Homeostatic levels of p62 control

cytoplasmic inclusion body formation in autophagy-deficient mice. Cell *131*, 1149-1163.

Kondapalli, C., Kazlauskaite, A., Zhang, N., Woodroof, H.I., Campbell, D.G., Gourlay, R., Burchell, L., Walden, H., Macartney, T.J., Deak, M., *et al.* (2012). PINK1 is activated by mitochondrial membrane potential depolarization and stimulates Parkin E3 ligase activity by phosphorylating Serine 65. Open Biol *2*, 120080.

Koshiba, T., Detmer, S.A., Kaiser, J.T., Chen, H., McCaffery, J.M., and Chan, D.C. (2004). Structural basis of mitochondrial tethering by mitofusin complexes. Science *305*, 858-862.

Koury, M.J., Koury, S.T., Kopsombut, P., and Bondurant, M.C. (2005). In vitro maturation of nascent reticulocytes to erythrocytes. Blood *105*, 2168-2174.

Koyano, F., Okatsu, K., Kosako, H., Tamura, Y., Go, E., Kimura, M., Kimura, Y., Tsuchiya, H., Yoshihara, H., Hirokawa, T., *et al.* (2014). Ubiquitin is phosphorylated by PINK1 to activate parkin. Nature *510*, 162-166.

Kraft, C., Deplazes, A., Sohrmann, M., and Peter, M. (2008). Mature ribosomes are selectively degraded upon starvation by an autophagy pathway requiring the Ubp3p/Bre5p ubiquitin protease. Nat Cell Biol *10*, 602-610.

Kraft, C., Peter, M., and Hofmann, K. (2010). Selective autophagy: ubiquitin-mediated recognition and beyond. Nat Cell Biol *12*, 836-841.

Kuma, A., Hatano, M., Matsui, M., Yamamoto, A., Nakaya, H., Yoshimori, T., Ohsumi, Y., Tokuhisa, T., and Mizushima, N. (2004). The role of autophagy during the early neonatal starvation period. Nature *432*, 1032-1036.

Kuznetsov, S.A., and Gelfand, V.I. (1987). 18 kDa microtubule-associated protein: identification as a new light chain (LC-3) of microtubule-associated protein 1 (MAP-1). FEBS Lett *212*, 145-148.

Lamark, T., Perander, M., Outzen, H., Kristiansen, K., Overvatn, A., Michaelsen, E., Bjorkoy, G., and Johansen, T. (2003). Interaction codes within the family of

mammalian Phox and Bem1p domain-containing proteins. J Biol Chem *278*, 34568-34581.

Lamb, C.A., Yoshimori, T., and Tooze, S.A. (2013). The autophagosome: origins unknown, biogenesis complex. Nat Rev Mol Cell Biol *14*, 759-774.

Lang, T., Schaeffeler, E., Bernreuther, D., Bredschneider, M., Wolf, D.H., and Thumm, M. (1998). Aut2p and Aut7p, two novel microtubule-associated proteins are essential for delivery of autophagic vesicles to the vacuole. The EMBO journal *17*, 3597-3607.

Langston, J.W., Ballard, P., Tetrud, J.W., and Irwin, I. (1983). Chronic Parkinsonism in humans due to a product of meperidine-analog synthesis. Science *219*, 979-980.

Lazarou, M., Jin, S.M., Kane, L.A., and Youle, R.J. (2012). Role of PINK1 binding to the TOM complex and alternate intracellular membranes in recruitment and activation of the E3 ligase Parkin. Dev Cell *22*, 320-333.

Lazarou, M., Narendra, D.P., Jin, S.M., Tekle, E., Banerjee, S., and Youle, R.J. (2013). PINK1 drives Parkin self-association and HECT-like E3 activity upstream of mitochondrial binding. J Cell Biol *200*, 163-172.

Lin, W., and Kang, U.J. (2008). Characterization of PINK1 processing, stability, and subcellular localization. J Neurochem *106*, 464-474.

Liu, L., Feng, D., Chen, G., Chen, M., Zheng, Q., Song, P., Ma, Q., Zhu, C., Wang, R., Qi, W., *et al.* (2012a). Mitochondrial outer-membrane protein FUNDC1 mediates hypoxia-induced mitophagy in mammalian cells. Nat Cell Biol *14*, 177-185.

Liu, L., Sakakibara, K., Chen, Q., and Okamoto, K. (2014). Receptor-mediated mitophagy in yeast and mammalian systems. Cell Res *24*, 787-795.

Liu, S., Sawada, T., Lee, S., Yu, W., Silverio, G., Alapatt, P., Millan, I., Shen, A., Saxton, W., Kanao, T., *et al.* (2012b). Parkinson's disease-associated kinase PINK1 regulates Miro protein level and axonal transport of mitochondria. PLoS Genet *8*, e1002537.

Loson, O.C., Liu, R., Rome, M.E., Meng, S., Kaiser, J.T., Shan, S.O., and Chan, D.C. (2014). The mitochondrial fission receptor MiD51 requires ADP as a cofactor. Structure *22*, 367-377.

Luo, S.M., Ge, Z.J., Wang, Z.W., Jiang, Z.Z., Wang, Z.B., Ouyang, Y.C., Hou, Y., Schatten, H., and Sun, Q.Y. (2013). Unique insights into maternal mitochondrial inheritance in mice. Proc Natl Acad Sci U S A *110*, 13038-13043.

Luoma, P., Melberg, A., Rinne, J.O., Kaukonen, J.A., Nupponen, N.N., Chalmers, R.M., Oldfors, A., Rautakorpi, I., Peltonen, L., Majamaa, K., *et al.* (2004). Parkinsonism, premature menopause, and mitochondrial DNA polymerase gamma mutations: clinical and molecular genetic study. Lancet *364*, 875-882.

Luoma, P.T., Eerola, J., Ahola, S., Hakonen, A.H., Hellstrom, O., Kivisto, K.T., Tienari, P.J., and Suomalainen, A. (2007). Mitochondrial DNA polymerase gamma variants in idiopathic sporadic Parkinson disease. Neurology *69*, 1152-1159.

Mao, K., Wang, K., Liu, X., and Klionsky, D.J. (2013). The scaffold protein Atg11 recruits fission machinery to drive selective mitochondria degradation by autophagy. Dev Cell *26*, 9-18.

Matsumoto, G., Wada, K., Okuno, M., Kurosawa, M., and Nukina, N. (2011). Serine 403 phosphorylation of p62/SQSTM1 regulates selective autophagic clearance of ubiquitinated proteins. Mol Cell *44*, 279-289.

Meeusen, S., DeVay, R., Block, J., Cassidy-Stone, A., Wayson, S., McCaffery, J.M., and Nunnari, J. (2006). Mitochondrial inner-membrane fusion and crista maintenance requires the dynamin-related GTPase Mgm1. Cell *127*, 383-395.

Meeusen, S., McCaffery, J.M., and Nunnari, J. (2004). Mitochondrial fusion intermediates revealed in vitro. Science *305*, 1747-1752.

Meissner, C., Lorenz, H., Weihofen, A., Selkoe, D.J., and Lemberg, M.K. (2011). The mitochondrial intramembrane protease PARL cleaves human Pink1 to regulate Pink1 trafficking. J Neurochem *117*, 856-867.

Melser, S., Chatelain, E.H., Lavie, J., Mahfouf, W., Jose, C., Obre, E., Goorden, S., Priault, M., Elgersma, Y., Rezvani, H.R., *et al.* (2013). Rheb regulates mitophagy induced by mitochondrial energetic status. Cell metabolism *17*, 719-730.

Mijaljica, D., Prescott, M., and Devenish, R.J. (2011). Microautophagy in mammalian cells: revisiting a 40-year-old conundrum. Autophagy *7*, 673-682.

Mishra, P., Carelli, V., Manfredi, G., and Chan, David C. Proteolytic Cleavage of OPA1 Stimulates Mitochondrial Inner Membrane Fusion and Couples Fusion to Oxidative Phosphorylation. Cell metabolism *19*, 630-641.

Mishra, P., Carelli, V., Manfredi, G., and Chan, D.C. (2014). Proteolytic cleavage of OPA1 stimulates mitochondrial inner membrane fusion and couples fusion to oxidative phosphorylation. Cell metabolism *19*, 630-641.

Mitra, K., Wunder, C., Roysam, B., Lin, G., and Lippincott-Schwartz, J. (2009). A hyperfused mitochondrial state achieved at G1-S regulates cyclin E buildup and entry into S phase. Proc Natl Acad Sci U S A *106*, 11960-11965.

Mizushima, N., Yamamoto, A., Matsui, M., Yoshimori, T., and Ohsumi, Y. (2004). In vivo analysis of autophagy in response to nutrient starvation using transgenic mice expressing a fluorescent autophagosome marker. Mol Biol Cell *15*, 1101-1111.

Moratalla, R., Quinn, B., DeLanney, L.E., Irwin, I., Langston, J.W., and Graybiel, A.M. (1992). Differential vulnerability of primate caudate-putamen and striosome-matrix dopamine systems to the neurotoxic effects of 1-methyl-4-phenyl-1,2,3,6-tetrahydropyridine. Proc Natl Acad Sci U S A *89*, 3859-3863.

Mozdy, A.D., McCaffery, J.M., and Shaw, J.M. (2000). Dnm1p GTPase-mediated mitochondrial fission is a multi-step process requiring the novel integral membrane component Fis1p. J Cell Biol *151*, 367-380.

Nakatogawa, H., Suzuki, K., Kamada, Y., and Ohsumi, Y. (2009). Dynamics and diversity in autophagy mechanisms: lessons from yeast. Nat Rev Mol Cell Biol *10*, 458-467.

Narendra, D., Kane, L.A., Hauser, D.N., Fearnley, I.M., and Youle, R.J. (2010a). p62/SQSTM1 is required for Parkin-induced mitochondrial clustering but not mitophagy; VDAC1 is dispensable for both. Autophagy *6*, 1090-1106.

Narendra, D., Tanaka, A., Suen, D.-F., and Youle, R.J. (2008). Parkin is recruited selectively to impaired mitochondria and promotes their autophagy. The Journal of Cell Biology *183*, 795-803.

Narendra, D.P., Jin, S.M., Tanaka, A., Suen, D.F., Gautier, C.A., Shen, J., Cookson, M.R., and Youle, R.J. (2010b). PINK1 is selectively stabilized on impaired mitochondria to activate Parkin. PLoS Biol *8*, e1000298.

Neutzner, A., Benard, G., Youle, R.J., and Karbowski, M. (2008). Role of the ubiquitin conjugation system in the maintenance of mitochondrial homeostasis. Ann N Y Acad Sci *1147*, 242-253.

Nicklas, W.J., Vyas, I., and Heikkila, R.E. (1985). Inhibition of NADH-linked oxidation in brain mitochondria by 1-methyl-4-phenyl-pyridine, a metabolite of the neurotoxin, 1-methyl-4-phenyl-1,2,5,6-tetrahydropyridine. Life Sci *36*, 2503-2508.

Nishimura, Y., Yoshinari, T., Naruse, K., Yamada, T., Sumi, K., Mitani, H., Higashiyama, T., and Kuroiwa, T. (2006). Active digestion of sperm mitochondrial DNA in single living sperm revealed by optical tweezers. Proc Natl Acad Sci U S A *103*, 1382-1387.

Noda, T., and Ohsumi, Y. (1998). Tor, a phosphatidylinositol kinase homologue, controls autophagy in yeast. J Biol Chem *273*, 3963-3966.

Novak, I., Kirkin, V., McEwan, D.G., Zhang, J., Wild, P., Rozenknop, A., Rogov, V., Lohr, F., Popovic, D., Occhipinti, A., *et al.* (2010). Nix is a selective autophagy receptor for mitochondrial clearance. EMBO Rep *11*, 45-51.

Okatsu, K., Saisho, K., Shimanuki, M., Nakada, K., Shitara, H., Sou, Y.S., Kimura, M., Sato, S., Hattori, N., Komatsu, M., *et al.* (2010). p62/SQSTM1 cooperates with Parkin for perinuclear clustering of depolarized mitochondria. Genes Cells *15*, 887-900.

Okatsu, K., Uno, M., Koyano, F., Go, E., Kimura, M., Oka, T., Tanaka, K., and Matsuda, N. (2013). A dimeric PINK1-containing complex on depolarized mitochondria stimulates Parkin recruitment. J Biol Chem *288*, 36372-36384.

Olichon, A., Baricault, L., Gas, N., Guillou, E., Valette, A., Belenguer, P., and Lenaers, G. (2003). Loss of OPA1 perturbates the mitochondrial inner membrane structure and integrity, leading to cytochrome c release and apoptosis. J Biol Chem *278*, 7743-7746.

Onoue, K., Jofuku, A., Ban-Ishihara, R., Ishihara, T., Maeda, M., Koshiba, T., Itoh, T., Fukuda, M., Otera, H., Oka, T., *et al.* (2013). Fis1 acts as a mitochondrial recruitment factor for TBC1D15 that is involved in regulation of mitochondrial morphology. J Cell Sci *126*, 176-185.

Ordureau, A., Sarraf, S.A., Duda, D.M., Heo, J.M., Jedrychowski, M.P., Sviderskiy, V.O., Olszewski, J.L., Koerber, J.T., Xie, T., Beausoleil, S.A., *et al.* (2014). Quantitative proteomics reveal a feedforward mechanism for mitochondrial PARKIN translocation and ubiquitin chain synthesis. Mol Cell *56*, 360-375.

Otera, H., Wang, C., Cleland, M.M., Setoguchi, K., Yokota, S., Youle, R.J., and Mihara, K. (2010a). Mff is an essential factor for mitochondrial recruitment of Drp1 during mitochondrial fission in mammalian cells. J Cell Biol *191*, 1141-1158.

Otera, H., Wang, C., Cleland, M.M., Setoguchi, K., Yokota, S., Youle, R.J., and Mihara, K. (2010b). Mff is an essential factor for mitochondrial recruitment of Drp1 during mitochondrial fission in mammalian cells. The Journal of Cell Biology *191*, 1141-1158.

Palacino, J.J., Sagi, D., Goldberg, M.S., Krauss, S., Motz, C., Wacker, M., Klose, J., and Shen, J. (2004). Mitochondrial dysfunction and oxidative damage in parkin-deficient mice. J Biol Chem *279*, 18614-18622.

Palikaras, K., and Tavernarakis, N. (2012). Mitophagy in neurodegeneration and aging. Frontiers in genetics *3*, 297.

Palmer, C.S., Osellame, L.D., Laine, D., Koutsopoulos, O.S., Frazier, A.E., and Ryan, M.T. (2011). MiD49 and MiD51, new components of the mitochondrial fission machinery. EMBO Rep *12*, 565-573.

Pankiv, S., Clausen, T.H., Lamark, T., Brech, A., Bruun, J.A., Outzen, H., Overvatn, A., Bjorkoy, G., and Johansen, T. (2007). p62/SQSTM1 binds directly to Atg8/LC3 to facilitate degradation of ubiquitinated protein aggregates by autophagy. J Biol Chem *282*, 24131-24145.

Papa, S., De Rasmo, D., Scacco, S., Signorile, A., Technikova-Dobrova, Z., Palmisano, G., Sardanelli, A.M., Papa, F., Panelli, D., Scaringi, R., *et al.* (2008). Mammalian complex I: a regulable and vulnerable pacemaker in mitochondrial respiratory function. Biochim Biophys Acta *1777*, 719-728.

Park, J., Lee, S.B., Lee, S., Kim, Y., Song, S., Kim, S., Bae, E., Kim, J., Shong, M., Kim, J.M., *et al.* (2006). Mitochondrial dysfunction in Drosophila PINK1 mutants is complemented by parkin. Nature *441*, 1157-1161.

Pennathur, S., Jackson-Lewis, V., Przedborski, S., and Heinecke, J.W. (1999). Mass spectrometric quantification of 3-nitrotyrosine, ortho-tyrosine, and o,o'-dityrosine in brain tissue of 1-methyl-4-phenyl-1,2,3, 6-tetrahydropyridine-treated mice, a model of oxidative stress in Parkinson's disease. J Biol Chem *274*, 34621-34628.

Pham, A.H., McCaffery, J.M., and Chan, D.C. (2012). Mouse lines with photo-activatable mitochondria (PhAM) to study mitochondrial dynamics. Genesis (New York, NY : 2000) *50*, 833-843.

Pickrell, A.M., and Youle, R.J. (2015). The roles of PINK1, parkin, and mitochondrial fidelity in Parkinson's disease. Neuron *85*, 257-273.

Plun-Favreau, H., Klupsch, K., Moisoi, N., Gandhi, S., Kjaer, S., Frith, D., Harvey, K., Deas, E., Harvey, R.J., McDonald, N., *et al.* (2007). The mitochondrial protease HtrA2 is regulated by Parkinson's disease-associated kinase PINK1. Nat Cell Biol *9*, 1243-1252.

Poole, A.C., Thomas, R.E., Yu, S., Vincow, E.S., and Pallanck, L. (2010). The mitochondrial fusion-promoting factor mitofusin is a substrate of the PINK1/parkin pathway. PLoS One *5*, e10054.

Pridgeon, J.W., Olzmann, J.A., Chin, L.S., and Li, L. (2007). PINK1 protects against oxidative stress by phosphorylating mitochondrial chaperone TRAP1. PLoS Biol *5*, e172.

Przedborski, S., Jackson-Lewis, V., Yokoyama, R., Shibata, T., Dawson, V.L., and Dawson, T.M. (1996). Role of neuronal nitric oxide in 1-methyl-4-phenyl-1,2,3,6-tetrahydropyridine (MPTP)-induced dopaminergic neurotoxicity. Proc Natl Acad Sci U S A *93*, 4565-4571.

Rambold, A.S., Kostelecky, B., Elia, N., and Lippincott-Schwartz, J. (2011). Tubular network formation protects mitochondria from autophagosomal degradation during nutrient starvation. Proc Natl Acad Sci U S A *108*, 10190-10195.

Ramirez, A., Heimbach, A., Grundemann, J., Stiller, B., Hampshire, D., Cid, L.P., Goebel, I., Mubaidin, A.F., Wriekat, A.L., Roeper, J., *et al.* (2006). Hereditary parkinsonism with dementia is caused by mutations in ATP13A2, encoding a lysosomal type 5 P-type ATPase. Nat Genet *38*, 1184-1191.

Ramsay, R.R., Salach, J.I., Dadgar, J., and Singer, T.P. (1986). Inhibition of mitochondrial NADH dehydrogenase by pyridine derivatives and its possible relation to experimental and idiopathic parkinsonism. Biochemical and biophysical research communications *135*, 269-275.

Rantanen, A., Jansson, M., Oldfors, A., and Larsson, N.G. (2001). Downregulation of Tfam and mtDNA copy number during mammalian spermatogenesis. Mammalian genome : official journal of the International Mammalian Genome Society *12*, 787-792.

Rantanen, A., and Larsson, N.G. (2000). Regulation of mitochondrial DNA copy number during spermatogenesis. Human reproduction (Oxford, England) *15 Suppl 2*, 86-91.

Ravikumar, B., Vacher, C., Berger, Z., Davies, J.E., Luo, S., Oroz, L.G., Scaravilli, F., Easton, D.F., Duden, R., O'Kane, C.J., *et al.* (2004). Inhibition of mTOR induces autophagy and reduces toxicity of polyglutamine expansions in fly and mouse models of Huntington disease. Nat Genet *36*, 585-595.

Reeve, A.K., Krishnan, K.J., and Turnbull, D. (2008). Mitochondrial DNA mutations in disease, aging, and neurodegeneration. Ann N Y Acad Sci *1147*, 21-29.

Richard, V.R., Leonov, A., Beach, A., Burstein, M.T., Koupaki, O., Gomez-Perez, A., Levy, S., Pluska, L., Mattie, S., Rafesh, R., *et al.* (2013). Macromitophagy is a longevity assurance process that in chronologically aging yeast limited in calorie supply sustains functional mitochondria and maintains cellular lipid homeostasis. Aging *5*, 234-269.

Rojo, M., Legros, F., Chateau, D., and Lombes, A. (2002). Membrane topology and mitochondrial targeting of mitofusins, ubiquitous mammalian homologs of the transmembrane GTPase Fzo. J Cell Sci *115*, 1663-1674.

Rossignol, R., Faustin, B., Rocher, C., Malgat, M., Mazat, J.P., and Letellier, T. (2003). Mitochondrial threshold effects. Biochem J *370*, 751-762.

Rote, K.V., and Rechsteiner, M. (1983). Degradation of microinjected proteins: effects of lysosomotropic agents and inhibitors of autophagy. Journal of cellular physiology *116*, 103-110.

Rozenknop, A., Rogov, V.V., Rogova, N.Y., Lohr, F., Guntert, P., Dikic, I., and Dotsch, V. (2011). Characterization of the interaction of GABARAPL-1 with the LIR motif of NBR1. J Mol Biol *410*, 477-487.

Rui, Y.N., Xu, Z., Patel, B., Chen, Z., Chen, D., Tito, A., David, G., Sun, Y., Stimming, E.F., Bellen, H.J., *et al.* (2015). Huntingtin functions as a scaffold for selective macroautophagy. Nat Cell Biol *17*, 262-275.

Sandoval, H., Thiagarajan, P., Dasgupta, S.K., Schumacher, A., Prchal, J.T., Chen, M., and Wang, J. (2008). Essential role for Nix in autophagic maturation of erythroid cells. Nature *454*, 232-235.

Sarraf, S.A., Raman, M., Guarani-Pereira, V., Sowa, M.E., Huttlin, E.L., Gygi, S.P., and Harper, J.W. (2013). Landscape of the PARKIN-dependent ubiquitylome in response to mitochondrial depolarization. Nature *496*, 372-376.

Sato, M., and Sato, K. (2011). Degradation of paternal mitochondria by fertilization-triggered autophagy in C. elegans embryos. Science *334*, 1141-1144.

Sawada, H., Sakai, N., Abe, Y., Tanaka, E., Takahashi, Y., Fujino, J., Kodama, E., Takizawa, S., and Yokosawa, H. (2002). Extracellular ubiquitination and proteasome-mediated degradation of the ascidian sperm receptor. Proc Natl Acad Sci U S A *99*, 1223-1228.

Schapira, A.H. (2006). Mitochondrial disease. Lancet *368*, 70-82.

Schweers, R.L., Zhang, J., Randall, M.S., Loyd, M.R., Li, W., Dorsey, F.C., Kundu, M., Opferman, J.T., Cleveland, J.L., Miller, J.L., *et al.* (2007). NIX is required for programmed mitochondrial clearance during reticulocyte maturation. Proc Natl Acad Sci U S A *104*, 19500-19505.

Scott, R.C., Schuldiner, O., and Neufeld, T.P. (2004). Role and regulation of starvation-induced autophagy in the Drosophila fat body. Dev Cell *7*, 167-178.

Sengupta, S., Peterson, T.R., and Sabatini, D.M. (2010). Regulation of the mTOR complex 1 pathway by nutrients, growth factors, and stress. Mol Cell *40*, 310-322.

Sha, D., Chin, L.S., and Li, L. (2010). Phosphorylation of parkin by Parkinson disease-linked kinase PINK1 activates parkin E3 ligase function and NF-kappaB signaling. Hum Mol Genet *19*, 352-363.

Shen, Q., Yamano, K., Head, B.P., Kawajiri, S., Cheung, J.T., Wang, C., Cho, J.H., Hattori, N., Youle, R.J., and van der Bliek, A.M. (2014). Mutations in Fis1 disrupt orderly disposal of defective mitochondria. Mol Biol Cell *25*, 145-159.

Shi, J., Fung, G., Deng, H., Zhang, J., Fiesel, F.C., Springer, W., Li, X., and Luo, H. (2015). NBR1 is dispensable for PARK2-mediated mitophagy regardless of the presence or absence of SQSTM1. Cell Death Dis *6*, e1943.

Shiba-Fukushima, K., Imai, Y., Yoshida, S., Ishihama, Y., Kanao, T., Sato, S., and Hattori, N. (2012). PINK1-mediated phosphorylation of the Parkin ubiquitin-like domain primes mitochondrial translocation of Parkin and regulates mitophagy. Sci Rep *2*, 1002.

Shpilka, T., Weidberg, H., Pietrokovski, S., and Elazar, Z. (2011). Atg8: an autophagy-related ubiquitin-like protein family. Genome Biol *12*, 226.

Silvestri, L., Caputo, V., Bellacchio, E., Atorino, L., Dallapiccola, B., Valente, E.M., and Casari, G. (2005). Mitochondrial import and enzymatic activity of PINK1 mutants associated to recessive parkinsonism. Hum Mol Genet *14*, 3477-3492.

Sims, J.J., Scavone, F., Cooper, E.M., Kane, L.A., Youle, R.J., Boeke, J.D., and Cohen, R.E. (2012). Polyubiquitin-sensor proteins reveal localization and linkage-type dependence of cellular ubiquitin signaling. Nat Methods *9*, 303-309.

Smirnova, E., Griparic, L., Shurland, D.L., and van der Bliek, A.M. (2001). Dynamin-related protein Drp1 is required for mitochondrial division in mammalian cells. Mol Biol Cell *12*, 2245-2256.

Song, W.-H., Ballard, J.W.O., Yi, Y.-J., and Sutovsky, P. (2014). Regulation of Mitochondrial Genome Inheritance by Autophagy and Ubiquitin-Proteasome System: Implications for Health, Fitness, and Fertility. BioMed Research International *2014*, 981867.

Song, Z., Chen, H., Fiket, M., Alexander, C., and Chan, D.C. (2007). OPA1 processing controls mitochondrial fusion and is regulated by mRNA splicing, membrane potential, and Yme1L. J Cell Biol *178*, 749-755.

Song, Z., Ghochani, M., McCaffery, J.M., Frey, T.G., and Chan, D.C. (2009). Mitofusins and OPA1 mediate sequential steps in mitochondrial membrane fusion. Mol Biol Cell *20*, 3525-3532.

Sou, Y.S., Waguri, S., Iwata, J., Ueno, T., Fujimura, T., Hara, T., Sawada, N., Yamada, A., Mizushima, N., Uchiyama, Y., *et al.* (2008). The Atg8 conjugation system is indispensable for proper development of autophagic isolation membranes in mice. Mol Biol Cell *19*, 4762-4775.

Spillantini, M.G., Schmidt, M.L., Lee, V.M., Trojanowski, J.Q., Jakes, R., and Goedert, M. (1997). Alpha-synuclein in Lewy bodies. Nature *388*, 839-840.

St John, J., Sakkas, D., Dimitriadi, K., Barnes, A., Maclin, V., Ramey, J., Barratt, C., and De Jonge, C. (2000). Failure of elimination of paternal mitochondrial DNA in abnormal embryos. Lancet *355*, 200.

Sugiura, A., McLelland, G.L., Fon, E.A., and McBride, H.M. (2014). A new pathway for mitochondrial quality control: mitochondrial-derived vesicles. The EMBO journal *33*, 2142-2156.

Sutovsky, P., Moreno, R.D., Ramalho-Santos, J., Dominko, T., Simerly, C., and Schatten, G. (1999). Ubiquitin tag for sperm mitochondria. Nature *402*, 371-372.

Sutovsky, P., Moreno, R.D., Ramalho-Santos, J., Dominko, T., Simerly, C., and Schatten, G. (2000). Ubiquitinated sperm mitochondria, selective proteolysis, and the regulation of mitochondrial inheritance in mammalian embryos. Biol Reprod *63*, 582-590.

Takeshige, K., Baba, M., Tsuboi, S., Noda, T., and Ohsumi, Y. (1992). Autophagy in yeast demonstrated with proteinase-deficient mutants and conditions for its induction. J Cell Biol *119*, 301-311.

Tanaka, A., Cleland, M.M., Xu, S., Narendra, D.P., Suen, D.F., Karbowski, M., and Youle, R.J. (2010). Proteasome and p97 mediate mitophagy and degradation of mitofusins induced by Parkin. J Cell Biol *191*, 1367-1380.

Tang, F., Wang, B., Li, N., Wu, Y., Jia, J., Suo, T., Chen, Q., Liu, Y.-J., and Tang, J. (2011). RNF185, a Novel Mitochondrial Ubiquitin E3 Ligase, Regulates Autophagy through Interaction with BNIP1. PLoS ONE *6*, e24367.

Tanida, I., Komatsu, M., Ueno, T., and Kominami, E. (2003). GATE-16 and GABARAP are authentic modifiers mediated by Apg7 and Apg3. Biochemical and biophysical research communications *300*, 637-644.

Taylor, E.B., and Rutter, J. (2011). Mitochondrial quality control by the ubiquitin-proteasome system. Biochemical Society transactions *39*, 1509-1513.

Thomas, K.J., McCoy, M.K., Blackinton, J., Beilina, A., van der Brug, M., Sandebring, A., Miller, D., Maric, D., Cedazo-Minguez, A., and Cookson, M.R.

(2011). DJ-1 acts in parallel to the PINK1/parkin pathway to control mitochondrial function and autophagy. Hum Mol Genet *20*, 40-50.

Thomas, R.E., Andrews, L.A., Burman, J.L., Lin, W.Y., and Pallanck, L.J. (2014). PINK1-Parkin pathway activity is regulated by degradation of PINK1 in the mitochondrial matrix. PLoS Genet *10*, e1004279.

Thompson, W.E., Ramalho-Santos, J., and Sutovsky, P. (2003). Ubiquitination of prohibitin in mammalian sperm mitochondria: possible roles in the regulation of mitochondrial inheritance and sperm quality control. Biol Reprod *69*, 254-260.

Thumm, M., Egner, R., Koch, B., Schlumpberger, M., Straub, M., Veenhuis, M., and Wolf, D.H. (1994). Isolation of autophagocytosis mutants of Saccharomyces cerevisiae. FEBS Lett *349*, 275-280.

Tondera, D., Grandemange, S., Jourdain, A., Karbowski, M., Mattenberger, Y., Herzig, S., Da Cruz, S., Clerc, P., Raschke, I., Merkwirth, C., *et al.* (2009). SLP-2 is required for stress-induced mitochondrial hyperfusion. The EMBO journal *28*, 1589-1600.

Tooze, S.A. (2013). Current views on the source of the autophagosome membrane. Essays Biochem *55*, 29-38.

Trifunovic, A., and Larsson, N.G. (2008). Mitochondrial dysfunction as a cause of ageing. J Intern Med *263*, 167-178.

Tsukada, M., and Ohsumi, Y. (1993). Isolation and characterization of autophagy-defective mutants of Saccharomyces cerevisiae. FEBS Lett *333*, 169-174.

Tsukamoto, S., Kuma, A., Murakami, M., Kishi, C., Yamamoto, A., and Mizushima, N. (2008). Autophagy is essential for preimplantation development of mouse embryos. Science *321*, 117-120.

Twig, G., Elorza, A., Molina, A.J.A., Mohamed, H., Wikstrom, J.D., Walzer, G., Stiles, L., Haigh, S.E., Katz, S., Las, G., *et al.* (2008). Fission and selective fusion govern mitochondrial segregation and elimination by autophagy. The EMBO journal *27*, 433-446.

Uttara, B., Singh, A.V., Zamboni, P., and Mahajan, R.T. (2009). Oxidative Stress and Neurodegenerative Diseases: A Review of Upstream and Downstream Antioxidant Therapeutic Options. Current Neuropharmacology *7*, 65-74.

Valente, E.M., Abou-Sleiman, P.M., Caputo, V., Muqit, M.M., Harvey, K., Gispert, S., Ali, Z., Del Turco, D., Bentivoglio, A.R., Healy, D.G., *et al.* (2004). Hereditary early-onset Parkinson's disease caused by mutations in PINK1. Science *304*, 1158-1160.

van Wijk, S.J., Fiskin, E., Putyrski, M., Pampaloni, F., Hou, J., Wild, P., Kensche, T., Grecco, H.E., Bastiaens, P., and Dikic, I. (2012). Fluorescence-based sensors to monitor localization and functions of linear and K63-linked ubiquitin chains in cells. Mol Cell *47*, 797-809.

Varastet, M., Riche, D., Maziere, M., and Hantraye, P. (1994). Chronic MPTP treatment reproduces in baboons the differential vulnerability of mesencephalic dopaminergic neurons observed in Parkinson's disease. Neuroscience *63*, 47-56.

Wang, X., Winter, D., Ashrafi, G., Schlehe, J., Wong, Y.L., Selkoe, D., Rice, S., Steen, J., LaVoie, M.J., and Schwarz, T.L. (2011). PINK1 and Parkin target Miro for phosphorylation and degradation to arrest mitochondrial motility. Cell *147*, 893-906.

Wei, Y.H. (1998). Mitochondrial DNA mutations and oxidative damage in aging and diseases: an emerging paradigm of gerontology and medicine. Proceedings of the National Science Council, Republic of China Part B, Life sciences *22*, 55-67.

Whitworth, A.J., Theodore, D.A., Greene, J.C., Benes, H., Wes, P.D., and Pallanck, L.J. (2005). Increased glutathione S-transferase activity rescues dopaminergic neuron loss in a Drosophila model of Parkinson's disease. Proc Natl Acad Sci U S A *102*, 8024-8029.

Williams, J.A., Ni, H.M., Ding, Y., and Ding, W.X. (2015). Parkin regulates mitophagy and mitochondrial function to protect against alcohol-induced liver injury and steatosis in mice. American journal of physiology Gastrointestinal and liver physiology *309*, G324-340.

Winklhofer, K.F., and Haass, C. (2010). Mitochondrial dysfunction in Parkinson's disease. Biochim Biophys Acta *1802*, 29-44.

Wu, W., Tian, W., Hu, Z., Chen, G., Huang, L., Li, W., Zhang, X., Xue, P., Zhou, C., Liu, L., *et al.* (2014). ULK1 translocates to mitochondria and phosphorylates FUNDC1 to regulate mitophagy. EMBO Reports *15*, 566-575.

Wurzer, B., Zaffagnini, G., Fracchiolla, D., Turco, E., Abert, C., Romanov, J., and Martens, S. (2015). Oligomerization of p62 allows for selection of ubiquitinated cargo and isolation membrane during selective autophagy. eLife *4*, e08941.

Xiong, H., Wang, D., Chen, L., Choo, Y.S., Ma, H., Tang, C., Xia, K., Jiang, W., Ronai, Z., Zhuang, X., *et al.* (2009). Parkin, PINK1, and DJ-1 form a ubiquitin E3 ligase complex promoting unfolded protein degradation. J Clin Invest *119*, 650-660.

Yamano, K., Fogel, A.I., Wang, C., van der Bliek, A.M., and Youle, R.J. (2014). Mitochondrial Rab GAPs govern autophagosome biogenesis during mitophagy. Elife *3*, e01612.

Yamano, K., and Youle, R.J. (2013). PINK1 is degraded through the N-end rule pathway. Autophagy *9*, 1758-1769.

Yang, J.Y., and Yang, W.Y. (2013). Bit-by-bit autophagic removal of parkin-labelled mitochondria. Nature communications *4*, 2428.

Yang, Y., Gehrke, S., Imai, Y., Huang, Z., Ouyang, Y., Wang, J.W., Yang, L., Beal, M.F., Vogel, H., and Lu, B. (2006). Mitochondrial pathology and muscle and dopaminergic neuron degeneration caused by inactivation of Drosophila Pink1 is rescued by Parkin. Proc Natl Acad Sci U S A *103*, 10793-10798.

Yang, Y., Ouyang, Y., Yang, L., Beal, M.F., McQuibban, A., Vogel, H., and Lu, B. (2008). Pink1 regulates mitochondrial dynamics through interaction with the fission/fusion machinery. Proc Natl Acad Sci U S A *105*, 7070-7075.

Yoon, Y., Krueger, E.W., Oswald, B.J., and McNiven, M.A. (2003). The mitochondrial protein hFis1 regulates mitochondrial fission in mammalian cells through an interaction with the dynamin-like protein DLP1. Molecular and cellular biology *23*, 5409-5420.

Yoshii, S.R., Kishi, C., Ishihara, N., and Mizushima, N. (2011). Parkin mediates proteasome-dependent protein degradation and rupture of the outer mitochondrial membrane. J Biol Chem *286*, 19630-19640.

Yun, J., Puri, R., Yang, H., Lizzio, M.A., Wu, C., Sheng, Z.H., and Guo, M. (2014). MUL1 acts in parallel to the PINK1/parkin pathway in regulating mitofusin and compensates for loss of PINK1/parkin. Elife *3*, e01958.

Zhao, J., Liu, T., Jin, S., Wang, X., Qu, M., Uhlen, P., Tomilin, N., Shupliakov, O., Lendahl, U., and Nister, M. (2011). Human MIEF1 recruits Drp1 to mitochondrial outer membranes and promotes mitochondrial fusion rather than fission. The EMBO journal *30*, 2762-2778.

Zhou, C., Huang, Y., Shao, Y., May, J., Prou, D., Perier, C., Dauer, W., Schon, E.A., and Przedborski, S. (2008). The kinase domain of mitochondrial PINK1 faces the cytoplasm. Proc Natl Acad Sci U S A *105*, 12022-12027.

Ziviani, E., Tao, R.N., and Whitworth, A.J. (2010). Drosophila parkin requires PINK1 for mitochondrial translocation and ubiquitinates mitofusin. Proc Natl Acad Sci U S A *107*, 5018-5023.

Chapter 2

PARKIN AND MUL1 PROMOTE MITOPHAGIC ELIMINATION OF PATERNAL MITOCHONDRIA IN MOUSE EMBRYOS

Rebecca Rojansky[1] and David C. Chan[1]

[1]Division of Biology and Biological Engineering
California Institute of Technology
Pasadena, CA 91125

This chapter is being reviewed by *Science*.

ABSTRACT

A defining feature of mitochondria is their maternal mode of inheritance. However, little is understood about the mechanism through which paternal mitochondria, delivered from the sperm, are eliminated from early mammalian embryos. We find that cultured mouse fibroblasts and early embryos use a common pathway for elimination of mitochondria. In both cases, mitochondrial elimination occurs by mitophagy, in which mitochondria are sequestered by autophagosomes and delivered to lysosomes for degradation. The E3 ubiquitin ligases PARKIN and MUL1 play redundant roles in elimination of paternal mitochondria. The process is associated with depolarization of paternal mitochondria and additionally requires the mitochondrial outer membrane protein FIS1, the autophagy adaptor P62, and PINK1 kinase. Our results elucidate the molecular mechanism of strict maternal transmission of mitochondria and uncover a collaboration between MUL1 and PARKIN in mitophagy.

One Sentence Summary: Paternal mitochondria in mouse embryos are eliminated by a mitophagic process that requires the E3 ubiquitin ligases PARKIN and MUL1.

MAIN TEXT

In most animals, including mammals, mitochondria are inherited strictly through the maternal lineage. Because sperm deliver mitochondria into the egg during fertilization, mechanisms must exist to eliminate paternal mitochondria from the early embryo. Uniparental inheritance of mitochondria ensures that only one haplotype of mitochondrial DNA (mtDNA) exists in the offspring, and this phenomenon underlies the maternal inheritance of mtDNA disease and the use of mtDNA to track human evolution. Mouse models suggest that heteroplasmy, the co-existence of more than one haplotype of mtDNA, is genetically unstable and associated with physiological abnormalities (1). In C. elegans, paternal mitochondria are eliminated by mitophagy (2, 3), whereby mitochondria are engulfed by autophagosomes and delivered to lysosomes for destruction. In D. melanogaster, paternal mitochondrial elimination involves autophagic components but occurs independently of Parkin (4), a Parkinson's disease-related E3 ubiquitin ligase that is central to the most heavily studied mitophagy pathway. It is unclear whether these insights from invertebrate model organisms extend to mammals, where the role of autophagy or even an active mechanism in paternal mitochondrial loss has been challenged (5).

We addressed this issue by first examining mitochondrial degradation in fibroblasts and then extending the study to early mouse embryos. To monitor mitophagy, we constructed a dual color fluorescence-quenching assay based on a mitochondrially localized EGFP-mCherry reporter. Normal mitochondria are

yellow, having both green and red fluorescence in the matrix, whereas mitochondria within acidic compartments show red-only fluorescence, due to the selective sensitivity of EGFP fluorescence to low pH. When mouse embryonic fibroblasts (MEFs) were cultured with a moderate concentration (10 mM) of glucose, a condition in which their metabolism relies largely on glycolysis, they showed few red-only mitochondria (Fig. 2.1A). We previously defined a glucose-free, acetoacetate-containing culture formulation that induces MEFs to upregulate OXPHOS activity (6). When cells were cultured for four days in this OXPHOS-inducing medium, many cells exhibited numerous red puncta (Fig. 2.1A), consistent with a study showing that glucose-free conditions promote increased turnover of mitochondria (7). Atg3 knockout MEFs did not form red puncta under the OXPHOS-inducing condition (Fig. 2.1B-C), indicating that formation of red puncta is dependent on the core autophagy machinery. Consistent with this idea, the level of lipidated LC3, another core component of the autophagy pathway, was elevated (Fig. 2.1D). Moreover, the red-only puncta co-localized extensively with mTurquoise2-LC3B, suggesting that they represent mitochondrial contents within the autophagosome pathway. In addition, a subset of the red puncta co-localize with LAMP1, likely indicating later intermediates that have progressed to lysosomes (Fig. 2.1F). In contrast, in glycolytic medium, mTurquoise2-LC3B did not colocalize with mitochondria (Fig. 2.1E). In addition, we found that P62, a protein implicated in autophagy (8) and mitophagy (9), localized to mitochondria only under the OXPHOS-inducing condition (Fig. 2.1G). Unlike LC3B and LAMP1, however, P62 was localized to both red punctate mitochondria and elongated

yellow mitochondria. These results indicate that the OXPHOS-inducing condition results in an increase in mitophagy intermediates.

With this cellular system, we sought to identify genes required for induced mitophagy. Previous studies suggested that mitochondrial dynamics, particularly mitochondrial fission, is important for efficient mitophagy (10, 11). To explore this idea, we examined the efficiency of OXPHOS-induced mitophagy in a panel of MEF cell lines deficient in mitochondrial fusion or fission genes: Mitofusin 1 (MFN1), Mitofusin 2 (MFN2), both MFN1 and MFN2 (MFN-dm), Optic atrophy 1 (OPA1), Mitochondrial fission factor (Mff), Dynamin-related protein 1 gene (Drp1), and Mitochondrial fission 1 (Fis1) (Fig. 2.2A). MEFs deficient in mitochondrial fusion were competent for mitophagy. In fact, MFN-dm cells and OPA1-/- cells showed substantial mitophagy even under glycolytic culture conditions, consistent with the finding that mitochondrial fusion protects against mitophagy (12, 13). Neither MFN-dm cells nor OPA1-/- cells were viable under oxidative conditions. Among cell lines deficient in mitochondrial fission, Drp1-/- and Mff-/- cells showed normal levels of mitophagy under OXPHOS conditions (Fig. 2.2A).

In contrast, Fis1-/- cells had dramatically reduced mitophagy under OXPHOS conditions (Fig. 2.2A-B), and a failure of both P62 and LC3 to co-localize with mitochondria (Fig. 2.2C-D). Although FIS1 is a central player in yeast mitochondrial fission, it does not play a prominent role in mammalian mitochondrial fission (14, 15). Instead, recent studies implicate FIS1 and its interacting protein TBC1D15 (16) in mitochondrial degradation, specifically in

PARKIN-dependent mitophagy (17, 18). Similar to Fis1 deletion, TBC1D15 knockdown efficiently blocked mitophagy and decreased LC3 and P62 localization to mitochondria (Fig. 2.2C-E). Because depletion of either FIS1 or TBC1D15 blocked mitophagy and abolished P62 localization to mitochondria, we tested whether P62 is required for mitophagy. Cells knocked down for P62, as well as p62 knockout cells, were deficient for OXPHOS-induced mitophagy (Fig. 2.2C, E; Fig. 2.S1A-B) and showed reduced mTurquoise2-LC3B localization to mitochondria. Conversely, expression of mTurquoise2-P62 restored red puncta formation in p62 knockout cells, consistent with a role for P62 in OXPHOS-induced mitophagy (Fig. 2.S1C). Taken together, these results place FIS1 and TBC1D15 upstream of P62 in promoting autophagic engulfment of mitochondria.

Because PINK1 and PARKIN (PARK2) are central components of the most widely studied pathway for mitophagy (19), we tested the role of these molecules in our mitophagy assay. Pink1-/- cells showed a substantial reduction in OXPHOS-induced mitophagy. Parkin knockout MEFs had normal mitophagy (Fig. 2.3A-B), a surprising observation given that PINK1 is known to operate upstream of PARKIN (20-22). This observation suggests that another molecule may compensate for the loss of PARKIN. Recently, the mitochondrial E3 ligase MULAN (MUL1/MAPL), has been shown to act in parallel to the PINK1/PARKIN pathway in ubiquitination and proteasomal degradation of mitofusin (23). We hypothesized that MULAN might work in parallel with PARKIN in OXPHOS-induced mitophagy, such that its presence would maintain mitophagy in the absence of PARKIN. Indeed, knockdown of MULAN by either of two independent shRNAs in the Parkin

knockout cell abolished mitophagy (Fig. 2.3A-B; Fig. 2.S1D). In contrast, loss of MULAN alone did not inhibit mitophagy. Inhibition of mitophagy due to loss of PINK1 or PARKIN/MULAN prevented co-localization of LC3 with mitochondria (Fig. 2.3C). These results reveal that MULAN and PARKIN have redundant functions in mitophagy.

We found that mitochondria from cells grown in OXPHOS media are ubiquitinated at least two-fold more than cells grown in glycolytic media (Fig. 2.3D,E). Loss of MULAN or PARKIN alone had little or no effect on the induction of mitochondrial ubiquitination under OXPHOS conditions. However, loss of both MULAN and PARKIN, or PINK1 alone, substantially reduced the ubiquitination of mitochondria, down to the level of glycolytic conditions (Fig. 2.3D,E). Taken together, these data suggest that MULAN and PARKIN act in concert to ubiquitinate mitochondrial substrates, and that a threshold level of ubiquitination may be required to sustain mitophagy under OXPHOS conditions. The level of mitochondrial ubiquitination is known to dynamically regulate mitophagy (24, 25).

With these molecular insights from the cellular assay, we tested whether the same pathway is involved in elimination of paternal mitochondria in the early embryo. To track paternal mitochondria, we utilized male PhAM mice, in which all mitochondria, including those in the sperm midpiece, are labeled with a mitochondrially-targeted version of the photoconvertable Dendra2 fluorescent protein (26) (Fig. 2.S2A). When male PhAM mice were mated with wild-type females, the resulting embryos contained brightly fluorescent paternal mitochondria. At 12 hours post-fertilization (Fig. 2.S2B), the paternal mitochondria

were found in a linear cluster, reflecting their original organization in the sperm midpiece. At 36 hours after fertilization (Fig. 2.S2C), this cluster began to disperse in cultured embryos, and thereafter, individual mitochondria were dispersed in the blastomeres. Over the next 2 days, paternal mitochondrial content progressively decreased (Fig. 2.S2D-F). At 84 hours after fertilization, 60-80% of embryos had lost all paternal mitochondria and the average number of paternal mitochondria per embryo had dropped to less than 5 (Fig. 2.S2E).

Because the time course of paternal mitochondrial loss was reproducible, we could test the role of the mitophagy proteins identified in our cell culture system. We microinjected 1-cell stage zygotes with lentivirus encoding mCherry and shRNA targeting mitophagy genes (Fig. 2.4A). Injected embryos began expressing the mCherry reporter within 48 hours of injection, 60 hours after fertilization (Fig. 2.S2G). We found that embryos expressing shRNA against P62, TBC1D15, or PINK1 showed strong suppression of paternal mitochondrial loss, compared to embryos expressing a non-targeting shRNA (Fig. 2.4B). When these mitophagy genes were knocked down, the majority of embryos retained five or more distinct clusters of paternal mitochondria (Fig. 2.4C). In contrast, less than 20% of embryos containing non-targeting shRNA retained significant paternal mitochondria, with the majority of embryos showing complete loss of paternal mitochondria. Depletion of either PARKIN or MULAN alone modestly reduced paternal mitochondrial elimination, but depletion of both had a severe effect. Although FIS1 is a key molecule in the OXPHOS-induced mitophagy pathway, the relevant FIS1 molecules are likely to be contributed by the sperm and not the egg.

Our shRNA approach can only knockdown proteins synthesized within the embryo. To circumvent this issue, we developed a dominant negative version of FIS1 (FIS1-DN) that lacks the C-terminal transmembrane domain. Retroviral overexpression of the FIS1-DN protein in MEFs strongly inhibits OXPHOS mitophagy (Fig. 2.S3A-B). FIS1-DN shows diffuse cytosolic localization (Fig. 2.S3C), consistent with the role of the transmembrane segment in mitochondrial localization. When FIS1-DN was expressed in embryos, we found that loss of paternal mitochondria was strongly inhibited, with less than 20% of embryos showing loss of paternal mitochondria (Fig. 2.4D-E).

The signal for selective degradation of paternal mitochondria in mammals is unknown, but some other forms of mitophagy are triggered by loss of mitochondrial membrane potential. Using the cationic dye TMRE (tetramethylrhodamine ethyl ester), we found robust staining of sperm isolated from the caudal epididymis of PhAM male mice, indicating intact mitochondrial membrane potential (Fig. 2.S4A,C). At 18 hours after fertilization, paternal mitochondria remained in a linear cluster and stained robustly with TMRE. However, over the next 36 hours, paternal mitochondria gradually lost TMRE staining, such that at 48 hours and later, nearly all paternal mitochondria failed to stain with TMRE, indicating a progressive and selective loss of membrane potential in paternal mitochondria (Fig. 2.S4B-C).

Our results indicate that uniparental inheritance of mitochondria in mouse occurs through a mitophagic process that eliminates paternal mitochondria. We find that either PARKIN or MULAN is sufficient to promote this process and

OXPHOS-induced mitophagy in MEFs. The redundant function of MULAN likely explains why PARKIN knockout mice show surprisingly mild and inconsistent mitochondrial phenotypes (27, 28). Upon entering the egg, sperm mitochondria progressively lose membrane potential, likely triggering activation of the PINK1/PARKIN and MULAN pathways to selectively ubiquitinate these mitochondria. Although uniparental inheritance of mitochondria is nearly universal in animals, its physiological function remains mysterious. The identification of molecules essential for this process may facilitate examination of this issue.

MATERIALS AND METHODS

Antibodies

The following commercially available antibodies were used: anti-actin (Mab1501R, Millipore), anti-Hsp60 (SC-1054, Santa Cruz Biotech), anti-Lamp1 (1D4B, Developmental Studies Hybridoma Bank), anti-P62 (PM045, MBL), anti-LC3B (2775S, Cell Signaling), anti-c-Myc (C3956, Sigma), and anti-Ubiquitin (P4D1, Cell Signaling).

Immunostaining

For immunofluorescence experiments, cells were fixed with 10% formalin, permeabilized with 0.1% Triton X-100 and stained with the primary antibodies listed above and with the following secondary antibodies: goat anti-mouse Alexa Fluor 633, donkey anti-goat Alexa Fluor 546, goat anti-rabbit Alexa Fluor 488, goat anti-rabbit Alexa Fluor 633 (Invitrogen). When used, DAPI (d1306, Invitrogen) was included in the last wash.

shRNA virus design and production

For experiments in MEFs, the retroviral vector pRetroX-H1, which contains the H1 promoter, was used to express shRNAs. shRNAs were cloned into the BglII/EcoRI sites. For embryo injection experiments, a third-generation lentiviral backbone was used to express shRNAs. The lentiviral vector FUGW-H1 (29) was modified by replacing the GFP reporter gene with mCherry and changing the shRNA cloning sites from Xba/SmaI to BamHI/EcoRI, generating FUChW-H1.

For dual knockdown experiments in embryos, a second H1 promoter was added, along with XbaI/NheI cloning sites 3' to the original H1 promoter, generating FUChW-H1H1.

The shRNA target sequences were:

p62:	TGGCCACTCTTTAGTGTTTGTGT
Tbc1d15:	GTGAGCGGGAAGATTATAT
Mulan sh1:	GAGCTAAGAAGATTCATCT
Mulan sh2:	GAGCTGTGCGGTCTGTTAA
Pink1:	GGCTGACAGGCTGAGAGAGAA
Parkin:	CCTCCAAGGAAACCATCAA
Non-targeting:	GACTAGAAGGCACAGAGGG

Lentiviral vectors were cotransfected into 293T cells with plasmids pMDLG/pRRE, pIVS-VSVG, and pRSV-Rev. Retroviral vectors were cotransfected into 293T cells with plasmids pVSVG and pUMVC. All transfections were done using calcium phosphate precipitation. For microinjection, virus was collected, filtered, concentrated by ultracentrifugation at 25,000 rpm for 2 hours, resuspended in PBS and stored at -80°C as described previously (30, 31). Viral titers were measured by infecting MEFs with serial dilutions of viral preparations, followed by flow cytometric analysis after 48 hr. Virus was used at 1x107 transducing units/μL.

Embryo microinjection

All mouse work was done according to protocols approved by the Institutional Animal Care and Use Committee at the California Institute of Technology. For each experiment, four C57/Bl6J wildtype female mice at 21-25 days old were superovulated by hormone priming as described previously (31), and then each was caged with a PhAM male (26). After euthanization of females by CO2 asphyxiation, the embryos were harvested and placed in M2 medium (MR-015-D, Millipore) at 12 hours after fertilization as described in (31). Approximately 60 to 100 embryos were collected per experiment. Embryos were divided into two equal groups and microinjected with 10 to 100 pl of viral stock into the perivitelline space as described in (30, 31). Embryos were washed with KSOM+AA medium (MR-106-D, Millipore) and cultured in that medium covered by oil (M8410, Sigma) at 37°C and 5% CO2. For each construct, at least three separate microinjection sessions were performed. In preparation for imaging, embryos were transferred to 10 µl droplets of KSOM+AA medium on glass-bottom dishes (FD35-100, World Precision Instruments).

Imaging

All images were acquired with a Zeiss LSM 710 confocal microscope with a Plan-Apochromat 63X/1.4 oil objective. All live imaging was performed in an incubated microscope stage at 37°C and 5% CO2. The 488 nm and 561 nm laser lines were used to excite cox8-EGFP-mCherry and imaging was done in line mode to minimize movement of mitochondria between acquisition of each channel. The 405 nm laser line was used to excite mTurquoise2 and DAPI. Alexa 488, Alexa

546, and Alexa 633, conjugated dyes were excited by the 488 nm laser, 561 nm laser, and the 633 nm laser, respectively.

For embryo imaging, optical slices were acquired at 1.1-μm thickness, and z stacks were oversampled at 0.467 μm. The 488 nm laser line was used to excite Dendra2 in the unconverted state. The mercury lamp was not used to avoid photoconversion. The same settings were used across all embryo-imaging experiments. Zen 2009 image analysis software was used to produce maximum intensity z-projections.

Isolation of spermatocytes

Sperm were isolated from 4-month-old PhAM male mice. Longitudinal cuts were made in the cauda epididymis and the tissue was incubated in PBS at 37°C to enable motile, mature sperm to swim out.

Membrane potential measurements

TMRE fluorescence was used to monitor mitochondrial membrane potential in spermatocytes and embryos. Samples were loaded with 20 nM TMRE for 20 min at 37°C and then washed into PBS (spermatocytes) or KSOM+AA (embryos). Samples were imaged live. Line analysis was performed using ImageJ.

Isolation of mitochondria

Mitochondria were isolated by differential centrifugation. Cells were washed in PBS, collected by scraping in isolation buffer (220 mM mannitol, 70

mM sucrose, 80 mM KCl, 5 mM MgCl2, 1 mM EGTA, 10 mM K+HEPES, pH7.4, and HALT protease inhibitors), and lysed on ice via sonication (amplitude 5, 5 seconds on, 5 seconds off, 3 cycles). Lysates were cleared of cell debris and nuclei with four 600 g spins. A crude mitochondrial fraction was isolated with a 10,000 g spin for 10 minutes and washed three times in isolation buffer.

Retroviral expression constructs

The Cox8-EGFP-mCherry retroviral vector (kindly provided by Dr. Prashant Mishra) consists of the Cox8 mitochondrial targeting sequence placed N-terminal to an EGFP- mCherry fusion. To clone mTurquoise2 fusion proteins, mTurquoise2 was amplified from pmTurquoise2-Mito (Addgene plasmid # 36208, Dorus Gadella, (32)). Human LC3B was amplified from pFCbW-EGFP-LC3. Mouse P62 was amplified from pMXs-puro GFP-p62 (Addgene plasmid # 38277, Noboru Mizushima, (33)). mTurquoise2 fusion proteins were cloned into the retroviral vector, pBABEpuro. The FIS1 dominant negative construct was cloned into pBABEpuro and consists of amino acids 1-121 of mouse FIS1, with 9 Myc tags at the N-terminus. The corresponding control construct consists of mCherry cloned into the pBABEpuro vector. All plasmids were verified by DNA sequence analysis. Stable cell lines were generated by retroviral infection followed by selection with 2 μg/μl puromycin.

Cell culture

MEFs were maintained in Dulbecco's Modified Eagle's Medium (DMEM) supplemented with 10% fetal bovine serum (FBS), 100 U/mL penicillin and 100 U/mL streptomycin at 37°C and 5% CO2. Glucose and acetoacetate containing media were made as previously described (6). For mitophagy experiments, cells were plated on Nunc Lab-Tek II Chambered Coverglass slides (155409, Thermo) in DMEM-based media. After cells had adhered, they were washed with PBS and glucose- or acetoacetate-containing medium was applied, after which cells were allowed to grow for four days and then imaged. Because cells grow more slowly in acetoacetate medium, a four-fold excess of cells was plated relative to glucose medium so that both samples were at the same density on the day of imaging.

Cell lines

The cells used included: Atg3-null MEFs (34) (kindly provided by Yu-Shin Sou and Masaaki Komatsu), p62-null MEFs (35) (kindly provided by Shun Kageyama and Masaaki Komatsu), Pink1-null, Parkin-null (both kindly provided by Clement Gautier and Jie Shen), and Drp1-null (36) (kindly provided by Katsuyoshi Mihara). MFN1-null, MFN2-null, MFN-dm, OPA1-null, Mff-null, and Fis1-null MEFs have been described previously (15, 37).

Analysis

Images were cropped when appropriate and image contrast and brightness were globally adjusted in Photoshop (Adobe). All quantifications were scored in triplicate with greater than 100 cells per experiment.

Western densitometry analysis was done using ImageJ. Density of ubiquitin signal was normalized to density of Hsp60 signal and the average of three separate experiments was taken.

For quantification of paternal mitochondria, maximum intensity z stacks were scored as having greater than 5, less than 5, or no distinct green puncta. Embryos from four females were pooled per experiment, and three or more independent replicate experiments were averaged.

FIGURE LEGENDS

Figure 2.1 Induction of mitophagy by OXPHOS-inducing medium. Mitophagy was examined in cells stably expressing Cox8-EGFP-mCherry. Wildtype (A) or *Atg3* knockout mouse embryonic fibroblasts (MEFs) (B) were grown in Glucose (Glu) or Acetoacetate (Ac) containing medium for four days and then imaged by fluorescence microscopy. The red puncta in (A) represent mitochondrial contents within acidic compartments. (C) Quantification of red-only puncta. **, $p < 0.01$. (D) Western blot analysis of LC3B expression in MEFs cultured in the indicated medium. Actin is a loading control. (E) Co-localization of LC3B with red puncta. MEFs expressing cox8-EGFP-mCherry and mTurquoise2-LC3B were grown in the indicated medium and imaged by fluorescence microscopy. Arrows indicate examples of mTurquoise2-LC3B co-localization with red mitochondrial puncta. (F) Co-localization of LAMP1 with red puncta. MEFs stably expressing cox8-EGFP-mCherry were grown in acetoacetate-containing medium and immunostained with anti-Lamp1 antibody (blue). Arrows and asterisks indicate red mitochondrial puncta that co-localized, or not, respectively, with LAMP1. Scale bar in (A) is 10 □m and applies to (A-F). (G) Co-localization of P62 with mitochondria. MEFs were grown in the indicated medium and immunostained with anti-P62 (green) and anti-HSP60 (red, mitochondrial marker). Error bars indicate SD. Scale bar, 10 μm.

Figure 2.2 Mitophagy under OXPHOS-inducing conditions requires Fis1, TBC1D15, and P62. (A) Mitophagy in cells with mutations in mitochondrial dynamics genes. MEFs of the indicated genotype were cultured in glucose or

acetoacetate medium, and mitophagy was quantified using the Cox8-EGFP-mCherry marker. (B) MEFs stably expressing Cox8-EGFP-mCherry were grown in acetoacetate containing medium and then imaged by fluorescence microscopy. *p62* and *Tbc1d15* shRNAs were stably introduced by retroviral infection. (C) Co-localization of mTurquoise2 with mitochondria. MEFs were grown in acetoacetate containing medium. Note that mTurquoise2 puncta localize to mitochondrial puncta only in WT cells. (D) Co-localization of P62 with mitochondria. MEFs were grown in acetoacetate containing medium and immunostained with anti-P62 (green) and anti-HSP60 (red). (E) Quantification of red-only puncta in WT cells and cells containing shRNA against Tbc1d15 or p62 cultured in glucose (Glu) or acetoacetate (Ac) medium. Error bars indicate SD.

Figure 2.3 MULAN and PARKIN have redundant functions in OXPHOS-induced mitophagy. (A) Quantification of red-only puncta in cells grown in the indicated medium. Presence (+) or absence (-) of *Pink1* gene, *Parkin* gene, or *Mulan* mRNA is indicated. (B) Mitophagy in wildtype and mutant cells. Cells stably expressing Cox8-EGFP-mCherry were grown in acetoacetate-containing medium and imaged by fluorescence microscopy. (C) Co-localization of LC3B with mitophagy intermediates. Wildtype and mutant cells were retrovirally transduced with mTurquoise2-LC3B, grown in acetoacetate containing medium and imaged by fluorescence microscopy. (D) Accumulation of polyubiquitinated proteins in mitochondria. Cells were grown in the indicated medium, and mitochondria were isolated by differential centrifugation. Mitochondrial lysates

were analyzed by Western blot for pan-Ubiquitin. HSP60 is a loading control. (E) Quantification of polyubiquitinated proteins in mitochondria. Three independent experiments were quantified by densitometry and averages are shown. Ubiquitin level was normalized to HSP60. Error bars indicate SD.

Figure 2.4 Clearance of paternal mitochondria in preimplantation embryos requires mitophagy genes. (A) Schematic of paternal mitochondrial elimination assay. Wildtype females are mated with *PhAM* males, whose sperm donate Dendra2-labeled mitochondria to the embryo upon fertilization. One-cell embryos are microinjected in the perivitelline space with concentrated lentivirus targeting candidate genes. During *in vitro* culture, embryos are periodically imaged live and monitored for loss of paternal mitochondria. (B) Clearance of paternal mitochondria upon inhibition of mitophagy genes. Embryos were injected with lentivirus targeting the indicated shRNA. The mitochondrial Dendra2 signal was imaged in live embryos by fluorescence microscopy at 60, 72, or 84 hours after fertilization. Images are maximum intensity projections. Scale bar, 10 μm. (C) Quantification of paternal mitochondrial elimination at 84 hours post-fertilization. Embryos were scored as having no paternal mitochondria (black bar), less than five clusters (white bar), or greater than five clusters (grey bar). Average of three independent injection experiments is shown. Error bars indicate standard deviation. (D) Clearance of paternal mitochondria in embryos expressing mCherry (control) or Fis1-DN. Same scale as (B). (E) Quantification of 84 hour results from (D). *p, <0.05; **, p<0.01;

***, $p<0.001$ (Student's t-test). *p*-values compare experimental embryos to control embryos with non-targeting shRNA or mCherry control. Error bars indicate SD.

Figure 2.S1 Defective mitophagy in *p62* and *Parkin/Mulan* deficient cells. (A) Quantification of red-only puncta in wildtype or *p62* knockout cells grown in medium containing glucose (Glu) or acetoacetate (Ac). Error bars indicate SD. (B) Representative image of *p62* knockout cell expressing cox8-EGFP-mCherry. Cells were grown in medium containing acetoacetate and imaged by fluorescent microscopy. Scale bar, 10 μm. (C) Rescue of mitophagy by P62 replacement. *p62* knockout cells stably expressing cox8-EGFP-mCherry were transduced with mTurquoise2-P62, grown in acetoacetate (Ac) containing medium, and imaged by fluorescence microscopy. Arrow indicates mitochondrial localization of mTurquoise2-P62. (D) Requirement for *Parkin/MULAN* in mitophagy. Quantification of red-only puncta in cells grown in medium containing acetoacetate. Wildtype (+) or *Parkin* knockout (-) cells were transduced with one of two independent *MULAN* shRNAs as indicated. Error bars indicate SD.

Figure 2.S2 Paternal mitochondria are degraded by 84 hours after fertilization. (A) Fluorescence of mito-Dendra2 in a live spermatocyte isolated from the cauda epididymis of a *PhAM* mouse. Scale bar, 10 μm. (B) Mito-Dendra2 in a 12-hour embryo. Note that mito-Dendra2 is circumscribed to a distinct rod-like structure. (C) Mito-Dendra2 in a 24-hour embryo. Note that mito-Dendra2 appears as puncta dispersed from the rod-like structure. Scale bar, 20 μm. (D) Mito-

Dendra2 in an 84-hour embryo. Note that distinct mito-Dendra2 puncta are lost. Scale bar, 10 μm. (E) Paternal mitochondrial elimination in control embryos injected with non-targeting shRNA. Mito-Dendra2 clusters were quantified at 36, 60, 72, and 84 hours after fertilization. Each data point represents the mean of 15 embryos. Error bars indicate SD. (F) Representative images of embryos analyzed in (E). Scale bars, 10 μm. (G) mCherry expression in embryos from (F). Note that mCherry expression is visible by 60 hours after fertilization. Bright aggregates at 36 and 60 hours are debris from viral prep, not from embryonic expression. Scale bars, 10 μm.

Figure 2.S3 Inhibition of OXPHOS-induced mitophagy by dominant negative FIS1. (A) Quantification of red-only puncta in wildtype (WT) cells or cells transduced with MYC-FIS1-DN retrovirus. Cells were grown in medium containing glucose (Glu) or acetoacetate (Ac). **, $p<0.01$ (Student's t-test). Error bars indicate SD. (B) Imaging of cox8-EGFP-mCherry in WT cells or cells transduced with MYC-FIS1-DN retrovirus. Cells were grown in medium containing acetoacetate. Scale bar, 10 μm. (C) Diffuse cytosolic localization of MYC-FIS1-DN. Scale bar, 10 μm.

Figure 2.S4 Membrane potential lost in paternal mitochondria after fertilization. (A) Mitochondrial membrane potential in live sperm cell. Spermatozoa were isolated from the cauda epididymis of a *PhAM* mouse, stained with 20 nM TMRE, washed, and imaged by fluorescent microscopy. Red signal is

TMRE; green signal is mito-Dendra2. The boxed region is enlarged below. Scale bar, 10 μm. (B) Membrane potential of paternal mitochondria in early embryos. Embryos, generated by mating wildtype females with *PhAM* males, were collected at 12 hours after fertilization and cultured *in vitro*. At 18, 48, or 72 hours after fertilization, the embryos were incubated in 20 nM TMRE, washed, and imaged by fluorescent microscopy. Dashed box indicates region enlarged below. Arrows indicate examples of mito-Dendra2 positive spots lacking TMRE signal. Scale bar, 10 μm. (C) Fluorescence line analysis of the boxed regions in (A and B). Each plot measures the TMRE and mito-Dendra2 signals along a one-pixel width line through the center of the boxed region. Note that the mito-Dendra2 and TMRE signals are co-incident at 18 hours after fertilization but not at 48 or 72 hours.

Figure 2.1

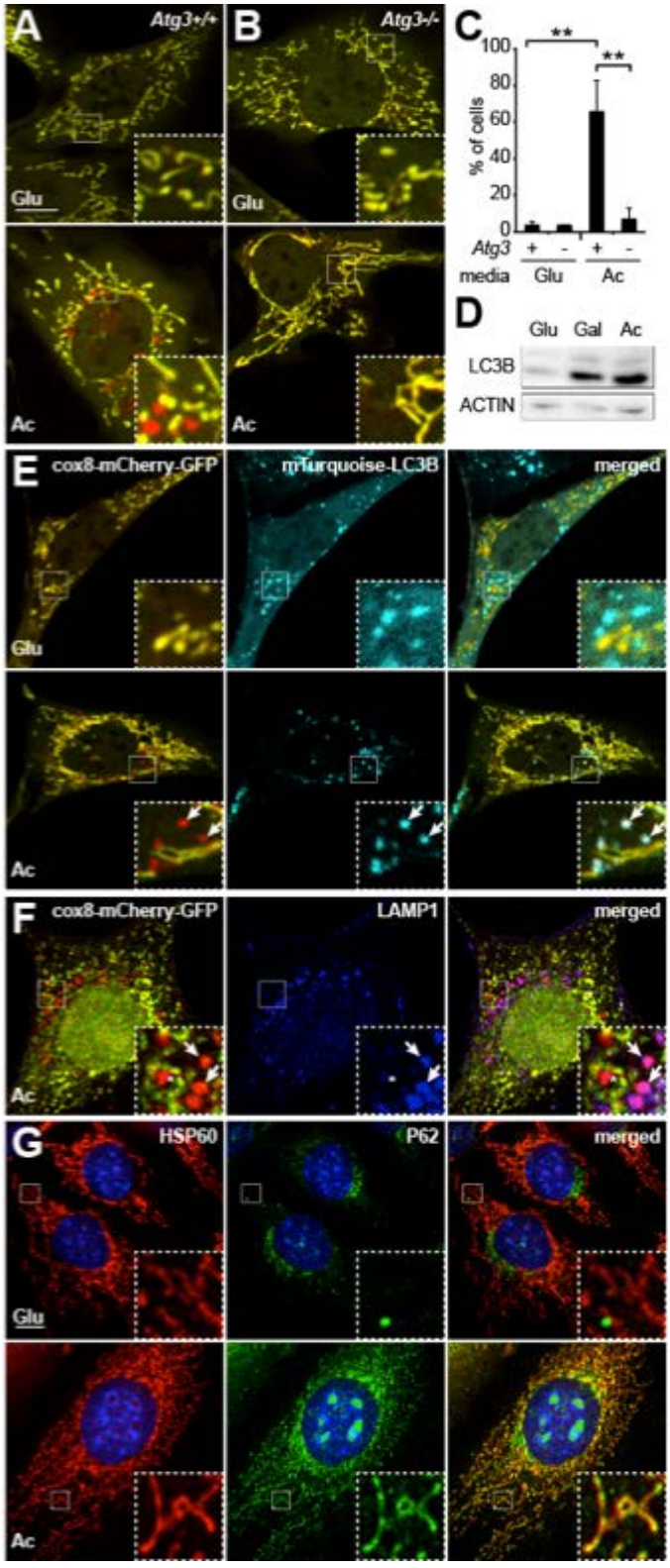
A
Atg3+/+
Glu
Ac
B
Atg3-/-
Glu
Ac
C
100
80
60
40
20
0
% of cells
**
**
Atg3
+
-
+
-
media
Glu
Ac
D
Glu
Gal
Ac
LC3B
ACTIN
E
cox8-mCherry-GFP
mTurquoise-LC3B
merged
Glu
Ac
F
cox8-mCherry-GFP
LAMP1
merged
Ac
G
HSP60
P62
merged
Glu
Ac

Figure 2.2

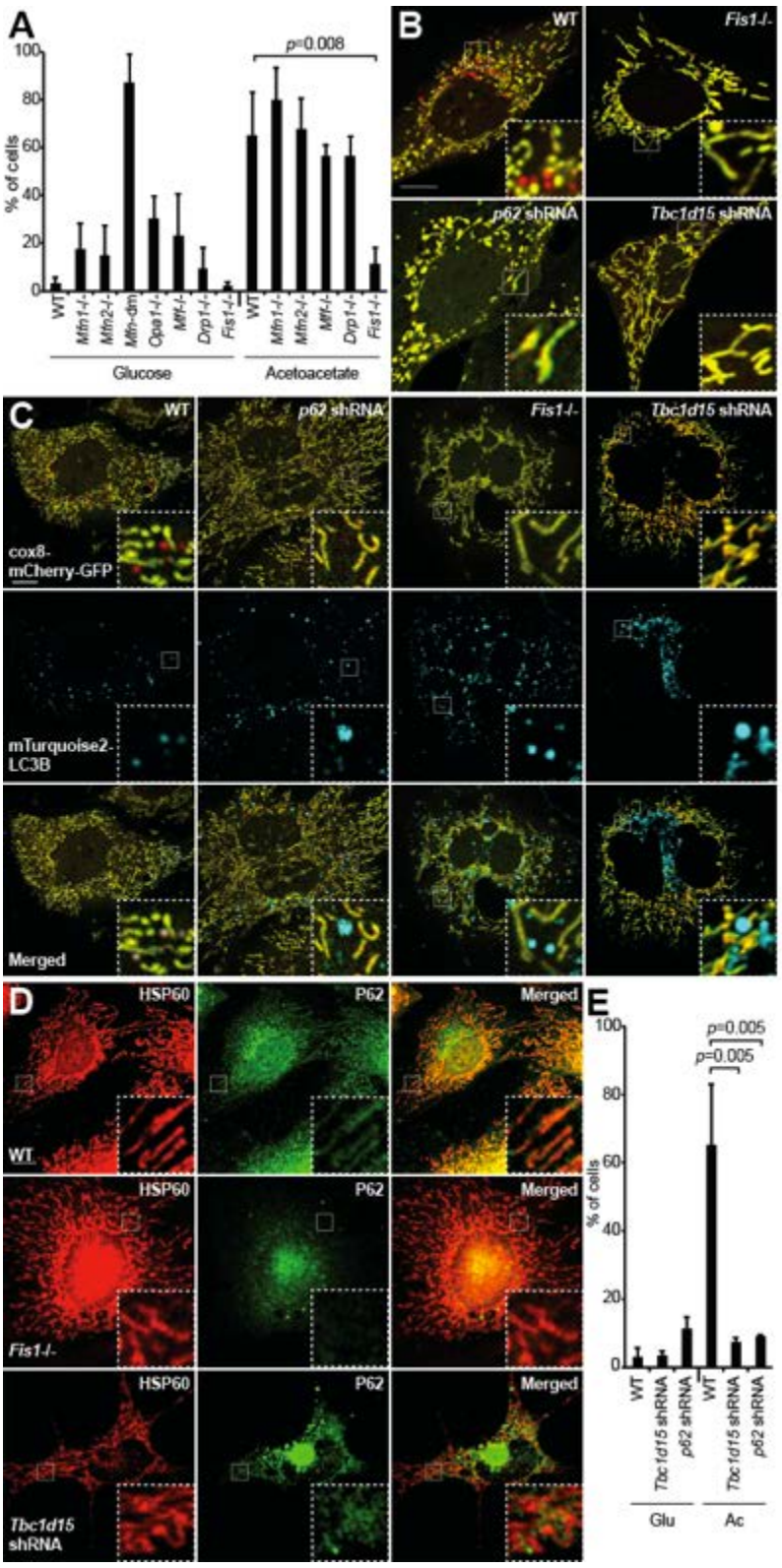
A
p=0.008
% of cells
WT
Mfn1-/-
Mfn2-/-
Mfn-dm
Opa1-/-
Mff-/-
Drp1-/-
Fis1-/-
Glucose
Acetoacetate
B
WT
Fis1-/-
p62 shRNA
Tbc1d15 shRNA
C
cox8-mCherry-GFP
mTurquoise2-LC3B
Merged
D
HSP60
P62
Merged
WT
Fis1-/-
Tbc1d15 shRNA
E
p=0.005
p=0.005
Glu
Ac

Figure 2.3

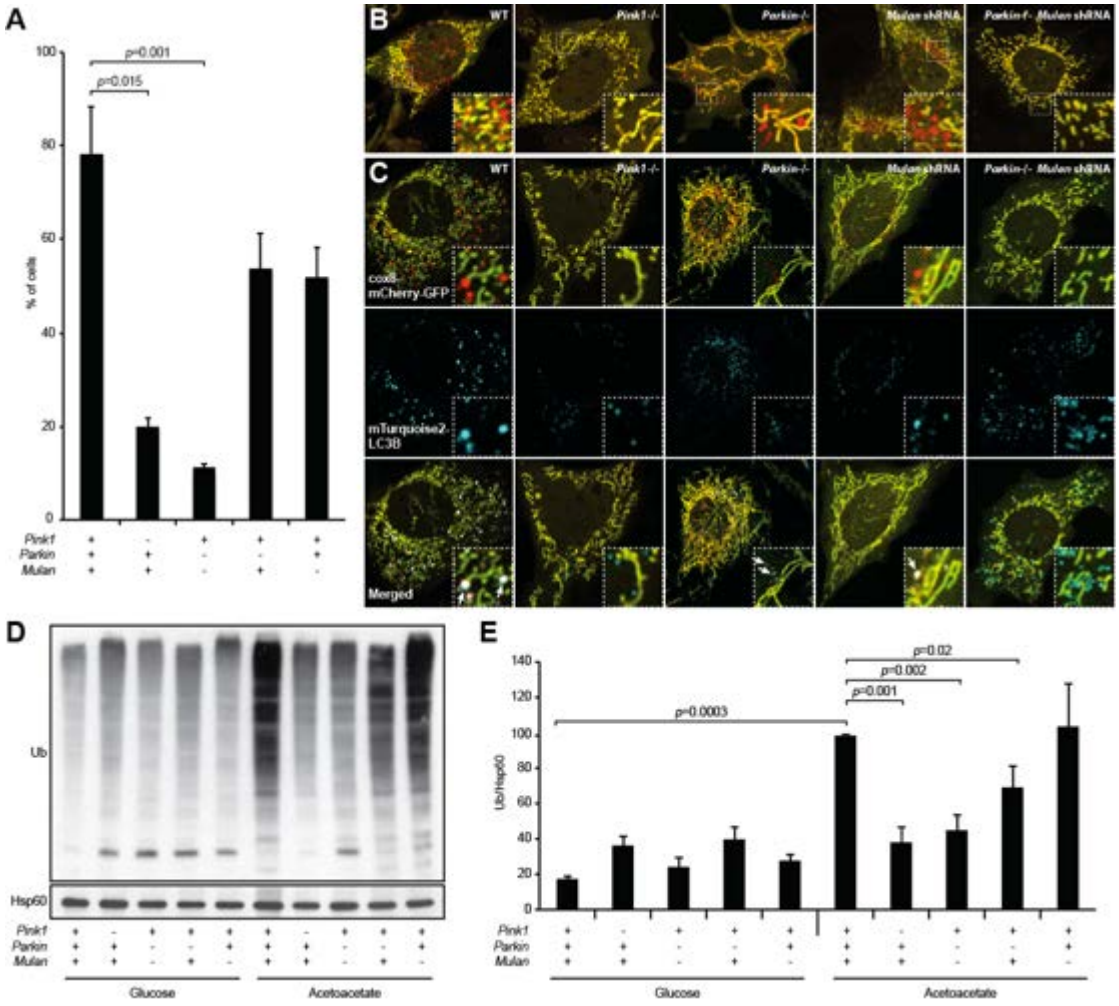
A
p=0.001
p=0.015
% of cells
Pink1
Parkin
Mulan
B
WT
Pink1-/-
Parkin-/-
Mulan shRNA
Parkin-/- Mulan shRNA
C
cox8-mCherry-GFP
mTurquoise2-LC3B
Merged
D
Ub
Hsp60
Glucose
Acetoacetate
E
p=0.0003
p=0.02
p=0.002
p=0.001
Ub/Hsp60
Glucose
Acetoacetate

Figure 2.4

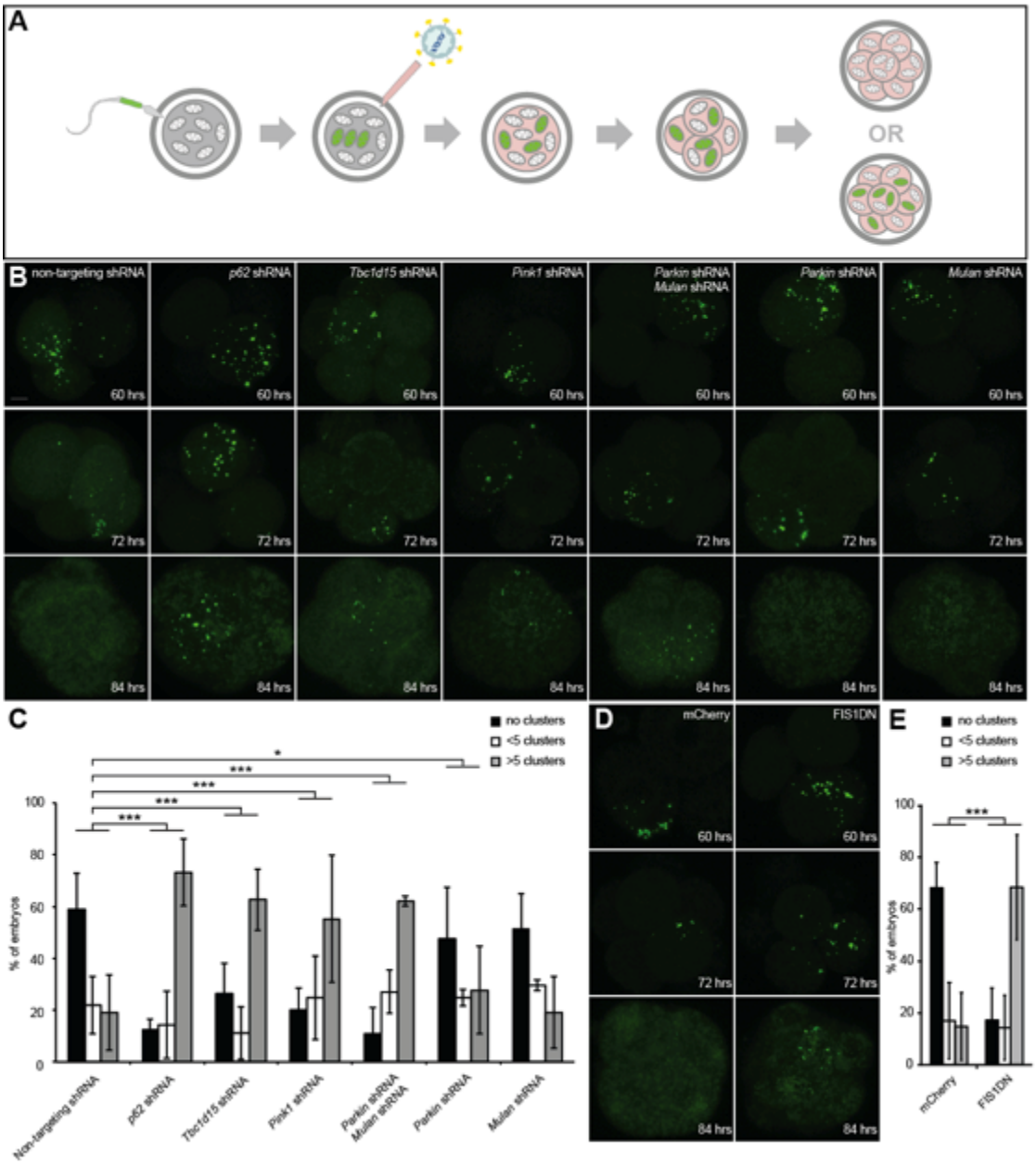
A
OR
B
non-targeting shRNA
p62 shRNA
Tbc1d15 shRNA
Pink1 shRNA
Parkin shRNA
Mulan shRNA
Parkin shRNA
Mulan shRNA
60 hrs
72 hrs
84 hrs
C
no clusters
<5 clusters
>5 clusters
% of embryos
Non-targeting shRNA
p62 shRNA
Tbc1d15 shRNA
Pink1 shRNA
Parkin shRNA Mulan shRNA
Parkin shRNA
Mulan shRNA
D
mCherry
FIS1DN
E
mCherry
FIS1DN

Figure 2.S1

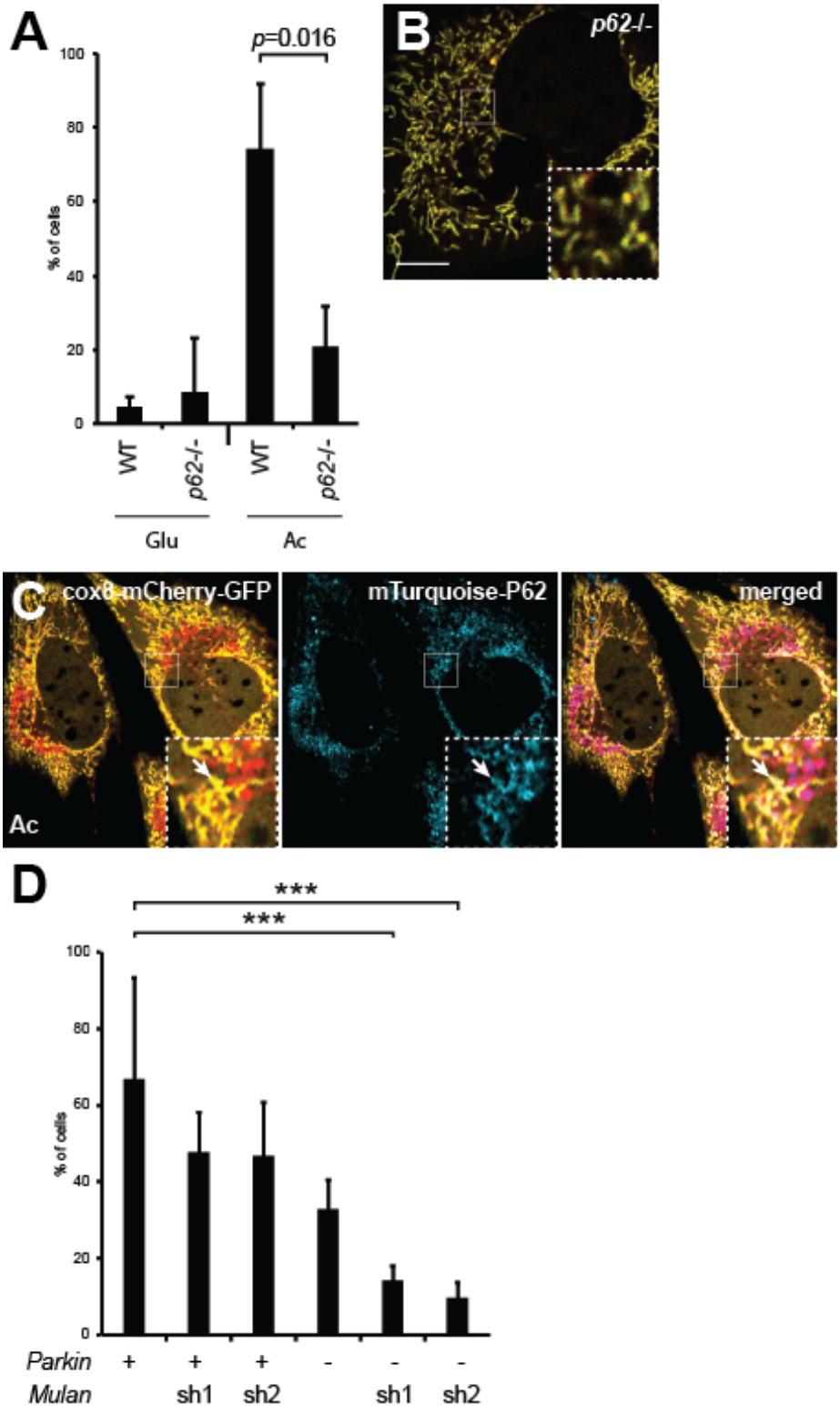
A
p=0.016
% of cells
100
80
60
40
20
0
WT
p62-/-
WT
p62-/-
Glu
Ac
B
p62-/-
C
cox8-mCherry-GFP
mTurquoise-P62
merged
Ac
D
***
***
% of cells
100
80
60
40
20
0
Parkin + + + - - -
Mulan sh1 sh2 sh1 sh2

Figure 2.S2

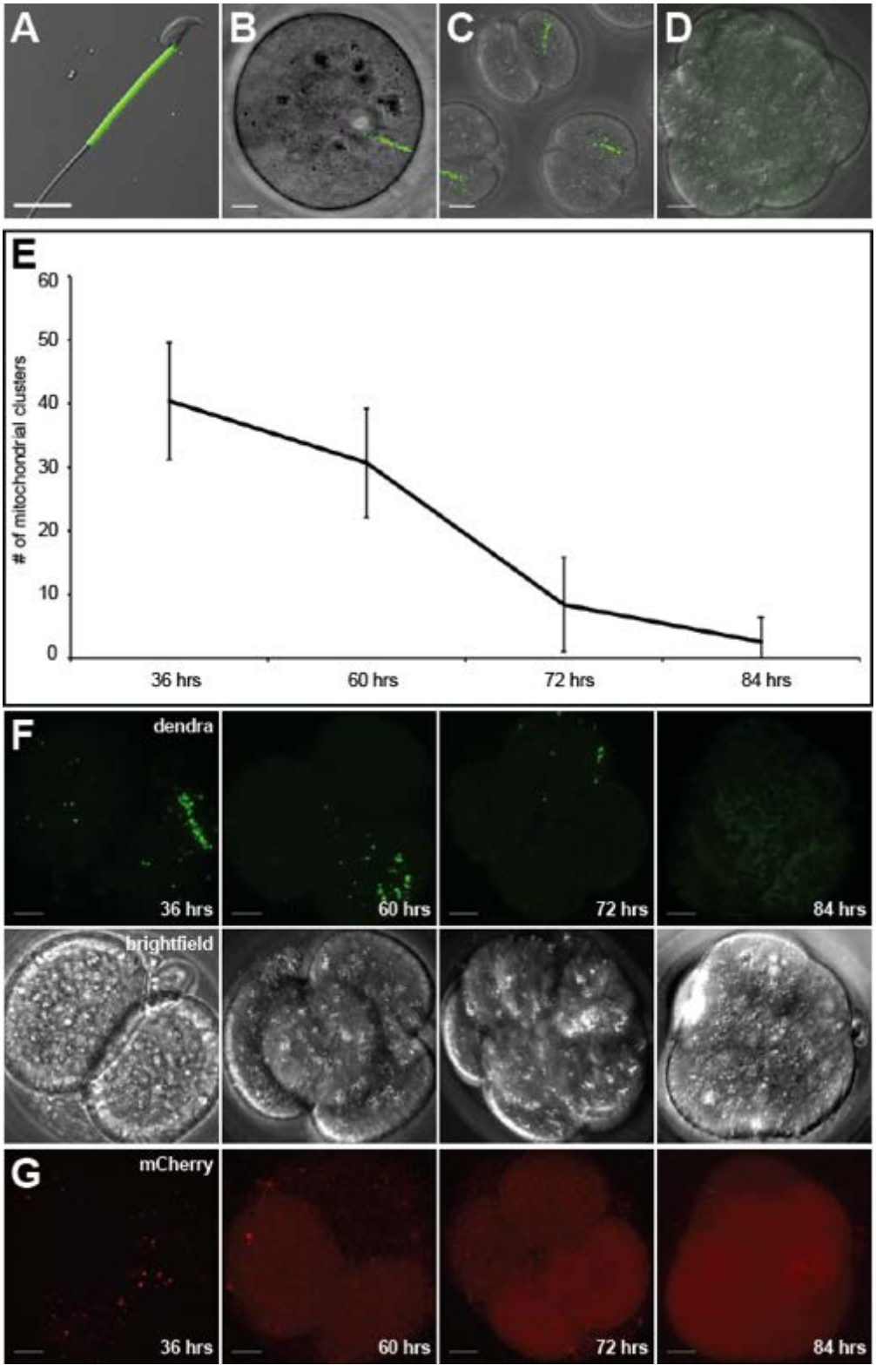
A
B
C
D
E
# of mitochondrial clusters
60
50
40
30
20
10
0
36 hrs
60 hrs
72 hrs
84 hrs
F
dendra
36 hrs
60 hrs
72 hrs
84 hrs
brightfield
G
mCherry
36 hrs
60 hrs
72 hrs
84 hrs

Figure 2.S3

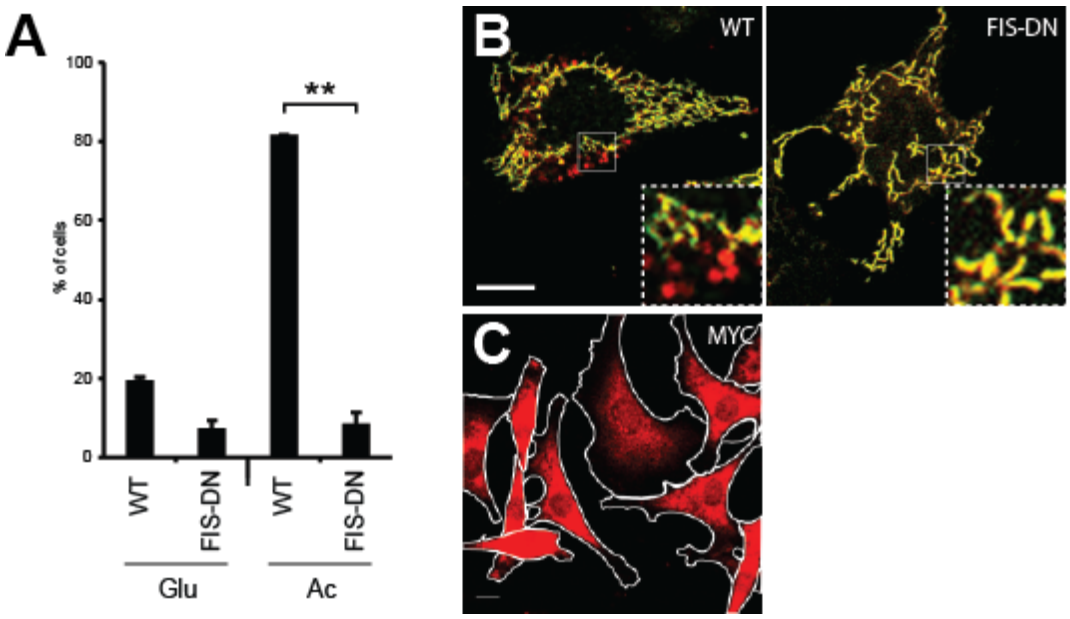
A
100
80
60
40
20
0
% of cells
**
WT
FIS-DN
WT
FIS-DN
Glu
Ac
B
WT
FIS-DN
C
MYC

Figure 2.S4

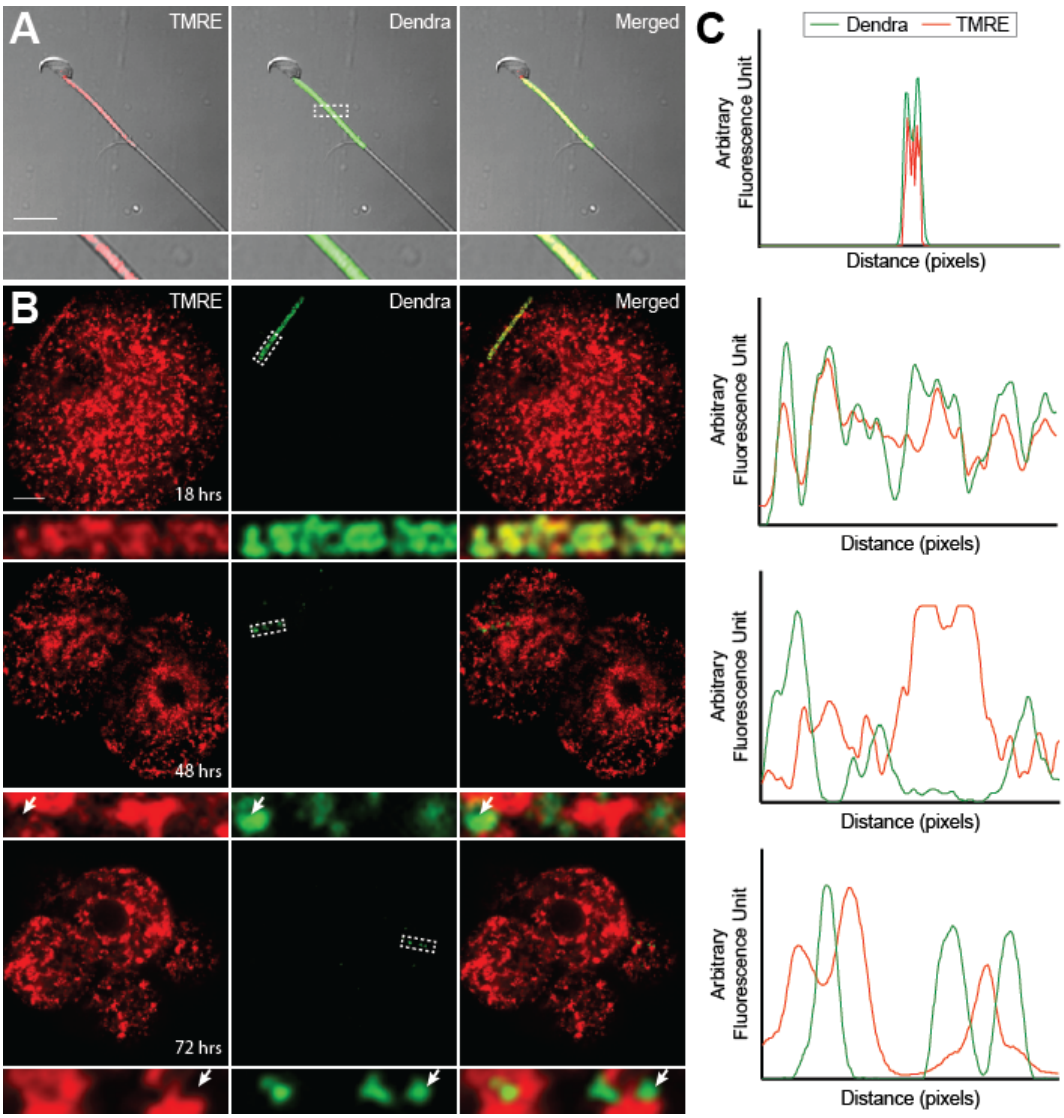
A
TMRE
Dendra
Merged
B
TMRE
Dendra
Merged
18 hrs
48 hrs
72 hrs
C
Dendra
TMRE
Arbitrary Fluorescence Unit
Distance (pixels)
Arbitrary Fluorescence Unit
Distance (pixels)
Arbitrary Fluorescence Unit
Distance (pixels)
Arbitrary Fluorescence Unit
Distance (pixels)

REFERENCES

1. M. S. Sharpley *et al.*, Heteroplasmy of mouse mtDNA is genetically unstable and results in altered behavior and cognition. *Cell* **151**, 333 (2012).
2. S. Al Rawi *et al.*, Postfertilization autophagy of sperm organelles prevents paternal mitochondrial DNA transmission. *Science* **334**, 1144 (2011).
3. M. Sato, K. Sato, Degradation of paternal mitochondria by fertilization-triggered autophagy in C. elegans embryos. *Science* **334**, 1141 (2011).
4. Y. Politi *et al.*, Paternal mitochondrial destruction after fertilization is mediated by a common endocytic and autophagic pathway in Drosophila. *Dev Cell* **29**, 305 (2014).
5. S. M. Luo *et al.*, Unique insights into maternal mitochondrial inheritance in mice. *Proc Natl Acad Sci U S A* **110**, 13038 (2013).
6. P. Mishra, V. Carelli, G. Manfredi, D. C. Chan, Proteolytic cleavage of OPA1 stimulates mitochondrial inner membrane fusion and couples fusion to oxidative phosphorylation. *Cell Metab* **19**, 630 (2014).
7. S. Melser *et al.*, Rheb regulates mitophagy induced by mitochondrial energetic status. *Cell Metab* **17**, 719 (2013).
8. S. Pankiv *et al.*, p62/SQSTM1 binds directly to Atg8/LC3 to facilitate degradation of ubiquitinated protein aggregates by autophagy. *J Biol Chem* **282**, 24131 (2007).

9. M. L. Seibenhener *et al.*, A role for sequestosome 1/p62 in mitochondrial dynamics, import and genome integrity. *Biochim Biophys Acta* **1833**, 452 (2013).

10. K. Mao, K. Wang, X. Liu, D. J. Klionsky, The scaffold protein Atg11 recruits fission machinery to drive selective mitochondria degradation by autophagy. *Dev Cell* **26**, 9 (2013).

11. A. Tanaka *et al.*, Proteasome and p97 mediate mitophagy and degradation of mitofusins induced by Parkin. *J Cell Biol* **191**, 1367 (2010).

12. A. S. Rambold, B. Kostelecky, N. Elia, J. Lippincott-Schwartz, Tubular network formation protects mitochondria from autophagosomal degradation during nutrient starvation. *Proc Natl Acad Sci U S A* **108**, 10190 (2011).

13. L. C. Gomes, G. Di Benedetto, L. Scorrano, During autophagy mitochondria elongate, are spared from degradation and sustain cell viability. *Nat Cell Biol* **13**, 589 (2011).

14. H. Otera *et al.*, Mff is an essential factor for mitochondrial recruitment of Drp1 during mitochondrial fission in mammalian cells. *J Cell Biol* **191**, 1141 (2010).

15. O. C. Loson, Z. Song, H. Chen, D. C. Chan, Fis1, Mff, MiD49, and MiD51 mediate Drp1 recruitment in mitochondrial fission. *Mol Biol Cell* **24**, 659 (2013).

16. K. Onoue *et al.*, Fis1 acts as a mitochondrial recruitment factor for TBC1D15 that is involved in regulation of mitochondrial morphology. *J Cell Sci* **126**, 176 (2013).

17. K. Yamano, A. I. Fogel, C. Wang, A. M. van der Bliek, R. J. Youle, Mitochondrial Rab GAPs govern autophagosome biogenesis during mitophagy. *Elife* **3**, e01612 (2014).

18. Q. Shen *et al.*, Mutations in Fis1 disrupt orderly disposal of defective mitochondria. *Mol Biol Cell* **25**, 145 (2014).

19. A. M. Pickrell, R. J. Youle, The roles of PINK1, parkin, and mitochondrial fidelity in Parkinson's disease. *Neuron* **85**, 257 (2015).

20. I. E. Clark *et al.*, Drosophila pink1 is required for mitochondrial function and interacts genetically with parkin. *Nature* **441**, 1162 (2006).

21. J. Park *et al.*, Mitochondrial dysfunction in Drosophila PINK1 mutants is complemented by parkin. *Nature* **441**, 1157 (2006).

22. Y. Yang *et al.*, Mitochondrial pathology and muscle and dopaminergic neuron degeneration caused by inactivation of Drosophila Pink1 is rescued by Parkin. *Proc Natl Acad Sci U S A* **103**, 10793 (2006).

23. J. Yun *et al.*, MUL1 acts in parallel to the PINK1/parkin pathway in regulating mitofusin and compensates for loss of PINK1/parkin. *Elife* **3**, e01958 (2014).

24. B. Bingol *et al.*, The mitochondrial deubiquitinase USP30 opposes parkin-mediated mitophagy. *Nature* **510**, 370 (2014).

25. T. Cornelissen *et al.*, The deubiquitinase USP15 antagonizes Parkin-mediated mitochondrial ubiquitination and mitophagy. *Hum Mol Genet* **23**, 5227 (2014).

26. A. H. Pham, J. M. McCaffery, D. C. Chan, Mouse lines with photo-activatable mitochondria to study mitochondrial dynamics. *Genesis* **50**, 833 (2012).

27. J. J. Palacino *et al.*, Mitochondrial dysfunction and oxidative damage in parkin-deficient mice. *J Biol Chem* **279**, 18614 (2004).

28. F. A. Perez, R. D. Palmiter, Parkin-deficient mice are not a robust model of parkinsonism. *Proc Natl Acad Sci U S A* **102**, 2174 (2005).

29. C. A. Fasano *et al.*, shRNA knockdown of Bmi-1 reveals a critical role for p21-Rb pathway in NSC self-renewal during development. *Cell Stem Cell* **1**, 87 (2007).

30. C. Lois, E. J. Hong, S. Pease, E. J. Brown, D. Baltimore, Germline transmission and tissue-specific expression of transgenes delivered by lentiviral vectors. *Science* **295**, 868 (2002).

31. S. Pease, C. Lois, *Mammalian and Avian Transgenesis – New Approaches*. (Springer-Verlag Berlin Heidelberg, Heidelberg, Germany, 2006).

32. J. Goedhart *et al.*, Structure-guided evolution of cyan fluorescent proteins towards a quantum yield of 93%. *Nat Commun* **3**, 751 (2012).

33. E. Itakura, N. Mizushima, p62 Targeting to the autophagosome formation site requires self-oligomerization but not LC3 binding. *J Cell Biol* **192**, 17 (2011).

34. Y. S. Sou *et al.*, The Atg8 conjugation system is indispensable for proper development of autophagic isolation membranes in mice. *Mol Biol Cell* **19**, 4762 (2008).

35. Y. Ichimura *et al.*, Structural basis for sorting mechanism of p62 in selective autophagy. *J Biol Chem* **283**, 22847 (2008).

36. N. Ishihara *et al.*, Mitochondrial fission factor Drp1 is essential for embryonic development and synapse formation in mice. *Nat Cell Biol* **11**, 958 (2009).

37. H. Chen, A. Chomyn, D. C. Chan, Disruption of fusion results in mitochondrial heterogeneity and dysfunction. *J Biol Chem* **280**, 26185 (2005).

ACKNOWLEDGMENTS

We thank Shirley Pease (Director, Transgenic Core at Caltech) for training and advice on embryo injection. We are grateful to Katherine Kim for assistance with the *MULAN* knockdown experiments, Kurt Reichermeier for advice on the ubiquitin assay, Ruohan Wang for technical assistance with *p62* overexpression, and Hsiuchen Chen for advice on animal work. R.R. is supported by an NIH NIGMS training grant (GM08042) and the UCLA Medical Scientist Training Program.

Chapter 3

UPREGULATION OF MITOPHAGY IN MITOCHONDRIAL FUSION-DEFICIENT CELLS IS DEPENDENT ON P62

Rebecca Rojansky[1] and David C. Chan[1]

[1]Division of Biology and Biological Engineering
California Institute of Technology
Pasadena, CA 91125

ABSTRACT

In addition to regulating mitochondrial morphology, mitochondrial fusion protects mitochondrial function, facilitating content mixing between mitochondria, including proteins, lipids, and mitochondrial DNA (mtDNA). Cells lacking mitochondrial fusion due to deletion of the mitochondrial GTPases, MFN1 and MFN2 (MFN-null cells) exhibit severe mitochondrial dysfunction, and heterogeneity of mtDNA, membrane potential, and proteins. Here we examine mitophagy in MFN-null cells. We find a high level of mitophagy in these cells that is dependent on the autophagy adaptor, p62 and independent of the structurally similar adaptor, NBR1. We show that p62 localizes to a subset of mitochondria that are depolarized and lack mtDNA, and that this localization is independent of the ubiquitin-binding domain of p62. Our results confirm a role for p62 in mitophagy, and suggest a novel ubiquitin-independent mechanism for its recruitment to mitochondria.

INTRODUCTION

Mitochondria are dynamic organelles that fuse and divide to maintain the functional status of the population (Detmer and Chan, 2007; Hoppins et al., 2007). In mammalian cells, three large dynamin-like GTPase proteins conduct coordinated fusion of the outer and inner mitochondrial membranes (OMM and IMM). In mammals, the early steps in membrane fusion involve the OMM resident proteins, mitofusin 1 (MFN1), and mitofusin 2 (MFN2) (Koshiba et al., 2004; Meeusen et al., 2004). The IMM protein, optic atrophy 1 (OPA1) is essential for IMM fusion (Meeusen et al., 2006; Song et al., 2009). Mitochondrial fusion is the key process underlying mitochondrial morphology (Chen et al., 2003); however, it also plays a role in maintaining mitochondrial function and mtDNA stability, and is thought to protect the functional status of the mitochondrial population by facilitating content mixing amongst mitochondria (Chen et al., 2007; Chen et al., 2010; Detmer and Chan, 2007).

Cells that lack mitochondrial fusion due to loss of MFN1 and MFN2 (MFN-null) have fragmented mitochondria as well as severe defects in respiratory capacity, cell growth rate, and mitochondrial membrane potential ($\Delta\Psi_m$) (Chen et al., 2005). In these cells, the fragmented mitochondria become functionally heterogeneous, with widely divergent $\Delta\Psi_m$, protein levels, and mtDNA levels and mutation load. This dysfunction has severe consequences for the organism. In mice, loss of mitochondrial fusion in skeletal muscle results in a lethal mitochondrial myopathy (Chen et al., 2010).

The fate of these dysfunctional mitochondria in MFN-null cells is unknown, however some evidence suggests that mitophagy may be involved in their removal (Narendra et al., 2008). Mitophagy is specialized form of macroautophagy, an intracellular degradation system mediated by the autophagosome and the lysosome. Mitochondria that are targeted for degradation are engulfed by a double-membrane vesicle called the isolation membrane or autophagophore, which ultimately fuses with the lysosome. The lysosomal low pH and hydrolase activity cooperate to degrade the autophagosomal inner membrane and contents (Nakamura et al., 1997). Specificity of this process is believed to be achieved by the recruitment of autophagy receptors, which are selective for specific cargoes (Johansen and Lamark, 2011).

Among the currently identified autophagy receptors are the structurally similar proteins, sequestosome 1 (SQSTM1) or p62 (hereafter referred to as p62), and neighbor of BRCA1 gene 1 (NBR1) (Geisler et al., 2010; Kirkin et al., 2009). Both were found to localize to the isolation membrane (Itakura and Mizushima, 2011a), and both contain at least four key domains.

The N-terminal PB1 domain mediates homo- and hetero-dimerization (Lamark et al., 2003). In vivo studies suggest that oligomerization of p62 is required for its association with cargo and for delivery to the autophagosome (Bjorkoy et al., 2005; Ichimura et al., 2008a; Itakura and Mizushima, 2011b), as well as for activation of the oxidative stress response regulation transcription factor NRF2 (Jain et al., 2010; Komatsu et al., 2010a).

Both p62 and NBR1 contain ZZ-type zinc finger domains. Their function is yet unknown; however, some evidence suggests that they may modulate protein-protein interactions (Lin et al., 2013).

Like most autophagy receptors, p62 and NBR1 contain LC3 binding motifs called LC3-interacting regions (LIR). P62 contains one LIR domain in the C-terminal half of the protein, whereas NBR1 contains two LIR domains with a coiled coil domain between them (Ichimura et al., 2008b; Noda et al., 2010; Pankiv et al., 2007). In mammalian cells, LC3 is present on both the outer and the inner membrane of the autophagosome, and it is generally thought that binding of receptors to LC3 may allow their cargo to be selectively engulfed by autophagosomes (Kirkin et al., 2009; Lamark et al., 2009), however LC3 independent mechanisms may exist (Cao et al., 2008). Of note, p62 localization to the isolation membrane was found to be independent of LC3 but dependent instead on self-oligomerization, suggesting that a simple LC3 focused model for cargo delivery to autophagosomes is incomplete (Itakura and Mizushima, 2011b).

Finally, the C-terminus of both p62 and NBR1 contains an ubiquitin association domain (UBA) (Long et al., 2010). This domain is commonly believed to be the means of cargo recognition by receptor proteins. The UBA domain of p62 preferentially interacts with K63-linked poly-ubiquitin chains, whereas the UBA domain of NBR1 shows less linkage preference (Geisler et al., 2010). The interaction of p62 with ubiquitin is modulated by phosphorylation of the UBA domain (Matsumoto et al., 2011). Ubiquitination of OMM proteins such as the mitofusins, or VDAC1 could be a mitophagy signal recognized by p62

(Sarraf et al., 2013). This ubiquitination is induced by loss of mitochondrial membrane potential ($\Delta\Psi_m$) and mediated by E3 ligases such as parkin RBR E3 ubiquitin protein ligase (PARKIN), mitochondrial ubiquitin ligase activator of NK-kB (MUL1), or ring finger protein 185 (RNF185) (Youle and Narendra, 2011; Yun et al., 2014a). Through an elegant $\Delta\Psi_m$ sensing mechanism, PARKIN is recruited specifically to depolarized mitochondria. In MFN-null cells a subset of mitochondria have low $\Delta\Psi_m$, and Narendra et al. reported selective accumulation of PARKIN on these mitochondria (Narendra et al., 2008). However, whether the UBA is essential for the function of p62 in autophagy generally and whether p62 is involved in MFN-null cells is unknown.

Roles for p62 and NBR1 in mitophagy have been suggested, but remain unclear. P62 was shown to colocalize with some mitochondria under basal conditions (Seibenhener et al., 2013b), and we have previously shown localization of p62 to mitochondria in mitophagy-inducing conditions (unpublished). Although work by Geisler et al. suggested that p62 may be essential for mitophagy, Narendra et al. suggested that it may only be required for mitochondrial clustering and not degradation (Geisler et al., 2010; Narendra et al., 2010a). NBR1 has been implicated in autophagic degradation of ubiquitinated substrates (Kirkin et al., 2009), and pexophagy specifically (Deosaran et al., 2013), and it has been proposed as a candidate mitophagy adaptor. Chan et al. found NBR1 in a screen of the mitochondrial proteome in HeLa cells undergoing CCCP-induced mitophagy (Chan et al., 2011). Shi et al. found the same by immunofluorescence, but further characterization of the functional role of NBR1

indicated that it may be dispensable for mitophagy under this condition (Shi et al., 2015). Thus, how and why p62 and NBR1 localize to mitochondria during mitophagy and what role they may play are open questions.

In this study, we investigate the roles of p62 and NBR1 in steady-state mitophagy in MFN-null MEFs. We find that NBR1 is dispensable for this process, and demonstrate that p62 is preferentially targeted to the subset of depolarized mitochondria that lack mtDNA, and that it is essential for their ubiquitination and delivery to lysosomes. Finally, we examine how p62 is recruited to mitochondria and find that the oligomerization or LC3 binding regions are independently sufficient to localize p62 to a subset of mitochondria, but that this localization is independent of the ubiquitin binding region of p62.

RESULTS

P62 is necessary for maintaining $\Delta\Psi_m$ in the absence of mitofusins

We performed stable isotope labeling by amino acids in cell culture (SILAC) analysis (Ong et al., 2002) to monitor changes in the mitochondrial proteome in mouse embryonic fibroblast (MEF) cells defective in mitochondrial fusion due to complete knock-out of mitofusins, *Mfn1* and *Mfn2* (MFN-null). By this approach, we quantified 2532 unique protein groups. Of these, 756 were mapped to proteins in the mouse MitoCarta database (Calvo et al., 2016), which contains 1158 mitochondrial proteins. This represents a 65 percent coverage of the mitochondrial proteome, which is highly comprehensive, given that fewer mitochondrial proteins are expressed in cultured cells than in tissues (Duborjal et al., 2002).

To sort through the proteins enriched on mitochondria in MFN-null cells, we considered only those with a calculated significance of <0.01 (Table 3.1). Amongst the top nine proteins enriched in MFN-null cells, six are involved in metabolism, and one is involved in mtDNA transcription. This is not surprising given that mitochondria from MFN-null cells are dysfunctional, with defective respiratory activity due to mtDNA loss and resulting Complex I deficiency (Chen et al., 2010). Of the remaining two proteins, one is a resident of the ER involved in ER stress response. This is not surprising, as ER-mitochondrial contacts are well established, and loss of MFN2 has been shown to increase the number of such contact points (Filadi et al., 2015). Finally, the autophagy adaptor/receptor protein, p62/SQSTM1 is increased six-fold on MFN-null mitochondria.

Mitochondrial localization of p62/SQSTM1 has been observed before (Seibenhener et al., 2013b); however, its enrichment on mitochondria in the absence of mitofusins has never been reported.

To confirm that p62, which is normally a cytosolic protein, localizes to mitochondria in MFN-null cells, we collected whole cell lysate or isolated mitochondria from wildtype and MFN-null cells, and probed for p62 by western blot (Figure 3.1A). Consistent with our SILAC results, we found that p62 is selectively enriched on mitochondria of MFN-null cells, but we detected no such enrichment in whole cell lysate from MFN-null cells, suggesting that p62 is recruited specifically to mitochondria. To further characterize the localization of p62, we immunostained wildtype and MFN-null cells for p62 and HSP60 (Figure 3.1C). MFN-null cells showed an overall increase in the abundance of p62, as well as an increase in the colocalization of p62 with mitochondria relative to wildtype cells, suggesting that p62 specifically localizes to mitochondria in the absence of mitochondrial fusion.

Interestingly, we found that p62 only localizes to a subset of on MFN-null mitochondria (Figure 3.1C). This finding is in contrast to what we previously reported for wildtype MEFs, in which mitophagy stimulation causes p62 localization to all mitochondria. Previous studies have demonstrated that MFN-null cells have dysfunctional mitochondria with heterogeneity of $\Delta\Psi_m$ (Chen et al., 2005; Chen et al., 2003). We wondered whether the increased p62 on MFN-null mitochondria might help maintain functional status of the mitochondrial population by targeting mitochondria with reduced $\Delta\Psi_m$ for degradation. If this

were true, loss of p62 in MFN-null cells would result in a reduction in the average $\Delta\Psi_m$ measured over all mitochondria in a cell. To test the dependence of membrane potential on p62, we first transduced MFN-null cells with one of two shRNAs targeting p62 (Figure 3.1B). The second of these shRNAs (sh2) reduced the level of p62 by 97%, and was used in all following experiments. To measure $\Delta\Psi_m$, wildtype and MFN-null cells were stained with the cyanine dye, JC-1 (5,5′,6,6′-tetrachloro-1,1′,3,3′-tetraethylbenzimidazolocarbo-cyanine iodide) (Reers et al., 1991; Smiley et al., 1991). JC-1 exists in either a monomeric or aggregated form. So called, J-aggregates, form at the high concentration reached inside of highly active mitochondria (those with high $\Delta\Psi_m$). When excited at 488 nm JC-1 monomers emit green fluorescence with a maximum at 530 nm, whereas J-aggregates emit orange-red fluorescence with a maximum at 595 nm. Therefore, mean fluorescence intensity of J-aggregates per cell represents average $\Delta\Psi_m$ of the mitochondrial population, whereas total fluorescence intensity of JC-1 monomer indicates total mitochondrial mass. Cells were imaged by confocal microscopy and mean fluorescence intensity per cell was measured (Figure 3.1D). Consistent with previous studies (Seibenhener et al., 2013b) we found that loss of p62 results in a 40 to 60 percent reduction in overall $\Delta\Psi_m$ in MFN-null cells (Figure 3.1E). Total mitochondrial mass, as indicated by JC-1 monomer fluorescence, was relatively unchanged by loss of p62 (Figure 3.1E), suggesting that p62 is required for maintenance of $\Delta\Psi_m$.

P62 is required for degradation of a subset of defective mitochondria by mitophagy in MFN-null cells.

Previous studies have shown that MFN-null cells have lower levels of mtDNA than wildtype cells (Chen et al., 2010). Mitochondria lacking mtDNA are unable to perform normal respiration because of a lack of key OXPHOS complex subunits. We wondered, therefore, whether the subset of mitochondria labeled with p62 contained mtDNA. We performed immunofluorescence staining of MFN-null cells with anti DNA and anti p62 antibodies (Figure 3.2A). Although many mitochondria that lacked mtDNA did not show p62 colocalization, p62 was never found to colocalize with mitochondria that contained mtDNA. Furthermore, p62 labeled mitochondria exhibited weaker Mitotracker Red staining than other mitochondria. Mitotracker Red accumulates in mitochondria in a $\Delta\Psi_m$ dependent manner (Perry et al., 2011), so this staining pattern indicates that p62 positive mitochondria have low $\Delta\Psi_m$. Taken together, these results are consistent with the idea that p62 localizes preferentially to dysfunctional mitochondria.

Previous studies have shown that p62 plays a role in maintenance of mitochondrial genome integrity in both mice and cultured cells. Overexpression of P62, even in wildtype cells, increases the levels of mtDNA (Seibenhener et al., 2013b). An alternate explanation, therefore, for the association of p62 with a subset of mitochondria apparently lacking mtDNA is that p62 promotes mtDNA replication in these mitochondria to restore mtDNA to detectable levels. If this were true, loss of p62 in MFN-null cells would reduce the total amount of mtDNA per cell, and increase the fraction of mitochondria lacking mtDNA. To

measure this we imaged cells labeled with the double-stranded DNA dye, PicoGreen, as well as the mitochondria-specific dye, Mitotracker Red-FM, and quantified the percent of mitochondria colocalizing with DNA stain (Figure 3.2B). To measure mtDNA content, we performed quantitative PCR on DNA from MFN-null cells with and without p62 shRNA (Figure 3.2C). We found that knockdown of p62 had no effect on the fraction of mitochondria lacking mtDNA (Figure 3.2B), or the amount of mtDNA (Figure 3.2C), suggesting that the role of p62 in MFN-null cells is not in mtDNA maintenance.

P62 is a known autophagy receptor (Johansen and Lamark, 2011), and more recently it has been implicated in mitophagy (Geisler et al., 2010; Narendra et al., 2010a). We previously reported that p62 is essential for mitophagy under OXPHOS-inducing growth conditions in MEF cells and that MFN-null cells have increased levels of mitophagy (Chapter 2). To test whether p62 is required for steady-state mitophagy in MFN-null cells, we utilized a dual-color fluorescence-quenching assay with a mitochondrially localized EGFP-mCherry reporter. When this construct is expressed, normal mitochondria are yellow, with both GFP and mCherry fluorescence visible in the matrix, whereas when mitochondria are in acidic compartments, such as the autolysosome, only mCherry fluorescence is intact, due to the selective sensitivity of EGFP fluorescence to low pH. We assayed mitophagy in MFN-null cells, MFN-null cells with p62 shRNA, and also MFN-null p62 knockdown cells with exogenous p62-Turquoise expression. Whereas close to 90% of control cells exhibit many red puncta constitutively, in p62 shRNA expressing cells red puncta are strongly reduced. Less than 20% of

cells showed red puncta. When p62 knockdown cells also expressed exogenous p62, the red puncta were restored (Figure 3.2D,E). To confirm that the red mitochondrial puncta observed in MFN-null cells at steady-state are in autophagosomes, we expressed an mTurquoise2 tagged version of LC3B, and imaged cells with and without p62 shRNA. We found that LC3B colocalizes with the red puncta, suggesting that they do represent mitochondria in autophagosomes (Figure 3.2E). Taken together, these results are consistent with a requirement for p62 in steady-state mitophagy of MFN-null mitochondria.

The PB1 and LIR domains but not the UBA of p62 are sufficient for its localization to mitochondria.

P62 contains four key domains and several binding motifs. The N-terminal PB1 domain mediates homo- and hetero-dimerization (Lamark et al., 2003). The ZZ-type zinc finger may modulate protein interactions, but is yet of unknown function (Lin et al., 2013). The LC3 interacting region (LIR) associates with the core autophagosomal protein, LC3 (Ichimura et al., 2008b; Pankiv et al., 2007), and the C-terminal UBA domain binds ubiquitinated substrates (Long et al., 2010). P62 is considered an autophagy receptor because it can recognize ubiquitinated proteins via its UBA domain, and link them to the autophagosome via its interaction with LC3; however, this function has not been proven with respect to mitochondria. We sought to determine how p62 localizes to mitochondria, whether by binding ubiquitinated proteins, or by some other method. First, we expressed a full-length mTurquoise2-p62 fusion protein in

MFN-null cells expressing the mitophagy marker, cox8-EGFP-mCherry. Similar to our observations by immunostaining, we again found that p62 localizes to only a subset of mitochondria in MFN-null MEFs, and interestingly, this subset consists exclusively of the red mitochondria that are undergoing mitophagy (Figure 3.3A). We next tested a series of truncated versions of p62 for localization to mitochondria (Figure 3.3B). Given that we observed p62 localization to acidic compartments in which GFP fluorescence is not detectable, we chose the acid-stable fluorescent proteins, mCherry and mTurquoise2 for our analysis. We co-expressed mCherry-tagged p62 constructs with mitochondrially targeted mTurquoise2 and imaged by confocal microscopy. As observed previously, full-length p62-mCherry (p62-Full) localizes to a subset of mTurquoise2 positive mitochondria. Interestingly, this localization pattern is recapitulated by the N-terminal half of p62 containing only the PB1 and ZZ domains, and lacking the LIR and UBA domains, and is maintained even when only the PB1 domain of p62 is expressed, without the ZZ domain. When the ZZ domain is expressed by itself, it is diffusely cytosolic with no obvious localization to mitochondria, suggesting that the PB1 domain alone is sufficient to localize p62 to mitochondria. This is consistent with previous work by Itakura and Mizushima who observed the same phenomenon with respect to p62 localization to the autophagosome formation site (Itakura and Mizushima, 2011b). The C-terminal half of p62 contains both the LIR and UBA domains, the two domains thought to be important in an autophagy adaptor. However, we found that the C-terminal half of p62 is predominantly cytosolic, with some localization to

mitochondria. This colocalization may be due to LIR domain interaction with autophagosomes, as the LIR domain alone produces the same localization pattern as the full C-terminus, whereas the UBA domain, alone, does not. This is surprising, given that ubiquitination of mitochondria often precedes mitophagy (Narendra et al., 2010b), and it is assumed that autophagy adaptors localize to their substrates via ubiquitin binding. The PB1 domain of p62 is a multifunctional domain that enables interaction with a variety of proteins, including dimerization and oligomerization of p62 itself (Lamark et al., 2003; Wilson et al., 2003). One possible explanation for the PB1 domain fragment localizing to mitochondria is that it can interact with endogenous p62 present in MFN-null cells. To address this issue, we expressed the PB1-mCherry construct in p62 knockout MEFs grown under OXPHOS-inducing conditions, which has been previously shown to induce mitophagy (Figure 3.3C) (Melser et al., 2013). In these cells, the PB1-mCherry construct also localizes to punctate mitochondria as in MFN-null cells under basal conditions, suggesting that the PB1 domain alone in the absence of endogenous p62 is sufficient to localize to mitochondria.

Ubiquitination of MFN-null mitochondria is dependent on p62

The observation that the UBA domain of p62 is neither necessary nor sufficient to localize p62 to mitochondria is surprising. We have previously shown that cells with high levels of mitophagy have mitochondria that are highly ubiquitinated (Chapter 2). We wondered, therefore, if the function or localization of p62 on mitochondria in MFN-null cells occurs upstream of ubiquitination. To

test this we isolated mitochondria from MFN-null cells with or without p62 shRNA and probed for ubiquitin by western blot. We found that the level of ubiquitin on MFN-null cells is decreased when p62 is knocked-down with either of two shRNAs (Figure 3.4A), consistent with a role for p62 upstream of ubiquitination of mitochondria.

To further test a possible interaction of the UBA domain of p62 with ubiquitinated mitochondria, we first measured mitophagy levels in MFN-null MEFs expressing the cytosolic UBA domain of p62. If p62 binding to mitochondria via its UBA domain is required for mitophagy, this construct may interfere with mitophagy in a dominant negative fashion, by impeding the binding of endogenous, full-length p62. The level of mitophagy in UBA expressing MFN-null cells was mildly reduced relative to control cells (Figure 3.4 B), suggesting a possible role for ubiquitin in facilitating mitophagy in MFN-null cells, and confirming that the UBA domain can act in a dominant negative fashion. However, the reduction we saw due to UBA expression was far less complete than when p62 was knocked down by shRNA, suggesting that ubiquitin binding cannot be the only mechanism for p62 function in mitophagy.

We also tested a role for the UBA domain in mitophagy of sperm mitochondria in the embryo. We retrovirally expressed UBA-mCherry in pre-implantation mouse embryos fertilized with sperm expressing the green fluorescent protein, Dendra, targeted to mitochondria. Mouse sperm mitochondria are ubiquitinated prior to fertilization (Sutovsky et al., 2000), and we have previously shown that p62 is involved in their degradation. If p62 binding to

ubiquitin on sperm mitochondria is an essential step in mitophagy, expression of the UBA domain of p62 might act as a dominant negative and interfere with the function of endogenous p62. We found, however, that the UBA domain had no effect on the degradation of paternal mitochondria, which proceeded normally such that all paternal mitochondria were degraded in UBA injected and control embryos by 84 hours after fertilization (Figure 3.4C,D). This result may either indicate that the p62 UBA domain does not act as a dominant negative in embryos, or it may suggest that the ubiquitin binding by p62 is not important for mitophagy of paternal mitochondria in embryos. Our observation of a decreased effect of the UBA in embryos relative to MEFs may be due to the higher sensitivity of the cell-culture assay. Taken together, these results suggest that p62 may have some function on mitochondria that is upstream of mitochondrial ubiquitination.

P62 homolog, Nbr1 is not required for mitophagy in MFN-null MEFs or embryos

Like p62, another structurally similar protein, neighbor of BRCA1 gene 1 (NBR1), is also selectively degraded by autophagy (Kirkin et al., 2009). NBR1 has been implicated in pexophagy (Deosaran et al., 2013), and was identified in a proteomic analysis of mitochondria undergoing CCCP-induced mitophagy (Chan et al., 2011). However, recent work suggests that its role in CCCP-induced mitophagy, if any, may be dispensable (Shi et al., 2015). We tested whether Nbr1 might be involved in steady-state MFN-null mitophagy using our mitophagy

marker in MFN-null cells with or without knockdown of NBR1. Consistent with Shi et al., we found that NBR1 knockdown had no effect on the percent of MFN-null cells undergoing steady-state mitophagy (Figure 3.5A).

We next examined the role of NBR1 in mitophagy in embryos. We retrovirally expressed shRNA against NBR1 in preimplantation embryos with fluorescent paternal mitochondria, and assessed the presence or absence of paternal mitochondria at 84 hours after fertilization. Consistent with our MFN-null results, we found that knockdown of NBR1 did not inhibit degradation of paternal mitochondria in the embryo (Figure 3.5B,C). In contrast, knockdown of p62 strongly inhibited degradation of paternal mitochondria, with the majority of embryos retaining more than five clusters of Dendra-positive paternal mitochondria at 84 hours post fertilization. Due to their structural similarity, p62 and NBR1 may have redundant functions, which may mask an effect of NBR1 in the presence of p62. Therefore, we assessed the effect of NBR1 knockdown with concurrent knockdown of p62. We found no difference in degradation of paternal mitochondria between knockdown of p62 alone, or knockdown of NBR1 and p62 together, suggesting that NBR1 is dispensable for mitophagy of paternal mitochondria in the presence or absence of p62.

DISCUSSION

Mitochondrial fusion is a protective process that increases respiration, safeguards mtDNA, and maintains $\Delta\Psi_m$. The heterogeneous mitochondrial dysfunction in cells deficient in mitochondrial fusion has been shown to be damaging to the organism (Chen et al., 2010); however, the mechanisms by which MFN-null cells cope with this state are unclear. Previous evidence suggests that the PARKIN mediated mitophagy pathway may be involved in clearing damaged mitochondria from MFN-null cells (Narendra et al., 2008). Here we investigate the role of mitophagy receptor proteins in this process, providing further evidence for preferential targeting of defective mitochondria by the mitophagy machinery, and linking mitophagy to mitochondrial dynamics.

Several lines of evidence suggest an intimate link between mitochondrial dynamics and mitophagy. Mitochondrial fusion has been shown to be a selective process. Mitochondria with intact $\Delta\Psi_m$ fuse preferentially with mitochondria of similar $\Delta\Psi_m$, generating a sub-population of dysfunctional mitochondria, and conversely, mitochondrial fission generates metabolically uneven daughters (Twig et al., 2008). Mitochondrial depolarization results in Parkin accumulation and can trigger mitophagy (Narendra et al., 2008). OPA1 overexpression, on the other hand, decreases mitophagy, presumably by activating fusion (Twig et al., 2008). Using a fluorescence-quenching assay we show that cells lacking mitochondrial fusion exhibit a high level of steady-state mitophagy (Figure 3.2D,E), confirming the downstream result of the PARKIN accumulation observed by Narendra et al.

Our results suggest that p62 may play a key role in maintaining the functional status of the mitochondrial population in cells lacking mitochondrial fusion. We find that p62 supports the maintenance of $\Delta\Psi_m$ of the mitochondrial population in MFN-null cells (Figure 3.1D,E), and that it is recruited to a subset of mitochondria that are depolarized and lack mtDNA, potentially priming them for clearance from the cell (Figure 3.2A).

We show a requirement for p62 in steady-state mitophagy in MFN-null cells (Figure 3.2D,E) that is novel. The requirement for p62 at steady-state may explain the phenotypes observed due to loss of p62 in wild-type cells including mitochondrial fragmentation, loss of mtDNA, and depolarization of mitochondria (Seibenhener et al., 2013b). Loss of p62 may impair basal mitochondrial quality control, and although fewer mitochondria may be damaged at any given time in wildtype cells, over time damaged mitochondria, which are prevented from fusing with healthy mitochondria, could accumulate leading to an increasingly fragmented, dysfunctional population.

Given the finding that p62 is required for mitophagy, it is surprising that we find no change in mitochondrial mass in the absence of p62 (Figure 3.1D). Given that our experiments utilize cells stably expressing p62 shRNA, it is possible that compensatory mechanisms are engaged in these cells to restore mitochondrial mass to baseline. It might be interesting to determine how acute verses chronic loss of p62 influences mitochondrial biosynthesis. How the mitophagy and biosynthetic machinery may interact is unknown.

There are many gaps in our knowledge of the signaling events during mitochondrial dysfunction leading to mitophagy. The mechanism by which p62 is targeted to mitochondria is one such unknown. It has been speculated that autophagy receptors are recruited to cargo through interaction with ubiquitin, however two of our findings contradict this model. First, sufficiency of the PB1 domain (Figure 3.3B), which does not bind ubiquitin to localize p62 to mitochondria argues against an important role for ubiquitin upstream of p62 recruitment to mitochondria. Secondly, the reduction in ubiquitination of mitochondria that we observed in MFN-null cells with p62 knockdown, suggests that p62 plays a role in mitophagy of MFN-null mitochondria upstream of ubiquitination of mitochondria (Figure 3.4A). This is a surprising finding given the traditional model for p62 function as an autophagy receptor that binds specifically to ubiquitinated substrates. One possibility is that p62 collaborates with an E3 ligase to ubiquitinate mitochondria, or, given that p62 is also known for its ability to form higher order complexes, that it forms a scaffold that recruits E3 ligases themselves, or other regulatory proteins. These mechanisms, however, are unprecedented. Furthermore, our results do not rule out possible ubiquitination of mitochondria prior to p62 binding. We also find that overexpression of the p62 UBA domain has some limited effect on mitophagy in MFN-null cells (Figure 3.4B), which is consistent with a role for ubiquitin in mitophagy in these cells. Interestingly, exogenous expression of the UBA domain has no effect on mitophagy in embryos (Figure 3.4C,D), consistent with a model in which the

function of p62 on mitochondria is independent of ubiquitin binding in that context.

Surprisingly, we found not just one, but two domains capable of localizing p62 to mitochondria. The LIR domain of p62 also co-localizes with a subpopulation of mitochondria. Interestingly, these mitochondria are located primarily in the periphery of the cell, consistent with the site of autophagosome formation (Jahreiss et al., 2008). One possible explanation for this dual targeting is that the PB1 domain is the primary domain responsible for p62 binding to mitochondria, whereas the LIR domain co-localization is due to its interaction with the LC3 on autophagosomes that already contain mitochondria. This model would be consistent with previous observations that the direct interaction of LC3 with p62 is not sufficient for efficient p62 degradation by autophagy (Ichimura et al., 2008b). Further investigation will be necessary to resolve this point.

The localization of p62 to a subpopulation of mitochondria that we observed in MFN-null cells (Figure 3.3A), while consistent with previous studies defining the heterogeneity of mitochondria in these cells (Chen et al., 2005) is in contrast to our observations in wildtype cells undergoing OXPHOS-induced mitophagy, where p62 localizes to all mitochondria (Chapter 2). This may point to a key difference in the signaling mechanisms that trigger autophagy in these two cases, a topic that is currently unexplored. In MFN-null cells, mitophagy occurs at steady state, and appears to be the result of sequestration of a subset of defective mitochondria. In OXPHOS-induced mitophagy, or in CCCP-induced mitophagy (where the localization of p62 to mitochondria has not been explored), the entire

mitochondrial population is equally subjected to the change in cellular conditions and needs to respond. In contrast to these metabolically or pharmacologically induced mitophagy systems, basal mitophagy levels in wildtype cells are believed to be very low and highly tissue specific (Katayama et al., 2011; Sun et al.). Mitophagy in MFN-null cells may better replicate basal mitophagy but at an amplified scale, since more mitochondria are dysfunctional at any given time. This may make MFN-null cells a tractable model system in which to study steady-state mitophagy, a phenomenon which has thus far been difficult to address.

In particular, the signaling mechanism that may be involved in p62 accumulation on different populations of mitochondria is currently unknown, although several well-characterized signaling cascades are candidates. P62 interacts with the transcription factor NRF2, stabilizing it, and thereby activating NRF2 target genes (Komatsu et al., 2010b). NRF2 is one of the main cellular defense mechanisms combatting oxidative stress (Itoh et al., 1997). This pathway could be involved in the signaling of either steady state or OXPHOS-induced mitophagy. Furthermore, the PB1 domain of p62 is known to interact with atypical protein kinase C (PKC) family members (Sanchez et al., 1998). The PKC pathway kinases have a breadth of tissue-specific effects, which are unexplored in relation to mitophagy. Furthermore, p62 has recently been shown to bind to Raptor, an integral part of the mTORC1 complex which senses nutrients (Duran et al., 2011). Recent evidence suggests that the mTORC1 pathway may interface with mitophagy (Gilkerson et al., 2012).

Further evidence for the specificity of the signaling upstream of p62 recruitment is our observation that NBR1, a protein that is very structurally similar to p62 and known to localize to mitochondria, is not required for mitophagy in MFN-null cells or embryos irrespective of the presence of p62 (Figure 3.5A-C). This is consistent with experiments in Parkin expressing wildtype cells treated with CCCP (Shi et al., 2015). This does not rule out a non-essential role for NBR1 in mitophagy, which could still be recruited to mitochondria via hetero-dimerization of its PB1 domain with that on p62.

One possible explanation for the preferential requirement for p62 over NBR1 could be a specific p62 binding partner on mitochondria. A candidate for this role might be TBC1D15, which is recruited to mitochondria by its binding partner, FIS1, and implicated in mitophagy (Yamano et al., 2014). We found an interaction between p62 and TBC1D15 by co-immunoprecipitation and mass spec analysis of p62 binding partners on MFN-null mitochondria (unpublished data). Some evidence suggests that high levels of exogenous FIS1 can drive mitophagy (Gomes and Scorrano, 2008), but whether endogenous FIS1 and TBC1D15 levels are increased specifically on dysfunctional mitochondria is currently unknown.

In summary, our data reinforce the link between mitochondrial dynamics and mitophagy. We identify p62 as a key player in steady-state mitophagy in MFN-null cells, and rule out Nbr1 as an essential mitophagy receptor in this context. We propose that p62 plays a role in mitophagy upstream of ubiquitination of mitochondria, and may instead be recruited by specific protein-protein interactions. Because of its specificity for a subpopulation of

mitochondria, mitophagy in MFN-null MEFs may be a tractable model system for the low level of steady-state mitophagy ongoing in wildtype cells.

MATERIALS AND METHODS

Cell lines

The cells used included: p62-null MEFs (Ichimura et al., 2008b) (kindly provided by Shun Kageyama and Masaaki Komatsu), MFN-null, and wildtype MEFs have been described previously (Chen et al., 2005).

Cell culture

MEFs were maintained in Dulbecco's Modified Eagle's Medium (DMEM) supplemented with 10% fetal bovine serum (FBS), 100 U/mL penicillin and 100 U/mL streptomycin at 37°C and 5% CO2. Acetoacetate containing media was made as previously described (Mishra et al., 2014). For mitophagy experiments, cells were plated on Nunc Lab-Tek II Chambered Coverglass slides (155409, Thermo) in DMEM-based media. MFN-null cells were imaged in this media one day after plating. P62 knockout MEFs were treated as follows: after cells had adhered, they were washed with PBS and acetoacetate-containing medium was applied, after which cells were allowed to grow for four days and then imaged.

Stable isotope labeling by amino acid in cell culture (SILAC)

SILAC, including isotope labeling, mitochondrial isolation and purification, isoelectric focusing of peptides, and mass spectrometric analysis, was performed as described in (Chan et al., 2011). Wildtype cells were passaged

ten-times in heavy medium before analysis. MFN-null cells were passaged in regular medium.

Isolation of mitochondria

For immunoblot analysis, mitochondria were isolated as previously described (Pagliarini et al., 2008). For SILAC, mitochondria were isolated as described in (Chan et al., 2011)

Data analysis

Raw data files were analyzed as described in (Chan et al., 2011) except that the IPI mouse database (v 3.54) was searched. Protein groups significantly different overall ratios ($P < 0.01$) and with significantly different ratios in both replicates ($P < 0.05$) were considered to be significantly altered. Mitochondrial annotations were derived from MitoCarta (Pagliarini et al., 2008).

Antibodies and reagents

The following commercially available antibodies were used: anti-Hsp60 (SC-1054, Santa Cruz Biotech), anti-P62 (PM045, MBL), anti-VDAC1 (4661S, Cell Signaling), anti-DNA (CBL186, Chemicon), and anti-Ubiquitin (P4D1, Cell Signaling). The following commercially available dyes were used: JC-1 dye (T3168, ThermoFisher), PicoGreen (P7581, Invitrogen), and MitoTracker Red FM (M22425, Invitrogen).

Immunostaining

For immunofluorescence experiments, cells were fixed with 10% formalin, permeabilized with 0.1% Triton X-100, and stained with the primary antibodies listed above and with the following secondary antibodies: goat anti-mouse Alexa Fluor 488, donkey anti-goat Alexa Fluor 546, goat anti-rabbit Alexa Fluor 488, and goat anti-rabbit Alexa Fluor 633 (Invitrogen). When used, DAPI (d1306, Invitrogen) was included in the last wash.

shRNA virus design and production

For experiments in MEFs, the retroviral vector pRetroX-H1, which contains the H1 promoter, was used to express shRNAs. shRNAs were cloned into the BglII/EcoRI sites. For embryo injection experiments, a third-generation lentiviral backbone was used to express shRNAs. The lentiviral vector FUGW-H1 (Fasano et al., 2007) was modified by replacing the GFP reporter gene with mCherry and changing the shRNA cloning sites from Xba/SmaI to BamHI/EcoRI, generating FUChW-H1. For dual knockdown experiments in embryos, a second H1 promoter was added, along with XbaI/NheI cloning sites 3' to the original H1 promoter, generating FUChW-H1H1.

The shRNA target sequences were:

p62 sh2:	TGGCCACTCTTTAGTGTTTGTGT
p62 sh1:	GACAACCCGTGTTTCCTTTATTA
NBR1:	GGAGTGGATTTACCAGTTATT

Non-targeting: GACTAGAAGGCACAGAGGG

Lentiviral vectors were cotransfected into 293T cells with plasmids pMDLG/pRRE, pIVS-VSVG, and pRSV-Rev. Retroviral vectors were cotransfected into 293T cells with plasmids pVSVG and pUMVC. All transfections were done using calcium phosphate precipitation. For microinjection, virus was collected, filtered, concentrated by ultracentrifugation at 25,000 rpm for 2 hours, resuspended in PBS, and stored at -80°C as described previously (30, 31). Viral titers were measured by infecting MEFs with serial dilutions of viral preparations, followed by flow cytometric analysis after 48 hr. Virus was used at 1x107 transducing units/μL.

Embryo microinjection

All mouse work was done according to protocols approved by the Institutional Animal Care and Use Committee at the California Institute of Technology. For each experiment, four C57/Bl6J wildtype female mice at 21-25 days old were superovulated by hormone priming as described previously (Pease and Lois, 2006), and then each was caged with a *PhAM* male (Pham et al., 2012b). After euthanization of females by CO_2 asphyxiation, the embryos were harvested and placed in M2 medium (MR-015-D, Millipore) at 12 hours after fertilization as described in (Pease and Lois, 2006). Approximately 60 to 100 embryos were collected per experiment. Embryos were divided into two equal groups and microinjected with 10 to 100 pl of viral stock into the perivitelline space as described in (Lois et al., 2002; Pease and Lois, 2006). Embryos were

washed with KSOM+AA medium (MR-106-D, Millipore) and cultured in that medium covered by oil (M8410, Sigma) at 37°C and 5% CO_2. For each construct, at least three separate microinjection sessions were performed. In preparation for imaging, embryos were transferred to 10 μl droplets of KSOM+AA medium on glass-bottom dishes (FD35-100, World Precision Instruments).

Imaging

All images were acquired with a Zeiss LSM 710 confocal microscope with a Plan-Apochromat 63X/1.4 oil objective. All live imaging was performed in an incubated microscope stage at 37°C and 5% CO_2. The 488 nm and 561 nm laser lines were used to excite cox8-EGFP-mCherry and imaging was done in line mode to minimize movement of mitochondria between acquisition of each channel. The 405 nm laser line was used to excite mTurquoise2 and DAPI. Alexa 488 conjugated dyes, the monomeric form of JC-1, and picoGreen were excited by the 488 nm laser. Alexa 546 conjugated dyes, the J-aggregate form of JC-1, mCherry, and Mitotracker Red were excited by the 561 nm laser. Alexa 633 conjugated dyes were excited by the 633 nm laser.

For embryo imaging, optical slices were acquired at 1.1-μm thickness, and z stacks were oversampled at 0.467 μm. The 488 nm laser line was used to excite Dendra2 in the unconverted state. The mercury lamp was not used to avoid photoconversion. The same settings were used across all embryo-imaging experiments. Zen 2009 image analysis software was used to produce maximum intensity z-projections.

Membrane potential measurements

Fluorescence of 5,5′,6,6′-tetrachloro-1,1′,3,3′ tetraethylbenzimidazolyl-carbocyanine iodide (JC-1) was used to monitor mitochondrial membrane potential. Samples were loaded with a 6000 fold dilution (100 ng/ml) of JC-1 in media for 30 minutes at 37°C and then washed into fresh media. Samples were imaged live. The same acquisition settings were used across experiments. Images were analyzed in ImageJ. Briefly, individual cell borders were outlined, and mean fluorescence intensity was recorded for each channel using the Measurement tool. Data for at least 30 cells was averaged and the ratio of shRNA-treated:control was averaged across three independent replicates.

PicoGreen nucleoid analysis

Cells were loaded with a 500 fold dilution of PicoGreen and 250nM MitoTracker Red FM in media for 15 minutes at 37°C and then washed into fresh, pre-incubated media. Samples were imaged live. The same acquisition settings were used across experiments. Images were analyzed in ImageJ using the JACoP plugin Objects based method. Images were filtered using a threshold set by JACoP and individual objects segmented in each channel. The center of mass method was used to determine object colocalization with a minimum particle size of 0 and a maximum of 25600. The ratio of colocalized objects:total mitotracker objects was taken and averaged across at least ten separate frames.

qPCR

qPCR of mtDNA was performed as described in (Chen et al., 2010)

Retroviral expression constructs

The *Cox8-EGFP-mCherry* retroviral vector (kindly provided by Dr. Prashant Mishra) consists of the *Cox8* mitochondrial targeting sequence placed N-terminal to an EGFP- mCherry fusion. The mito-targeted mTurquoise2 vector was pmTurquoise2-Mito (Addgene plasmid # 36208, Dorus Gadella, (Goedhart et al., 2012)). To clone LC3 and p62-full length mTurquoise2 fusion proteins mTurquoise2 was amplified from this vector. Mouse P62 isoform 1 was amplified from pMXs-puro GFP-p62 (Addgene plasmid # 38277, Noboru Mizushima, (Itakura and Mizushima, 2011b)). mTurquoise2 and mCherry fusion proteins were cloned into the retroviral vector, pBABEpuro that was modified by addition of AgeI and BglII sites inserted between BamHI and EcoRI. mCherry/mTurquoise2 were inserted between AgeI and BglII, and p62 or LC3 were cloned between EcoRI and SalI sites, resulting in a 12 amino acid linker between inserts. Truncation constructs of p62 were as follows:

Full Length: aa1-443

Nterm: aa1-233

PB1: aa1-102

ZZ: aa122-167

Cterm: aa234-443

LIR: aa321-349

UBA: aa386-438

All plasmids were verified by DNA sequence analysis. Stable cell lines were generated by retroviral infection followed by selection with 2 μg/μl puromycin.

Analysis

Images were cropped when appropriate and image contrast and brightness were globally adjusted in Photoshop (Adobe). Mitophagy quantifications were scored in triplicate with greater than 100 cells per experiment.

Western densitometry analysis was done using ImageJ. Density of p62 signal was normalized to density of VDAC1 signal and the average of two independent experiments was taken.

For quantification of paternal mitochondria, maximum intensity z stacks were scored as having greater than 5, less than 5, or no distinct green puncta. Embryos from four females were pooled per experiment. For Nbr1 shRNA experiments two or more independent replicate experiments were averaged. For UBA expression experiments, a single experiment is shown.

p values are the result of students two-tailed t test, except for embryo data, which are Chi-square analysis with two degrees of freedom.

FIGURE LEGENDS

Table 3.1 Proteins with increased abundance in the mitochondria of MFN-null cells. Summary of the most significantly increased proteins in mitochondria isolated from MFN-null MEFs. Ratios are MFN-null/wildtype.

Figure 3.1 Increased P62 on mitochondria in the absence of mitofusins is necessary for maintaining mitochondrial membrane potential. (**A**) Western blot analysis of p62 expression in wildtype and MFN-null MEFs from whole cell lysate (WCL) or isolated mitochondria (mitochondria). VDAC1 is a loading control. Quantitation by densitometry plotted below, reported as p62/VDAC1 normalized to wildtype. *, $p < 0.05$. (**B**) Western blot analysis of p62 expression in mitochondria isolated from MFN-null MEFs untreated (control) or treated with two different p62 shRNAs (p62 sh1 and sh2). VDAC1 is a loading control. Quantitation by densitometry plotted below, reported as p62/VDAC1 normalized to control. *, $p < 0.05$. (**C**) Co-localization of p62 with mitochondria. Wildtype or MFN-null MEFs were immunostained with anti p62 (green) and anti-HSP60 (red, mitochondrial marker). (**D**) JC-1 staining to measure relative $\Delta\Psi_m$ in MFN-null MEFs with or without p62 shRNA. Cells were loaded with 100ng/mL JC-1 and J-aggregates ($\Delta\Psi_m$ dependent) or monomers ($\Delta\Psi_m$ independent) were imaged as indicated. (**E**) Quantitation of JC-1 staining. Reported as mean fluorescence intensity per cell, averaged over three independent experiments. Note a significant reduction in J-aggregate accumulation ($\Delta\Psi_m$) in p62 shRNA cells with no change

in monomer uptake (mitochondrial mass). Error bars indicate SD. Scale bar, 10 μm.

Figure 3.2 P62 is required for degradation of a subset of defective mitochondria by mitophagy in MFN-null cells. (**A**) Co-localization of p62 with mtDNA and depolarized mitochondria. MFN-null MEFs stably expressing mTurquoise2-p62 (blue) were stained with MitoTracker Red (red, $\Delta\Psi_m$ dependent mitochondrial marker) and immunostained with anti DNA (green). Arrows indicate mitochondria that co-localized with DNA but not with p62, arrowheads indicate mitochondria that co-localized with p62 but not with DNA. Note reduced MitoTracker intensity of mitochondria co-localized with p62. Scale bar, 10 μm. (**B**) Co-localization of mtDNA with mitochondria. MFN-null MEFs with or without p62 shRNA were stained with PicoGreen (green) and MitoTracker Red (red) and imaged. Quantitation on right is percent of mitochondria that co-localize with PicoGreen. Note equivalent mtDNA co-localization with or without p62 shRNA. Scale bar, 10 μm. *p* value non-significant (ns) obtained from unpaired t test. Error bars indicate SD. (**C**) Mitochondrial copy number in MFN-null MEFs with and without p62 knockdown. P62 knockdown with two different shRNAs as indicated. To obtain the mtDNA level for a single DNA sample, quantitative PCR was performed in triplicate. p values non-significant (ns) obtained from unpaired t tests. Error bars indicate SD. (**D**) Mitophagy in MFN-null cells with and without p62 shRNA (sh2) or with p62 shRNA and exogenous full-length p62 (sh2 + p62-Full). MEFs stably expressing Cox8-EGFP-mCherry mitophagy marker were

imaged by fluorescence microscopy. P62 shRNA and/or full-length p62 were stably introduced by retroviral infection. Note that red-only puncta represent mitochondrial contents within acidic compartments. (**E**) Quantitation of percent of cells containing puncta from (**D**). Experiment performed in triplicate, greater than 100 cells counted per experiment. ***, p <0.001. Scale bar, 10 μm. Error bars indicate SD. (**F**) Co-localization of LC3B with red-only puncta. MFN-null MEFs, with or without p62 shRNA, stably expressing cox8-EGFP-mCherry and mTurquoise2-LC3B were imaged by fluorescence microscopy. Note that mTurquoise2-LC3B puncta localize to mitochondrial puncta only in the absence of p62 shRNA. Scale bar, 10 μm.

Figure 3.3 The PB1 and LIR domains but not the UBA of p62 are sufficient for its localization to mitochondria. (**A**) Co-localization of p62 with red-only mitochondria. MFN-null MEFs stably expressing Cox8-EGFP-mCherry and p62-Turquoise were imaged. Arrows indicate yellow mitochondria (red + green) that do not co-localize with p62. Arrowheads indicate red-only mitochondria that co-localize with p62. Scale bar, 10 μm. (**B**) MFN-null MEFs stably expressing cox8-Turquoise2 (green, mitochondrial marker) and mCherry-p62Full (wildtype, 1-443 amino acids), mCherry-p62Nterm (1-233 amino acids), mCherry-p62PB1 (1-102 amino acids), mCherry-p62ZZ (122-167 amino acids), mCherry-p62Cterm (234-443 amino acids), mCherry-p62LIR (321-349 amino acids), or mCherry-p62UBA (386-438 amino acids) (all in red) were imaged by confocal microscopy. Note that mitochondria co-localize predominantly with p62Full, p62Nterm, and p62PB1,

and to a lesser extent with p62Cterm and p62LIR, but not with p62UBA. Scale bar, 10 μm applies to (**B**) and (**C**). (**C**) Co-localization of p62PB1 with mitochondria in p62-KO MEFs. P62-KO MEFs stably expressing cox8-Turquoise2 (green, mitochondrial marker), and mCherry-p62PB1 were grown in OXPHOS-inducing media to induce mitophagy. Note that p62PB1 co-localizes with mitochondrial puncta in the absence of endogenous p62.

Figure 3.4 Ubiquitination of MFN-null mitochondria is dependent on p62. (**A**) Accumulation of polyubiquitinated proteins in mitochondria. Mitochondria from MFN-null MEFs with or without p62 shRNA were isolated by differential centrifugation. Mitochondrial lysates were analyzed by western blot for pan-Ubiquitin. VDAC1 is a loading control. Note the reduced ubiquitin level in p62 shRNA expressing cells. (**B**) Mitophagy in MFN-null cells with and without p62UBA. MEFs stably expressing Cox8-EGFP-mCherry mitophagy marker and mTurquoise2-p62UBA were imaged by fluorescence microscopy and percent of cells containing red-only puncta were counted. Note a slightly reduced percent of cells with puncta in the presence of p62-UBA. Experiment performed in triplicate, greater than 100 cells counted per experiment. ***, $p < 0.001$. Error bars indicate SD. (**C**) Clearance of paternal mitochondria. Wildtype females were mated with male *PhAM* mice, and embryos were collected 12 hours after fertilization. Retrovirus encoding mCherry-p62UBA was injected in the perivitelline space. Control is un-injected. The mitochondrial Dendra2 signal was imaged live by fluorescence microscopy at 84 hours after fertilization. Images are representative

maximum intensity projections. Scale bar, 10 μm. (**D**) Quantitation of paternal mitochondrial elimination at 84 hours post-fertilization. Embryos were scored as having no paternal mitochondria (black bar), less than five clusters (white bar), or greater than five clusters (green bar).

Figure 3.5 P62 homolog, Nbr1 is not required for mitophagy in MFN-null MEFs or embryos. (**A**) Mitophagy in MFN-null cells with and without NBR1 shRNA. MEFs stably expressing Cox8-EGFP-mCherry mitophagy marker and NBR1 shRNA were imaged by fluorescence microscopy and percent of cells with red-only puncta were counted. Note that red-only puncta are observed at similar frequency in either case. Scale bar, 10 μm. Experiment performed in triplicate, greater than 100 cells counted per experiment. *p* value not significant (ns), student's t-test, unpaired. Error bars indicate SD. (**B**) Clearance of paternal mitochondria. Wildtype females were mated with male *PhAM* mice, and embryos were collected 12 hours after fertilization. Lentivirus encoding non-targeting shRNA, p62 shRNA, NBR1 shRNA, or both p62 shRNA and NBR1 shRNA was injected in the perivitelline space. The mitochondrial Dendra2 signal was imaged live by fluorescence microscopy at 84 hours after fertilization. Images are representative maximum intensity projections. Scale bar, 10 μm. (**C**) Quantitation of paternal mitochondrial elimination at 84 hours post-fertilization. Embryos were scored as having no paternal mitochondria (black bar), less than five clusters (white bar), or greater than five clusters (green bar). The average of two

independent injection experiments is shown. *p* value not significant (ns), student's t-test, unpaired. Error bars indicate SD.

Table 3.1

Proteins with increased abundance in the mitochondria of MFN-null cells

Protein	**Localization**	**Biological Function**	**SILAC ratio[a]**	**Significance[b]**
GATM	Mitochondria	Creatine synthesis	26.7	8.16E-12
PON3	Unknown	Metabolism	11.7	4.86E-07
THBS1	ER	UPR	7.2	1.34E-05
CBR2	Mitochondria	Metabolism	6.9	2.61E-05
CA5B	Mitochondria	Metabolism	6.5	4.37E-05
p62/SQSTM1	Cytosol	Autophagy receptor	6.0	1.56E-03
POLRMT	Mitochondria	mtDNA transcription	4.8	3.21E-04
FAHD2	Mitochondria	Metabolism	3.7	6.50E-04
ECH1	Mitochondria	Metabolism	3.5	2.36E-03

[a]Combined SILAC ratio from two independent mass spectrometry experiments. The ratio represents the protein level in MFN-null mitochondria divided by the level in wild-type cells.

[b]Corresponds to the significance calculated in MaxQuant.

Figure 3.1

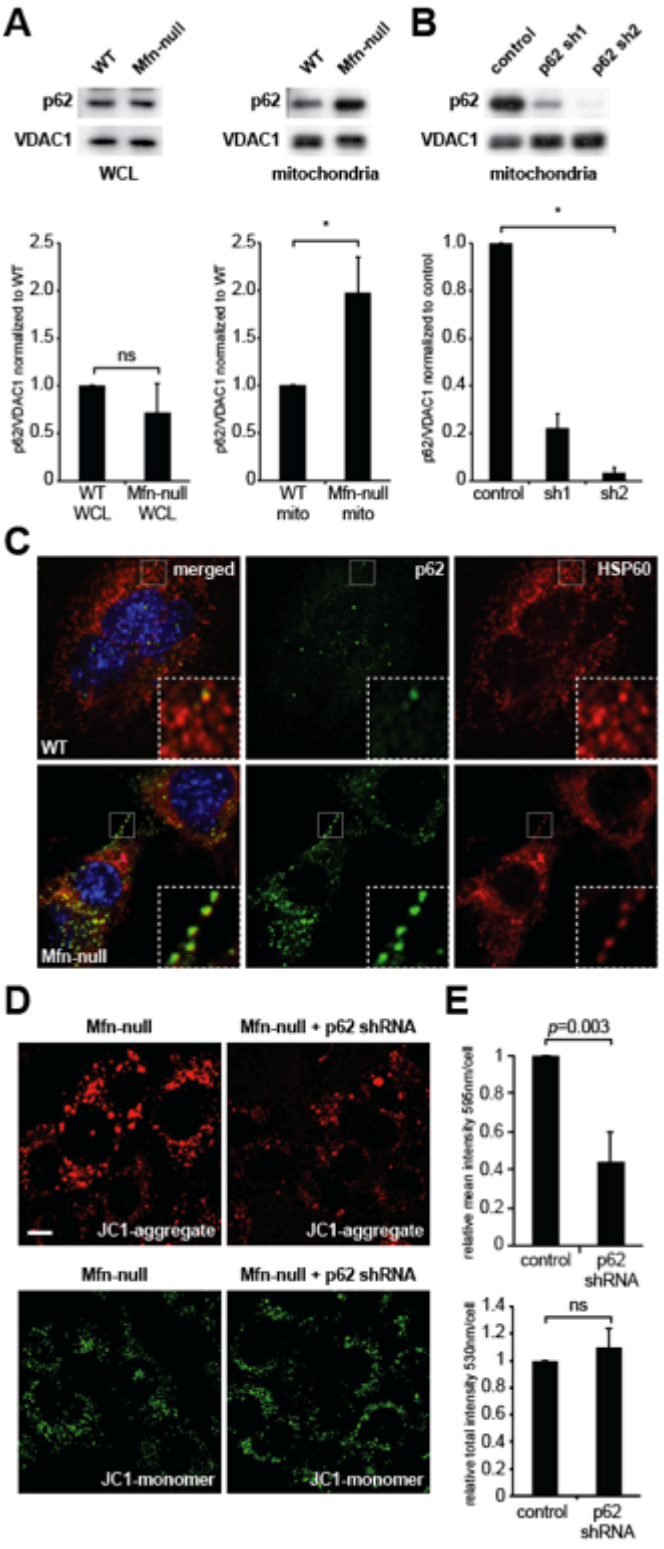
A
WT
Mfn-null
p62
VDAC1
WCL
mitochondria
B
control
p62 sh1
p62 sh2
p62/VDAC1 normalized to WT
ns
WT WCL
Mfn-null WCL
WT mito
Mfn-null mito
p62/VDAC1 normalized to control
control
sh1
sh2
C
merged
p62
HSP60
WT
Mfn-null
D
Mfn-null
Mfn-null + p62 shRNA
JC1-aggregate
JC1-monomer
E
p=0.003
relative mean intensity 595nm/cell
control
p62 shRNA
ns
relative total intensity 530nm/cell

Figure 3.2

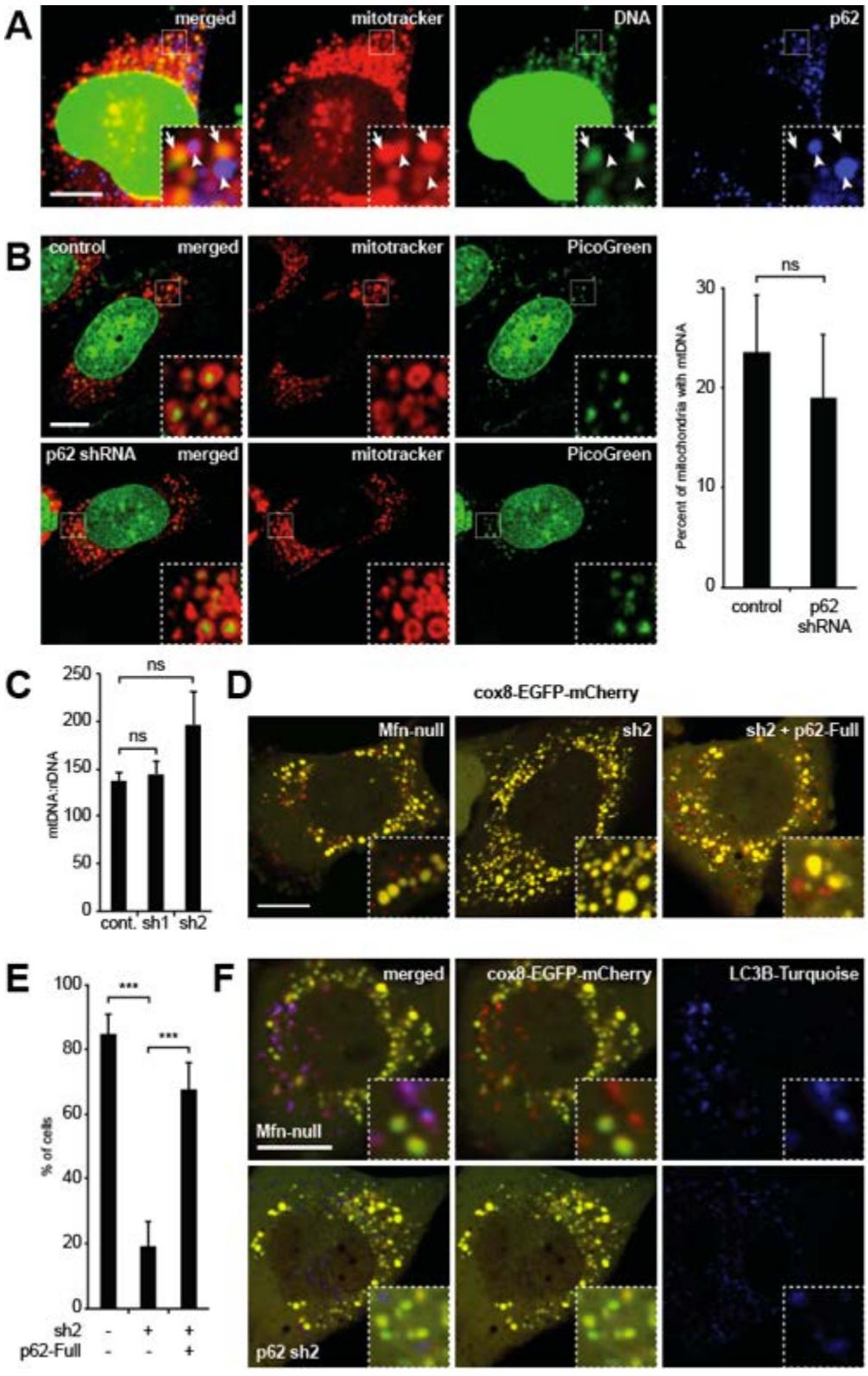
A
merged
mitotracker
DNA
p62
B
control
merged
mitotracker
PicoGreen
p62 shRNA
merged
mitotracker
PicoGreen
ns
Percent of mitochondria with mtDNA
30
20
10
0
control
p62 shRNA
C
mtDNA:nDNA
250
200
150
100
50
0
ns
ns
cont.
sh1
sh2
D
cox8-EGFP-mCherry
Mfn-null
sh2
sh2 + p62-Full
E
% of cells
100
80
60
40
20
0
***
***
sh2 - + +
p62-Full - - +
F
merged
cox8-EGFP-mCherry
LC3B-Turquoise
Mfn-null
p62 sh2

Figure 3.3

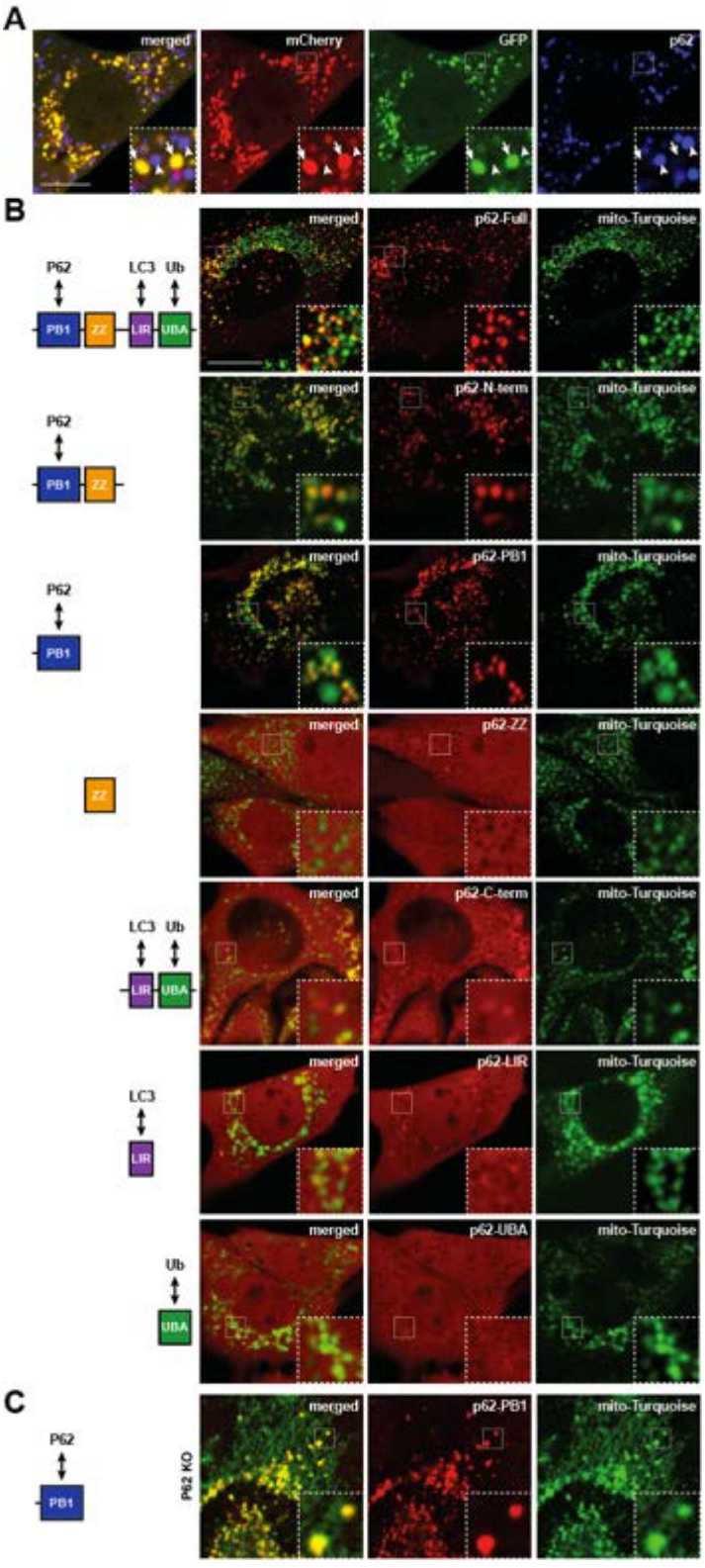
A
merged
mCherry
GFP
p62
B
P62
LC3
Ub
PB1
ZZ
LIR
UBA
merged
p62-Full
mito-Turquoise
merged
p62-N-term
mito-Turquoise
merged
p62-PB1
mito-Turquoise
merged
p62-ZZ
mito-Turquoise
merged
p62-C-term
mito-Turquoise
merged
p62-LIR
mito-Turquoise
merged
p62-UBA
mito-Turquoise
C
P62
PB1
P62 KO
merged
p62-PB1
mito-Turquoise

Figure 3.4

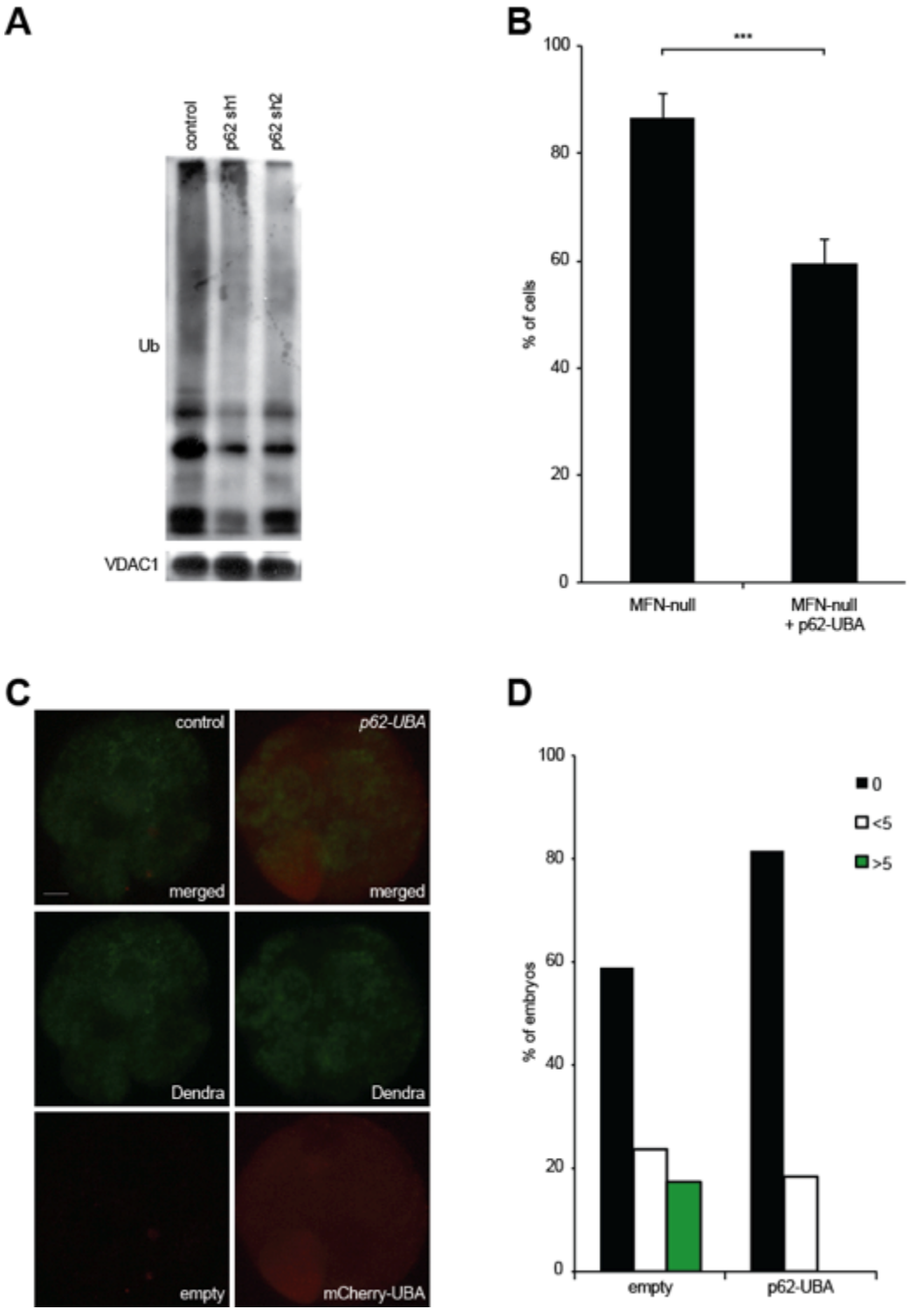
A
control
p62 sh1
p62 sh2
Ub
VDAC1
B
***
100
80
60
40
20
0
% of cells
MFN-null
MFN-null
+ p62-UBA
C
control
p62-UBA
merged
merged
Dendra
Dendra
empty
mCherry-UBA
D
100
80
60
40
20
0
% of embryos
0
<5
>5
empty
p62-UBA

Figure 3.5

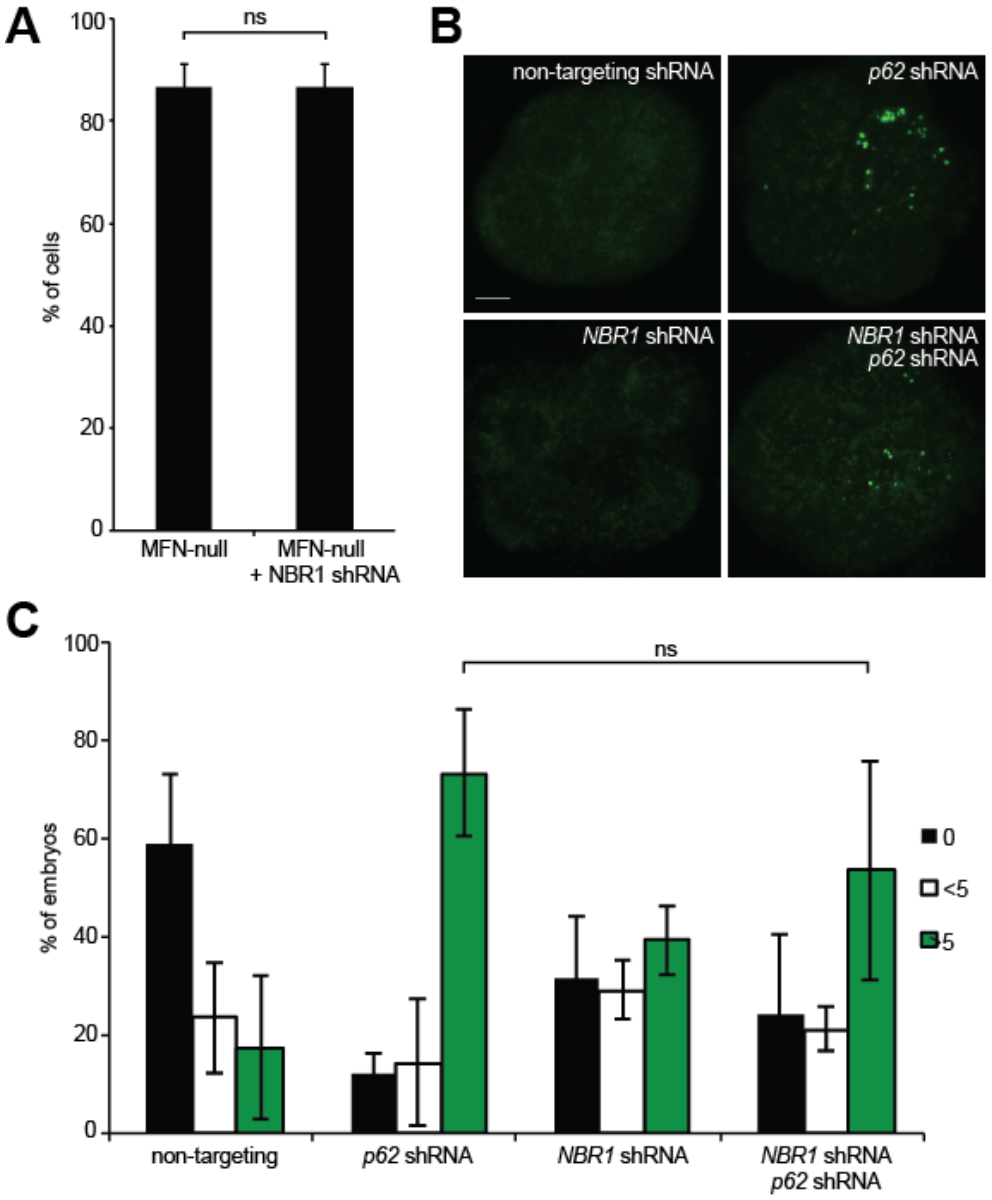
A
100
80
60
40
20
0
% of cells
ns
MFN-null
MFN-null
+ NBR1 shRNA
B
non-targeting shRNA
p62 shRNA
NBR1 shRNA
NBR1 shRNA
p62 shRNA
C
100
80
60
40
20
0
% of embryos
ns
0
<5
5
non-targeting
p62 shRNA
NBR1 shRNA
NBR1 shRNA
p62 shRNA

REFERENCES

Bjorkoy, G., Lamark, T., Brech, A., Outzen, H., Perander, M., Overvatn, A., Stenmark, H., and Johansen, T. (2005). p62/SQSTM1 forms protein aggregates degraded by autophagy and has a protective effect on huntingtin-induced cell death. J Cell Biol *171*, 603-614.

Calvo, S.E., Clauser, K.R., and Mootha, V.K. (2016). MitoCarta2.0: an updated inventory of mammalian mitochondrial proteins. Nucleic Acids Res *44*, D1251-1257.

Cao, Y., Cheong, H., Song, H., and Klionsky, D.J. (2008). In vivo reconstitution of autophagy in Saccharomyces cerevisiae. The Journal of Cell Biology *182*, 703-713.

Chan, N.C., Salazar, A.M., Pham, A.H., Sweredoski, M.J., Kolawa, N.J., Graham, R.L., Hess, S., and Chan, D.C. (2011). Broad activation of the ubiquitin-proteasome system by Parkin is critical for mitophagy. Hum Mol Genet *20*, 1726-1737.

Chen, H., Chomyn, A., and Chan, D.C. (2005). Disruption of fusion results in mitochondrial heterogeneity and dysfunction. J Biol Chem *280*, 26185-26192.

Chen, H., Detmer, S.A., Ewald, A.J., Griffin, E.E., Fraser, S.E., and Chan, D.C. (2003). Mitofusins MFN1 and MFN2 coordinately regulate mitochondrial fusion and are essential for embryonic development. J Cell Biol *160*, 189-200.

Chen, H., McCaffery, J.M., and Chan, D.C. (2007). Mitochondrial fusion protects against neurodegeneration in the cerebellum. Cell *130*, 548-562.

Chen, H., Vermulst, M., Wang, Y.E., Chomyn, A., Prolla, T.A., McCaffery, J.M., and Chan, D.C. (2010). Mitochondrial fusion is required for mtDNA stability in skeletal muscle and tolerance of mtDNA mutations. Cell *141*, 280-289.

Deosaran, E., Larsen, K.B., Hua, R., Sargent, G., Wang, Y., Kim, S., Lamark, T., Jauregui, M., Law, K., Lippincott-Schwartz, J., *et al.* (2013). NBR1 acts as an autophagy receptor for peroxisomes. J Cell Sci *126*, 939-952.

Detmer, S.A., and Chan, D.C. (2007). Functions and dysfunctions of mitochondrial dynamics. Nat Rev Mol Cell Biol *8*, 870-879.

Duborjal, H., Beugnot, R., Mousson de Camaret, B., and Issartel, J.P. (2002). Large functional range of steady-state levels of nuclear and mitochondrial transcripts coding for the subunits of the human mitochondrial OXPHOS system. Genome Res *12*, 1901-1909.

Duran, A., Amanchy, R., Linares, J.F., Joshi, J., Abu-Baker, S., Porollo, A., Hansen, M., Moscat, J., and Diaz-Meco, M.T. (2011). p62 is a key regulator of nutrient sensing in the mTORC1 pathway. Mol Cell *44*, 134-146.

Fasano, C.A., Dimos, J.T., Ivanova, N.B., Lowry, N., Lemischka, I.R., and Temple, S. (2007). shRNA knockdown of Bmi-1 reveals a critical role for p21-Rb pathway in NSC self-renewal during development. Cell Stem Cell *1*, 87-99.

Filadi, R., Greotti, E., Turacchio, G., Luini, A., Pozzan, T., and Pizzo, P. (2015). Mitofusin 2 ablation increases endoplasmic reticulum-mitochondria coupling. Proc Natl Acad Sci U S A *112*, E2174-2181.

Geisler, S., Holmstrom, K.M., Skujat, D., Fiesel, F.C., Rothfuss, O.C., Kahle, P.J., and Springer, W. (2010). PINK1/Parkin-mediated mitophagy is dependent on VDAC1 and p62/SQSTM1. Nat Cell Biol *12*, 119-131.

Gilkerson, R.W., De Vries, R.L.A., Lebot, P., Wikstrom, J.D., Torgyekes, E., Shirihai, O.S., Przedborski, S., and Schon, E.A. (2012). Mitochondrial autophagy in cells with mtDNA mutations results from synergistic loss of transmembrane potential and mTORC1 inhibition. Human Molecular Genetics *21*, 978-990.

Goedhart, J., von Stetten, D., Noirclerc-Savoye, M., Lelimousin, M., Joosen, L., Hink, M.A., van Weeren, L., Gadella, T.W., Jr., and Royant, A. (2012). Structure-guided evolution of cyan fluorescent proteins towards a quantum yield of 93%. Nat Commun *3*, 751.

Gomes, L.C., and Scorrano, L. (2008). High levels of Fis1, a pro-fission mitochondrial protein, trigger autophagy. Biochimica et Biophysica Acta (BBA) - Bioenergetics *1777*, 860-866.

Hoppins, S., Lackner, L., and Nunnari, J. (2007). The machines that divide and fuse mitochondria. Annu Rev Biochem *76*, 751-780.

Ichimura, Y., Kominami, E., Tanaka, K., and Komatsu, M. (2008a). Selective turnover of p62/A170/SQSTM1 by autophagy. Autophagy *4*, 1063-1066.

Ichimura, Y., Kumanomidou, T., Sou, Y.S., Mizushima, T., Ezaki, J., Ueno, T., Kominami, E., Yamane, T., Tanaka, K., and Komatsu, M. (2008b). Structural basis for sorting mechanism of p62 in selective autophagy. J Biol Chem *283*, 22847-22857.

Itakura, E., and Mizushima, N. (2011a). p62 Targeting to the autophagosome formation site requires self-oligomerization but not LC3 binding. J Cell Biol *192*, 17-27.

Itakura, E., and Mizushima, N. (2011b). p62 targeting to the autophagosome formation site requires self-oligomerization but not LC3 binding. The Journal of Cell Biology *192*, 17-27.

Itoh, K., Chiba, T., Takahashi, S., Ishii, T., Igarashi, K., Katoh, Y., Oyake, T., Hayashi, N., Satoh, K., Hatayama, I., *et al.* (1997). An Nrf2/small Maf heterodimer mediates the induction of phase II detoxifying enzyme genes through antioxidant response elements. Biochemical and biophysical research communications *236*, 313-322.

Jahreiss, L., Menzies, F.M., and Rubinsztein, D.C. (2008). The Itinerary of Autophagosomes: From Peripheral Formation to Kiss-and-Run Fusion with Lysosomes. Traffic (Copenhagen, Denmark) *9*, 574-587.

Jain, A., Lamark, T., Sjøttem, E., Bowitz Larsen, K., Atesoh Awuh, J., Øvervatn, A., McMahon, M., Hayes, J.D., and Johansen, T. (2010). p62/SQSTM1 Is a Target Gene for Transcription Factor NRF2 and Creates a Positive Feedback Loop by Inducing Antioxidant Response Element-driven Gene Transcription. Journal of Biological Chemistry *285*, 22576-22591.

Johansen, T., and Lamark, T. (2011). Selective autophagy mediated by autophagic adapter proteins. Autophagy *7*, 279-296.

Katayama, H., Kogure, T., Mizushima, N., Yoshimori, T., and Miyawaki, A. (2011). A sensitive and quantitative technique for detecting autophagic events based on lysosomal delivery. Chemistry & biology *18*, 1042-1052.

Kirkin, V., Lamark, T., Sou, Y.S., Bjorkoy, G., Nunn, J.L., Bruun, J.A., Shvets, E., McEwan, D.G., Clausen, T.H., Wild, P., *et al.* (2009). A role for NBR1 in autophagosomal degradation of ubiquitinated substrates. Mol Cell *33*, 505-516.

Komatsu, M., Kurokawa, H., Waguri, S., Taguchi, K., Kobayashi, A., Ichimura, Y., Sou, Y.-S., Ueno, I., Sakamoto, A., Tong, K.I., *et al.* (2010a). The selective autophagy substrate p62 activates the stress responsive transcription factor Nrf2 through inactivation of Keap1. Nat Cell Biol *12*, 213-223.

Komatsu, M., Kurokawa, H., Waguri, S., Taguchi, K., Kobayashi, A., Ichimura, Y., Sou, Y.S., Ueno, I., Sakamoto, A., Tong, K.I., *et al.* (2010b). The selective autophagy substrate p62 activates the stress responsive transcription factor Nrf2 through inactivation of Keap1. Nat Cell Biol *12*, 213-223.

Koshiba, T., Detmer, S.A., Kaiser, J.T., Chen, H., McCaffery, J.M., and Chan, D.C. (2004). Structural basis of mitochondrial tethering by mitofusin complexes. Science *305*, 858-862.

Lamark, T., Kirkin, V., Dikic, I., and Johansen, T. (2009). NBR1 and p62 as cargo receptors for selective autophagy of ubiquitinated targets. Cell Cycle *8*, 1986-1990.

Lamark, T., Perander, M., Outzen, H., Kristiansen, K., Overvatn, A., Michaelsen, E., Bjorkoy, G., and Johansen, T. (2003). Interaction codes within the family of mammalian Phox and Bem1p domain-containing proteins. J Biol Chem *278*, 34568-34581.

Lin, X., Li, S., Zhao, Y., Ma, X., Zhang, K., He, X., and Wang, Z. (2013). Interaction domains of p62: a bridge between p62 and selective autophagy. DNA Cell Biol *32*, 220-227.

Lois, C., Hong, E.J., Pease, S., Brown, E.J., and Baltimore, D. (2002). Germline transmission and tissue-specific expression of transgenes delivered by lentiviral vectors. Science *295*, 868-872.

Long, J., Garner, T.P., Pandya, M.J., Craven, C.J., Chen, P., Shaw, B., Williamson, M.P., Layfield, R., and Searle, M.S. (2010). Dimerisation of the UBA domain of p62 inhibits ubiquitin binding and regulates NF-kappaB signalling. J Mol Biol *396*, 178-194.

Matsumoto, G., Wada, K., Okuno, M., Kurosawa, M., and Nukina, N. (2011). Serine 403 phosphorylation of p62/SQSTM1 regulates selective autophagic clearance of ubiquitinated proteins. Mol Cell *44*, 279-289.

Meeusen, S., DeVay, R., Block, J., Cassidy-Stone, A., Wayson, S., McCaffery, J.M., and Nunnari, J. (2006). Mitochondrial inner-membrane fusion and crista maintenance requires the dynamin-related GTPase Mgm1. Cell *127*, 383-395.

Meeusen, S., McCaffery, J.M., and Nunnari, J. (2004). Mitochondrial fusion intermediates revealed in vitro. Science *305*, 1747-1752.

Melser, S., Chatelain, E.H., Lavie, J., Mahfouf, W., Jose, C., Obre, E., Goorden, S., Priault, M., Elgersma, Y., Rezvani, H.R., *et al.* (2013). Rheb regulates mitophagy induced by mitochondrial energetic status. Cell metabolism *17*, 719-730.

Mishra, P., Carelli, V., Manfredi, G., and Chan, D.C. (2014). Proteolytic cleavage of OPA1 stimulates mitochondrial inner membrane fusion and couples fusion to oxidative phosphorylation. Cell metabolism *19*, 630-641.

Nakamura, N., Matsuura, A., Wada, Y., and Ohsumi, Y. (1997). Acidification of vacuoles is required for autophagic degradation in the yeast, Saccharomyces cerevisiae. J Biochem *121*, 338-344.

Narendra, D., Kane, L.A., Hauser, D.N., Fearnley, I.M., and Youle, R.J. (2010a). p62/SQSTM1 is required for Parkin-induced mitochondrial clustering but not mitophagy; VDAC1 is dispensable for both. Autophagy *6*, 1090-1106.

Narendra, D., Tanaka, A., Suen, D.-F., and Youle, R.J. (2008). Parkin is recruited selectively to impaired mitochondria and promotes their autophagy. The Journal of Cell Biology *183*, 795-803.

Narendra, D.P., Jin, S.M., Tanaka, A., Suen, D.F., Gautier, C.A., Shen, J., Cookson, M.R., and Youle, R.J. (2010b). PINK1 is selectively stabilized on impaired mitochondria to activate Parkin. PLoS Biol *8*, e1000298.

Noda, N.N., Ohsumi, Y., and Inagaki, F. (2010). Atg8-family interacting motif crucial for selective autophagy. FEBS Letters *584*, 1379-1385.

Ong, S.E., Blagoev, B., Kratchmarova, I., Kristensen, D.B., Steen, H., Pandey, A., and Mann, M. (2002). Stable isotope labeling by amino acids in cell culture, SILAC, as a simple and accurate approach to expression proteomics. Mol Cell Proteomics *1*, 376-386.

Pagliarini, D.J., Calvo, S.E., Chang, B., Sheth, S.A., Vafai, S.B., Ong, S.E., Walford, G.A., Sugiana, C., Boneh, A., Chen, W.K., *et al.* (2008). A mitochondrial protein compendium elucidates complex I disease biology. Cell *134*, 112-123.

Pankiv, S., Clausen, T.H., Lamark, T., Brech, A., Bruun, J.A., Outzen, H., Overvatn, A., Bjorkoy, G., and Johansen, T. (2007). p62/SQSTM1 binds directly to Atg8/LC3 to facilitate degradation of ubiquitinated protein aggregates by autophagy. J Biol Chem *282*, 24131-24145.

Pease, S., and Lois, C. (2006). Mammalian and Avian Transgenesis – New Approaches (Heidelberg, Germany: Springer-Verlag Berlin Heidelberg).

Perry, S.W., Norman, J.P., Barbieri, J., Brown, E.B., and Gelbard, H.A. (2011). Mitochondrial membrane potential probes and the proton gradient: a practical usage guide. BioTechniques *50*, 98-115.

Pham, A.H., McCaffery, J.M., and Chan, D.C. (2012). Mouse lines with photo-activatable mitochondria to study mitochondrial dynamics. Genesis (New York, NY : 2000) *50*, 833-843.

Reers, M., Smith, T.W., and Chen, L.B. (1991). J-aggregate formation of a carbocyanine as a quantitative fluorescent indicator of membrane potential. Biochemistry *30*, 4480-4486.

Sanchez, P., De Carcer, G., Sandoval, I.V., Moscat, J., and Diaz-Meco, M.T. (1998). Localization of atypical protein kinase C isoforms into lysosome-targeted endosomes through interaction with p62. Molecular and cellular biology *18*, 3069-3080.

Sarraf, S.A., Raman, M., Guarani-Pereira, V., Sowa, M.E., Huttlin, E.L., Gygi, S.P., and Harper, J.W. (2013). Landscape of the PARKIN-dependent ubiquitylome in response to mitochondrial depolarization. Nature *496*, 372-376.

Seibenhener, M.L., Du, Y., Diaz-Meco, M.T., Moscat, J., Wooten, M.C., and Wooten, M.W. (2013). A role for sequestosome 1/p62 in mitochondrial dynamics, import and genome integrity. Biochim Biophys Acta *1833*, 452-459.

Shi, J., Fung, G., Deng, H., Zhang, J., Fiesel, F.C., Springer, W., Li, X., and Luo, H. (2015). NBR1 is dispensable for PARK2-mediated mitophagy regardless of the presence or absence of SQSTM1. Cell Death Dis *6*, e1943.

Smiley, S.T., Reers, M., Mottola-Hartshorn, C., Lin, M., Chen, A., Smith, T.W., Steele, G.D., Jr., and Chen, L.B. (1991). Intracellular heterogeneity in mitochondrial membrane potentials revealed by a J-aggregate-forming lipophilic cation JC-1. Proc Natl Acad Sci U S A *88*, 3671-3675.

Song, Z., Ghochani, M., McCaffery, J.M., Frey, T.G., and Chan, D.C. (2009). Mitofusins and OPA1 mediate sequential steps in mitochondrial membrane fusion. Mol Biol Cell *20*, 3525-3532.

Sun, N., Yun, J., Liu, J., Malide, D., Liu, C., Rovira, Ilsa I., Holmström, Kira M., Fergusson, Maria M., Yoo, Young H., Combs, Christian A., *et al.* Measuring In Vivo Mitophagy. Molecular Cell *60*, 685-696.

Sutovsky, P., Moreno, R.D., Ramalho-Santos, J., Dominko, T., Simerly, C., and Schatten, G. (2000). Ubiquitinated sperm mitochondria, selective proteolysis, and the regulation of mitochondrial inheritance in mammalian embryos. Biol Reprod *63*, 582-590.

Twig, G., Elorza, A., Molina, A.J.A., Mohamed, H., Wikstrom, J.D., Walzer, G., Stiles, L., Haigh, S.E., Katz, S., Las, G., *et al.* (2008). Fission and selective fusion govern mitochondrial segregation and elimination by autophagy. The EMBO journal *27*, 433-446.

Wilson, M.I., Gill, D.J., Perisic, O., Quinn, M.T., and Williams, R.L. (2003). PB1 domain-mediated heterodimerization in NADPH oxidase and signaling complexes of atypical protein kinase C with Par6 and p62. Mol Cell *12*, 39-50.

Yamano, K., Fogel, A.I., Wang, C., van der Bliek, A.M., and Youle, R.J. (2014). Mitochondrial Rab GAPs govern autophagosome biogenesis during mitophagy. eLife *3*, e01612.

Youle, R.J., and Narendra, D.P. (2011). Mechanisms of mitophagy. Nat Rev Mol Cell Biol *12*, 9-14.

Yun, J., Puri, R., Yang, H., Lizzio, M.A., Wu, C., Sheng, Z.-H., and Guo, M. (2014). MUL1 acts in parallel to the PINK1/parkin pathway in regulating mitofusin and compensates for loss of PINK1/parkin. eLife *3*, e01958.

Chapter 4

FUTURE DIRECTIONS

MUL1 and the PINK1/PARKIN pathway

We identified the E3 ligase, MUL1, as a protein that could partially compensate for loss of PARKIN in OXPHOS induced mitophagy and degradation of paternal mitochondria. The regulation of MUL1 in this context remains ambiguous. In contrast to PARKIN, which is a cytosolic protein recruited to mitochondria only under conditions of mitochondrial dysfunction, MUL1 is a resident mitochondrial protein. By what mechanism mitochondrial dysfunction might influence MUL1 mediated ubiquitination is unknown. Further mechanistic studies of MUL1 would help illuminate this issue. For instance, experiments to assess post-translational modifications on MUL1 under OXPHOS-induced mitophagy conditions would shed light on the changes that might take place to alter MUL1 function under those conditions. A direct test of a possible relationship between PINK1 and MUL1 would be assessment of MUL1 phosphorylation in a PINK1 wildtype or knockout background. Although MUL1 has two possible phosphorylation sites that are exposed to the cytoplasm, no such phosphorylation has been reported.

Additionally, the interaction of MUL1 with the PINK1/PARKIN pathway is uncertain. In one model, MUL1 functions independently of PINK1 and PARKIN; in another, MUL1 acts downstream of PINK1, either directly or indirectly. Previous

work in *Drosophila* has shown that MUL1 acts in parallel to the PINK1/PARKIN pathway in ubiquitination of MFN. Overexpression of MUL1 suppresses dPink1/dParkin mutant phenotypes (Yun et al., 2014a). In this case, it was found that MUL1 is not a downstream target of PINK1. However, in our system PINK1 knockout or PARKIN knockout with MUL1 knockdown impairs mitophagy whereas PARKIN knockout alone does not. Currently, PARKIN is the only E3 ligase shown to act in a PINK1 dependent manner; however, the difference between PINK1 knockout and PARKIN knockout phenotypes that we observed might suggest that there are other essential mitophagy factors downstream of PINK1 other than PARKIN, or that PINK1 has another role in mitophagy beyond activating PARKIN. It is possible that MUL1 is such a factor. Therefore it would be informative to further analyze the relationship of MUL1 with PINK1 in mammalian cells. Ubiquitination of mitochondria is a quantitative readout that might facilitate epistasis analysis. Preliminary experiments with PINK-knockout MEFS in which MULAN has been knocked down suggest that there is no additive loss of ubiquitination of mitochondria, which might imply that it acts downstream of PINK1; however, this may be due to residual MUL1 protein. Construction of a MULAN/PINK1 double knockout might be more informative. Furthermore, so far we have analyzed ubiquitination of mitochondria in a linkage-independent fashion, using a pan-ubiquitin antibody. It might be important to assess the role of MULAN in facilitating specific polyubiquitin chain linkages, specifically K63-linked ubiquitin, since this is more reflective of autophagy-specific ubiquitination. It is also worth noting that the level of ubiquitination of mitochondria in PINK1

knockout cells is very low. Firstly, this may mean that the dynamic range of the ubiquitination assay in PINK1 knockout cells is not sufficient to detect a further decrease due to MUL1 knockout, in which case a more sensitive mass spectrometry based assay might be beneficial. Secondly, this may suggest that there are several downstream targets of PINK1, which are currently unknown. Consistent with this, a recent phosphoproteomic screen identified three RAB GTPases, Rab8A, 8B and 13 that are phosphorylated at a conserved residue in response to PINK1 activation (Lai et al., 2015). How these proteins may function in mitophagy is unknown. Finally, the interesting way in which PINK1 is spared from degradation by depolarization of mitochondria may not be specific to PINK1. Perhaps other proteins are regulated in a similar manner. Identification of such proteins might help illuminate this issue as well.

The work in *Drosophila* also suggested that MUL1 acts by ubiquitinating MFN. However, the changes that we observed in ubiquitination of mitochondria were quite profound, suggesting that perhaps MUL1 ubiquitinates more than just MFN. Also, the high level of mitophagy observed in MFN-null MEFs suggests that mitophagy can proceed in the absence of MFN. Further studies in two directions would help clarify this. Identification of other MUL1 substrates would be informative, particularly if these substrates are not also substrates of PARKIN. A number of mass spectrometry based approaches could be taken to answer this question. Comparison of ubiquitinated proteins in PARKIN knockout cells verses PARKIN/MUL1 double knockout cells is one possibility, but overexpression of

functional MUL1 or a ligase-dead MUL1 would be another. The dependence of such ubiquitination on PINK1 could also be assessed by this method.

Tools for studying mitophagy: high throughput screening, and mitophagy mouse

The PINK1/PARKIN-mediated mitophagy mechanism is an elegant cascade of events that links mitochondrial membrane potential to ubiquitination. It is unclear, however, if this is the only, or even the primary means by which mitochondrial dysfunction gets translated into mitophagy. Furthermore, there are significant differences in the players already identified in mitophagy triggered under different conditions, although some amount of mitochondrial stress is probably present in most of these cases. High throughput screening of shRNA libraries under various cellular stresses is made possible by the fluorescence-quenching mitophagy assay that we have developed. Automated imaging of cells in a 96-well glass-bottom plate format coupled with image segmentation algorithms to distinguish red mitochondrial puncta could facilitate identification of the networks of proteins that are involved in each of these mitophagy contexts. Comparison of these networks could reveal common and unique mechanisms and help parse the currently scattered information we have about mitophagy pathways.

Our embryo experiments suggest a potential physiological relevance for the mitophagy proteins that we identified in our cell-culture assay, and the involvement of NIX in erythrocyte differentiation makes it clearly relevant to normal physiology. However, one long-puzzling conundrum is that although mutations in

PINK1 and PARKIN are found in Parkinson's disease patients, PINK1 and PARKIN knockout mouse models show surprisingly subtle phenotypes (Cookson, 2012). This may be due to complementation with other proteins, and our results regarding MUL1 support this idea, but it also suggests that there is much we do not understand about mitophagy in the whole organism context. The fluorescence-quenching assay that we have shown can be used as tool to monitor mitophagy in the mouse. Indeed, Sun et al., have created a transgenic mouse expressing a similar matrix-targeted pH dependent construct utilizing the fluorescent reporter Keima (mt-Keima) (Sun et al., 2015). This mouse can be used to address the physiological relevance of the mitophagy players so far identified, and the potential tissue specificity of each.

Persistence of paternal mitochondria in mice

One puzzling question regarding the maternal mode of mtDNA inheritance is a teleological one. Why doesn't paternal mtDNA persist? Is it because heteroplasmy in general is detrimental to the organism (Sharpley et al., 2012), or is it a selfish act on the part of the female that has no phenotypic outcome (Agnati et al., 2009)? The principles of natural selection would suggest that there must be some deleterious effect of paternal mtDNA persistence. Some evidence exists suggesting that heteroplasmy causes altered behavior, respiratory exchange ratio, and cognitive impairment in mice (Sharpley et al., 2012), and some sporadic cases of Parkinson's disease in humans show increased heteroplasmy, although it is not specifically localized to the substantia nigra so a case for a causal relationship to the

disease phenotype is difficult to envision (Schnopp et al., 1996). An alternate model is based on the observation that mtDNA can exhibit so-called “selfish selection” which favors mtDNA haplotypes with a replication advantage despite any deleterious effect on cell fitness (Aanen et al., 2014; Ma et al., 2014). Matrilinear inheritance of mtDNA restricts the opportunities for selfish mtDNA mutations to spread. The phenotypic effect of persistent paternal mitochondria, however, has been difficult to test in the absence of specific genes involved in the process.

We have shown that loss of mitophagy proteins in mouse embryos can inhibit or delay degradation of paternal mitochondria. We do not know, however, whether the paternal mitochondria that we detect in pre-implantation embryos with mitophagy protein knockdown would persist in an adult animal, or whether another mechanism exists that would later degrade these mitochondria. If the paternal mitochondria were maintained in adult animals, potential phenotypes in these animals could be investigated.

One way to answer this question is by PCR of mtDNA from mouse pups born of a cross between parents with differing mtDNA haplotypes. A previous paper demonstrated the feasibility of this approach (Luo et al., 2013); however, they found that mtDNA from the male parent could be detected stochastically at a low frequency in wildtype animals, suggesting that perhaps degradation mechanisms are not normally completely efficient. Nonetheless, a quantitative version of this technique might be able to determine whether mtDNA from the male parent is more often detected in offspring that are mitophagy protein mutants. Of the proteins we identified as being important in mitophagy of paternal mitochondria, knockout mice

of PINK1 and p62 have been made and are viable (Gautier et al., 2008; Harada et al., 2013). FIS1 knockout males do not produce viable sperm, and since this protein is expected to be important on the paternal mitochondria, rather than in the egg cytoplasm, it is difficult to test the involvement of FIS1 by this method. To our knowledge a TBC1D15 knockout mouse does not exist. Relatively rapid generation of genetically modified mice is now possible using the CRISPR/Cas-mediated genome engineering method (Yang et al., 2014), and this could be employed to generate a TBC1D15 knockout. One challenge with this approach is that the offspring of a homozygous mutant female and wildtype male are heterozygotes, which would only facilitate testing the function of these proteins prior to the maternal-zygotic transition. Furthermore, germ cells generally contain protein contributed by the parental support cells, which could contaminate such an experiment. A better experiment would involve a cross wherein both parents are mutants, which would first require generation of a new mutant line with an alternate mtDNA haplotype.

In our embryo experiments, we introduced virus by microinjection of fertilized oocytes, which is a laborious technique, limiting the number of proteins that can be screened. Another interesting possibility that would enable higher throughput screening of shRNAs is incubation of denuded embryos (zona pellucidae removed) in media containing a virus. This method was shown to generate transgenic mice at a similar frequency to embryo microinjection (Lois et al., 2002). By this method, embryos could be collected from fertilized females, denuded, and incubated with virus in a multiplexed format, wherein they could be

imaged. The high variability amongst embryos would necessitate a relatively large number of embryos to be collected, but this method could nonetheless yield rapid results and would help control for variability in the multiplicity of infection due to differences in the amount of virus injected in each embryo.

The role of p62 on mitochondria

We have shown here that loss of mitochondrial fusion results in an increase in mitophagy, which is consistent with previous studies suggesting a protective role for fusion, which facilitates mixing of mitochondrial contents, allowing complementation of function (Sato et al., 2006). As well as with studies showing that overexpression of FIS1 drives mitophagy (Alirol et al., 2006) and that fission helps segregate dysfunctional mitochondria which are prevented from fusing with the functional pool (Twig et al., 2008). The latter study suggests that functional status, as evinced by $\Delta\Psi_m$ determines mitophagy rather than fragmentation per se. We have shown a critical role for p62 in mitophagy in MFN-null cells. It is not clear, however, what dictates p62 translocation to mitochondria, since we find that the UBA domain of p62 is dispensable for this localization. Interestingly, previous studies have implicated p62 in mitochondrial morphology, protein import, and maintenance of mtDNA (Seibenhener et al., 2013a). Could p62 be a direct sensor of mitochondrial function rather than simply an adaptor to the autophagosome? To address this question, further studies of the localization of p62 to mitochondria are needed. In particular, to which sub-compartment of mitochondria p62 localizes will be informative. It is likely to be associated with the OMM, since it does not contain

a mitochondrial localization sequence. Furthermore, identification of p62 binding partners on the mitochondria would be informative in understanding the mechanisms by which it senses and/or influences mitochondrial stress. A preliminary co-immunoprecipitation experiment suggests that there may be an association between p62 and the complex that forms the mitochondrial OMM-cristae junctions, but this remains to be validated. The PB1 domain of p62 appears to be a key determinant of p62 localization to mitochondria. It would be useful to learn which proteins on mitochondria specifically bind to this domain, and how these proteins are altered under conditions of stress.

Another interesting facet of the $\Delta\Psi_m$ mediated mitophagy model is that mitochondria are highly dynamic. As illustrated by the Crabtree effect in cultured cells (Diaz-Ruiz et al., 2011), mitochondria can readily increase and decrease OXPHOS activity. It would seem wasteful for the attendant changes in $\Delta\Psi_m$ to invariably lead to mitophagy. It stands to reason, therefore, that there might be some threshold $\Delta\Psi_m$ below which loss of fusion and mitophagy occurs. A quantitative analysis of the correlation between $\Delta\Psi_m$ and mitophagy that could reveal such a threshold, or perhaps a linear relationship might be enlightening in this regard.

REFERENCES:

Aanen, D.K., Spelbrink, J.N., and Beekman, M. (2014). What cost mitochondria? The maintenance of functional mitochondrial DNA within and across generations. Philosophical Transactions of the Royal Society B: Biological Sciences *369*, 20130438.

Agnati, L.F., Barlow, P.W., Baldelli, E., and Baluška, F. (2009). Are maternal mitochondria the selfish entities that are masters of the cells of eukaryotic multicellular organisms? Communicative & Integrative Biology *2*, 194-200.

Alirol, E., James, D., Huber, D., Marchetto, A., Vergani, L., Martinou, J.-C., and Scorrano, L. (2006). The Mitochondrial Fission Protein hFis1 Requires the Endoplasmic Reticulum Gateway to Induce Apoptosis. Molecular Biology of the Cell *17*, 4593-4605.

Cookson, M.R. (2012). Parkinsonism Due to Mutations in PINK1, Parkin, and DJ-1 and Oxidative Stress and Mitochondrial Pathways. Cold Spring Harbor Perspectives in Medicine *2*, a009415.

Diaz-Ruiz, R., Rigoulet, M., and Devin, A. (2011). The Warburg and Crabtree effects: On the origin of cancer cell energy metabolism and of yeast glucose repression. Biochimica et Biophysica Acta (BBA) - Bioenergetics *1807*, 568-576.

Gautier, C.A., Kitada, T., and Shen, J. (2008). Loss of PINK1 causes mitochondrial functional defects and increased sensitivity to oxidative stress. Proc Natl Acad Sci U S A *105*, 11364-11369.

Harada, H., Warabi, E., Matsuki, T., Yanagawa, T., Okada, K., Uwayama, J., Ikeda, A., Nakaso, K., Kirii, K., Noguchi, N., *et al.* (2013). Deficiency of p62/Sequestosome 1 causes hyperphagia due to leptin resistance in the brain. J Neurosci *33*, 14767-14777.

Lai, Y.C., Kondapalli, C., Lehneck, R., Procter, J.B., Dill, B.D., Woodroof, H.I., Gourlay, R., Peggie, M., Macartney, T.J., Corti, O., *et al.* (2015). Phosphoproteomic screening identifies Rab GTPases as novel downstream targets of PINK1. The EMBO journal *34*, 2840-2861.

Lois, C., Hong, E.J., Pease, S., Brown, E.J., and Baltimore, D. (2002). Germline transmission and tissue-specific expression of transgenes delivered by lentiviral vectors. Science *295*, 868-872.

Luo, S.M., Ge, Z.J., Wang, Z.W., Jiang, Z.Z., Wang, Z.B., Ouyang, Y.C., Hou, Y., Schatten, H., and Sun, Q.Y. (2013). Unique insights into maternal mitochondrial inheritance in mice. Proc Natl Acad Sci U S A *110*, 13038-13043.

Ma, H., Xu, H., and O'Farrell, P.H. (2014). Transmission of mitochondrial mutations and action of purifying selection in Drosophila melanogaster. Nat Genet *46*, 393-397.

Sato, A., Nakada, K., and Hayashi, J. (2006). Mitochondrial dynamics and aging: Mitochondrial interaction preventing individuals from expression of respiratory deficiency caused by mutant mtDNA. Biochim Biophys Acta *1763*, 473-481.

Schnopp, N.M., Kosel, S., Egensperger, R., and Graeber, M.B. (1996). Regional heterogeneity of mtDNA heteroplasmy in parkinsonian brain. Clinical neuropathology *15*, 348-352.

Seibenhener, M.L., Du, Y., Diaz-Meco, M.-T., Moscat, J., Wooten, M.C., and Wooten, M.W. (2013). A Role for Sequestosome1/p62 in Mitochondrial Dynamics, Import and Genome Integrity. Biochimica et biophysica acta *1833*, 452-459.

Sharpley, M.S., Marciniak, C., Eckel-Mahan, K., McManus, M., Crimi, M., Waymire, K., Lin, C.S., Masubuchi, S., Friend, N., Koike, M., *et al.* (2012). Heteroplasmy of mouse mtDNA is genetically unstable and results in altered behavior and cognition. Cell *151*, 333-343.

Sun, N., Yun, J., Liu, J., Malide, D., Liu, C., Rovira, II, Holmstrom, K.M., Fergusson, M.M., Yoo, Y.H., Combs, C.A., *et al.* (2015). Measuring In Vivo Mitophagy. Mol Cell *60*, 685-696.

Twig, G., Elorza, A., Molina, A.J.A., Mohamed, H., Wikstrom, J.D., Walzer, G., Stiles, L., Haigh, S.E., Katz, S., Las, G., *et al.* (2008). Fission and selective fusion govern mitochondrial segregation and elimination by autophagy. The EMBO journal *27*, 433-446.

Yang, H., Wang, H., and Jaenisch, R. (2014). Generating genetically modified mice using CRISPR/Cas-mediated genome engineering. Nat Protocols *9*, 1956-1968.

Yun, J., Puri, R., Yang, H., Lizzio, M.A., Wu, C., Sheng, Z.-H., and Guo, M. (2014). MUL1 acts in parallel to the PINK1/parkin pathway in regulating mitofusin and compensates for loss of PINK1/parkin. eLife *3*, e01958.